

September 23, 2020

Lauderdale County Seismic and Liquefaction Hazard Maps
(HUD Grant Year Three Products)

Chris H. Cramer, Roy B. Van Arsdale, Valarie Harrison, Karim Bouzeid, David Arellano, Hamed Tohidi, Shahram Pezeshk, Stephan P. Horton, Roshan Bhattarai, Nima Nazemi, and Ali Farhadi

Abstract

A five-year seismic and liquefaction hazard mapping project for five western Tennessee counties began in 2017 under a Disaster Resilience Competition grant from the U.S. Department of Housing and Urban Development to the State of Tennessee. The project supports natural hazard (flood and earthquake) mitigation efforts in these five counties. The seismic hazard maps for Lauderdale County in western Tennessee were completed in 2020. Additional geological, geotechnical, and geophysical information has been gathered in Lauderdale Co. to improve the base northern Mississippi Embayment hazard maps of Dhar and Cramer (2018). Information gathered includes additional geological and geotechnical subsurface exploration logs, water table level data collection and measurements, new measurements of shallow and deep shear-wave velocity (V_s) profiles, and the compilation of existing V_s profiles in and around the county. Improvements were made in the 3D geological model, water table model, the geotechnical liquefaction probability curves, and the V_s correlation with lithology model for Lauderdale Co. Resulting improved soil response amplification distributions on a 0.5 km grid were combined with the 2014 U.S. Geological Survey seismic hazard model (Petersen et al., 2014) sources and attenuation models to add the effect of local geology for Lauderdale Co. Resulting products are an improved 3D-geology, geotechnical, seismic hazard, and liquefaction hazard models and maps for Lauderdale Co. Seismic hazard maps at PGA and 1.0 s show a 10-70% decrease in hazard at short periods and a 10-100% increase at long periods compared with USGS NSHMP maps.

Introduction

As part of the 2015 Disaster Resilience Competition, the State of Tennessee received funds from the Department of Housing and Urban Development (HUD) for several grants for flood hazard mitigation efforts. The University of Memphis received one of the grants for flood and seismic hazard mapping efforts in five western Tennessee counties (Figure 1) covering a five-year period starting in 2017. The third-year seismic hazard mapping effort is for Lauderdale County seismic and liquefaction hazard maps (this report).

The goal for the seismic hazard mapping project is to develop seismic and liquefaction hazard maps for use in flood hazard mitigation efforts in other portions of the HUD grant effort via the University of Memphis. The hazard maps will also be useful for other earthquake hazard mitigation efforts in the five western Tennessee counties.

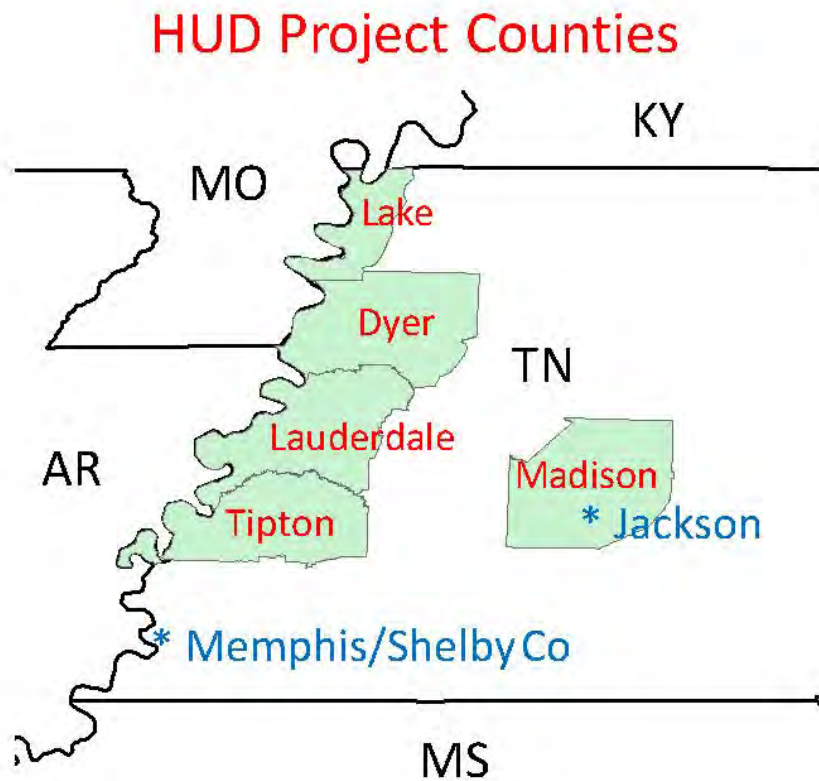


Figure 1: Five western Tennessee counties of the HUD grant supported seismic hazard study. AR – Arkansas, KY – Kentucky, MO – Missouri, MS – Mississippi, and TN – Tennessee.

The major elements to the seismic and liquefaction hazard mapping in this project are (1) geological 3D model development, (2) geotechnical (soil response to ground motions) model development, (3) seismological data gathering, and (4) hazard maps generation. The 3D geological model of sediments above bedrock involves the gathering and interpretation of boring logs, entering geological information into a geographic information system (GIS), and developing maps of the depth to the tops of key geological sediment layers. The accompanying geotechnical model involves the gathering of geotechnical information (sediment properties and water table levels) from boring logs, and modeling liquefaction potential of the shallow sediments. Seismological data gathering includes collecting published sediment velocity profiles with depth, and making new measurements of sediment velocity with depth in the study area. The final step is to integrate the geological, geotechnical, and seismological data into a county wide hazard model and maps that included the effects of local geology (sediments).

Geological Model

Introduction

Lauderdale County in western Tennessee was mapped as part of a five-county earthquake hazard mapping program (Figure 2) (Cramer et al., 2018b; Weathers and Van Arsdale, 2019). Located immediately southeast of the New Madrid seismic zone, Lauderdale County is vulnerable to both earthquake ground shaking and liquefaction in the event of future large earthquakes (Chiou et al., 1992; Cramer, 2006; Csontos and Van Arsdale, 2008; Cramer and Boyd, 2014; Cramer et al., 2018a and b).

The topography of Lauderdale County consists of lowland floodplains of the Mississippi, Hatchie, and South Fork of the Forked Deer rivers and loess covered terraces of these rivers (Figure 3). Beneath the near-surface Pliocene and Quaternary sediments are Eocene (~34 Ma) strata that overlie older Paleogene, Late Cretaceous, and Paleozoic strata (Hardeman, 1966; Weathers and Van Arsdale, 2019). Structurally, the county overlies the east-bounding faults of the Cambrian Reelfoot rift (Parrish and Van Arsdale, 2004; Csontos et al., 2008), which has revealed Quaternary reactivation at Porter's Gap (Fig. 4) (Cox et al., 2001; 2006). The surface and subsurface geology of a region influences how the landscape will move during a large earthquake. In this study we present geologic maps of Lauderdale County that provide important information for companion seismologic and liquefaction hazard modeling studies.

Methods

A Lidar based 10-meter digital elevation model (DEM) of Lauderdale County was the base map upon which surface and near-surface geology was mapped. River terraces along the Hatchie and South Fork of the Forked Deer rivers in Figure 3 were derived from previously published west Tennessee terrace maps by Saucier (1987) and Rodbell (1996). Subsurface geologic drill hole data were acquired from North American Coal Company, Tennessee Department of Transportation, petroleum exploration wells, Tennessee Department of Environmental Control, and the Center of Applied Earth Science and Engineering Research at the University of Memphis. The lithologic boring logs were geologically interpreted and entered into Excel spread sheets. Geologic mapping was conducted down to the top of the Paleozoic strata, which is at an average depth of 832 m below Lauderdale County.

The near-surface Pliocene and Quaternary geology was mapped using 2,330 bore holes (Figure 2) and the top of the Eocene was mapped using 2,630 borings (Figure 5). The contact between the fine-grained Eocene sediment and the overlying Pliocene and Quaternary alluvium is identified by the basal conglomeratic facies of the alluvium. Within the Eocene section is the Memphis Sand (Martin and Van Arsdale, 2017). The Memphis Sand is the major aquifer for western Tennessee and there are 95 wells in this study that penetrate its uppermost surface. The underlying top of the Cretaceous and top of the Paleozoic were mapped from DOW

Chemical seismic reflection lines (e.g. Figure 4B) and oil-exploration wells (Parrish and Van Arsdale, 2004).

Structure contour maps were made of the elevation of the tops of the Eocene, Memphis Sand, Cretaceous, and Paleozoic strata beneath Lauderdale County and within a peripheral zone (Figures 5B, 6A-8A). These maps were made using the Natural Neighbor contouring algorithm. Bedrock faults have been mapped beneath Lauderdale County (Parrish and Van Arsdale, 2004; Martin and Van Arsdale, 2008). These previously mapped faults (Figure 4) were used in our mapping to produce faulted structure contour maps of the tops of the Eocene, Memphis Sand, Cretaceous, and Paleozoic using the Spline with Barriers contouring algorithm (Figures 5C, 6B-8B).

Isopach (unit thickness) maps were made of the Lowland floodplain alluvium and the silt/clay uppermost portion of the Lowlands floodplain alluvium (Figure 9).

Results

Near-Surface Geologic Map

Near-surface geology of Lauderdale County was geologically differentiated into three mapping units (Lowlands, Intermediate, Uplands) that differ in their elevation and near-surface geology (Figure 3A). The Figure 3B cross section does not represent a particular place on the map but is a general depiction of the near-surface geology. Unit surface elevations and unit thicknesses in Figure 3B are averages from multiple values measured throughout the county.

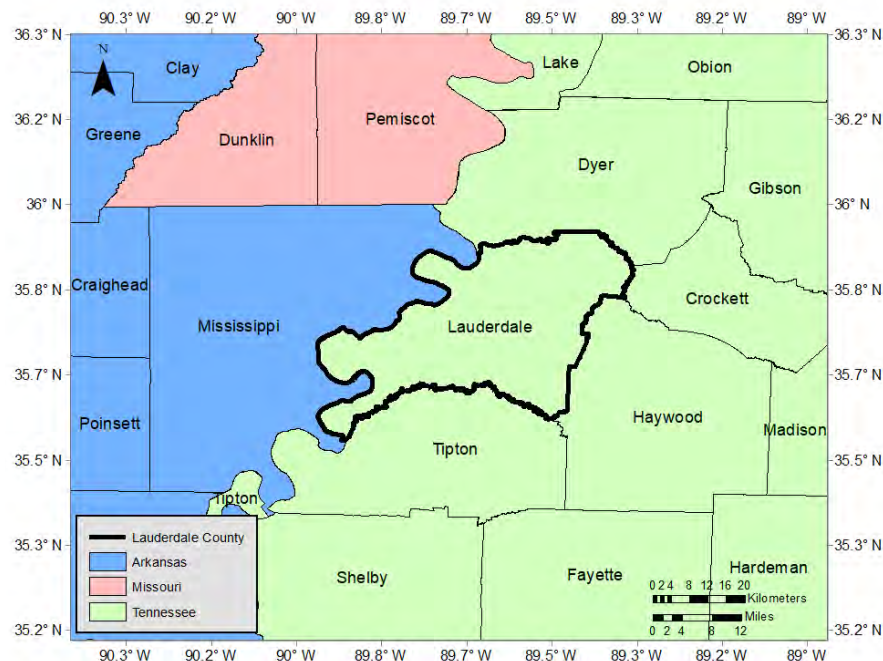
The Lowlands are at an elevation of less than 81 m and consists of Holocene (< 12 ka) river floodplain alluvium (Saucier, 1994; Rittenour et al., 2007). In general, the alluvium consists of surface silt and clay overbank sediment that overlies laterally accreted sand and gravel sediment. Between elevations of > 81 m and 107 m are the Intermediate units. Intermediate units are differentiated into river terraces that are former high-level floodplains of the South Fork of the Forked Deer and Hatchie rivers. The terraces have been mapped from topographically highest to lowest as the Humboldt, Hatchie, and Finley terraces (Saucier, 1987; Rodbell, 1996). We have also mapped an Intermediate surface that is not a terrace and consists of loess overlying Eocene strata. All Intermediate units are covered with Peoria loess (wind-blown silt) that is less than 20 ka. The Hatchie and Humboldt terraces have older loess beneath the Peoria loess (Rodbell, 1996) that have not been mapped in this study because our data do not provide this information. Beneath the loess, the terrace alluvium consists of silt and clay overbank sediment and underlying laterally accreted sand and gravel sediment that is ~ 22 ka (Finley) and > 65 ka (Hatchie and Humboldt). The Upland unit is at an elevation > 107 m and is a loess covered high-level terrace of the ancestral (~ 3.6 Ma) Mississippi/Ohio river (Van Arsdale et al., 2007; Odum et al., in press). This high-level terrace alluvium, called the Upland Complex, consists of sand and gravel that is regionally a major source of aggregate (Van Arsdale et al., 2012; Lumsden et al., 2016).

Structure Contour Maps

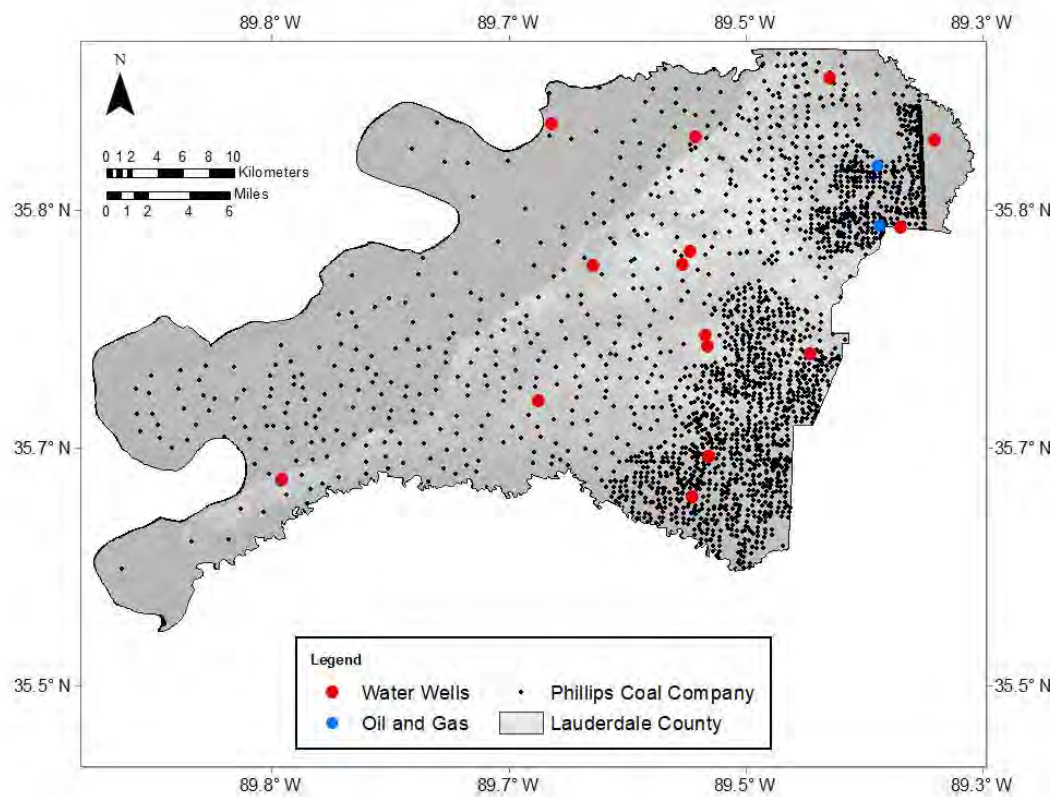
The top of the Eocene strata is presented as an un-faulted surface and as a faulted surface (Figure 5). There is a lot of subsurface relief on the top of the Eocene because the Eocene has been eroded by the Mississippi, Hatchie, and South Fork of the Forked Deer rivers and because it has undergone structural deformation. When inserting the bedrock faults into this data set and contouring it with the Spline with Barriers contouring algorithm, fault displacement is apparent. Although poorly constrained due to only 95 wells, the top of the Memphis Sand illustrates a westerly slope (Figure 6). When the bedrock faults are inserted, the top of the Memphis Sand reveals fault displacement. Also poorly constrained, the tops of the Cretaceous strata and Paleozoic strata were contoured without faults (Figures 7A and 8A). These surfaces slope westerly. When inserting the faults, the tops of Cretaceous and Paleozoic reveal fault displacements (Figures 7B and 8B).

Isopach Maps

The Lowland floodplain alluvium, in general, consists of two layers. A surface silt and clay layer that averages 8 m thick and an underlying sand and gravel layer that averages 23 m thick. The isopach map of the thickness of the entire Lowland floodplain alluvium reveals variation in thickness due to rivers of different sizes and scour depths (Figure 9a). Thickness of the uppermost silt and clay layer is also variable (Figure 9b).

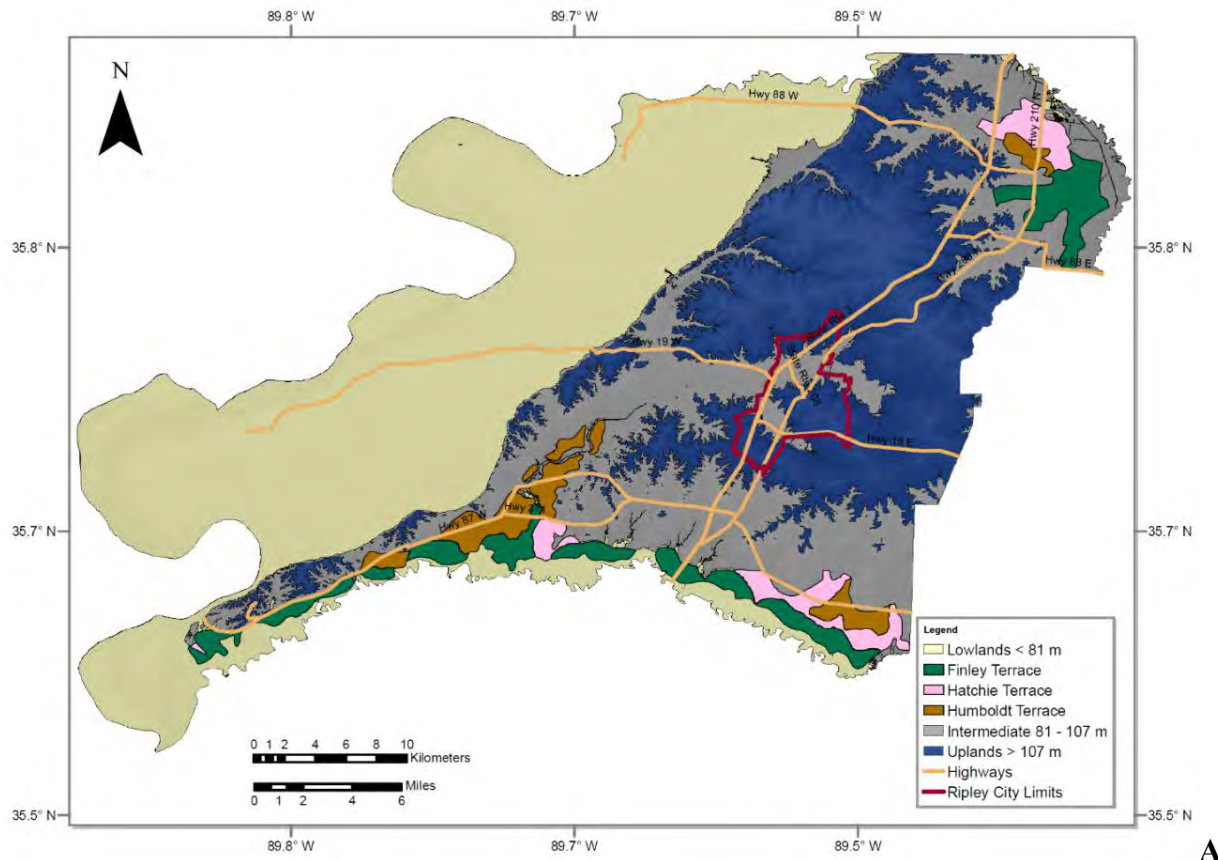


A

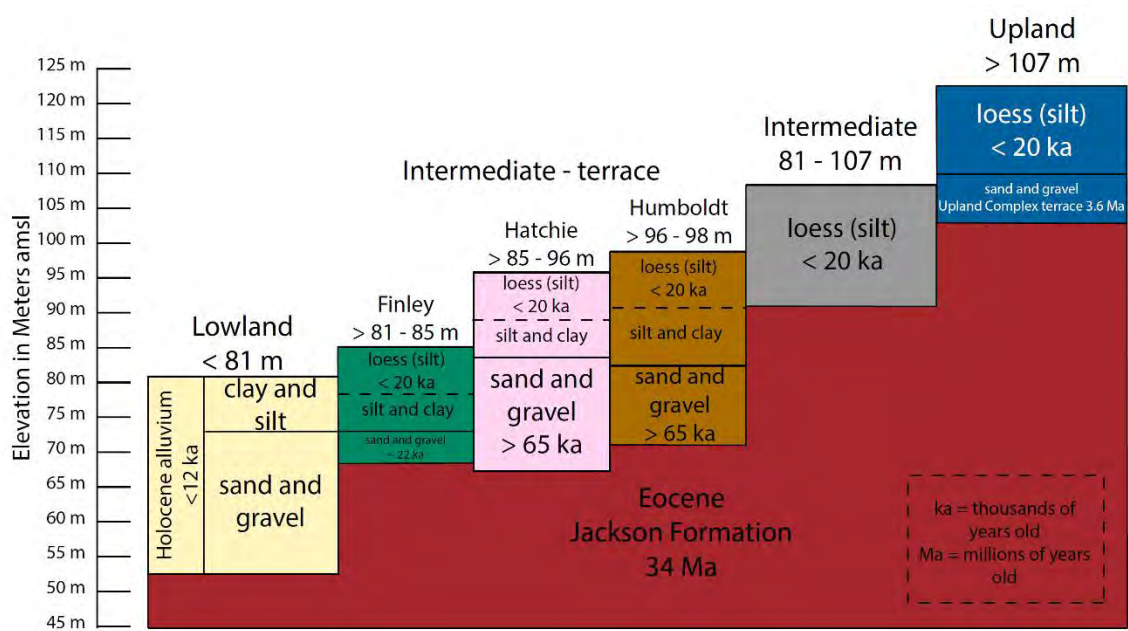


B

Figure 2: A) Lauderdale County in western Tennessee. B) Dots show geologic drill holes used in near-surface mapping of Lauderdale County.



A



B

Figure 3: A) Geologic map of Lauderdale County. B) General geologic cross section illustrating the near-surface geology beneath the Lowland, Intermediate, and Upland surfaces in Lauderdale County.

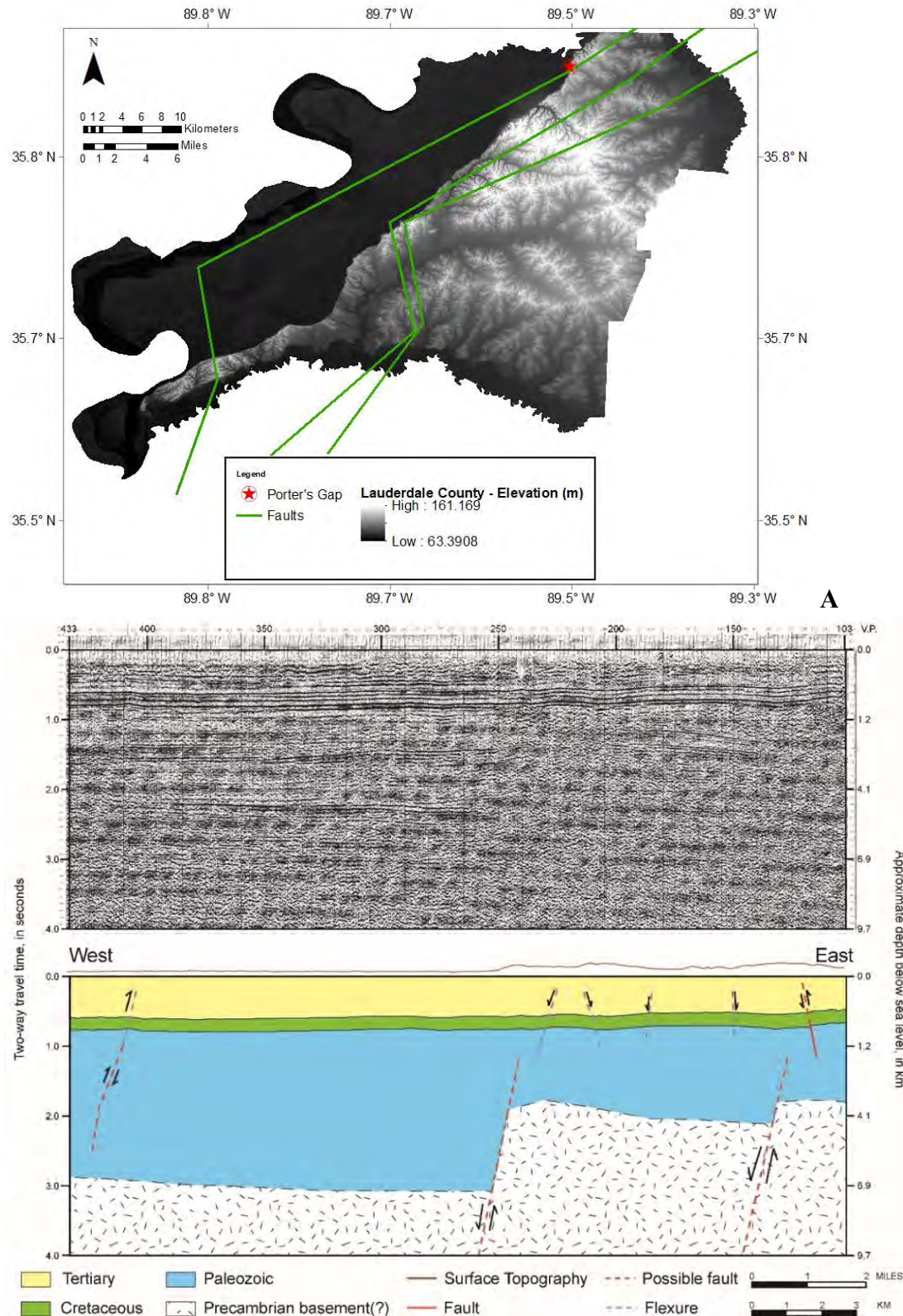
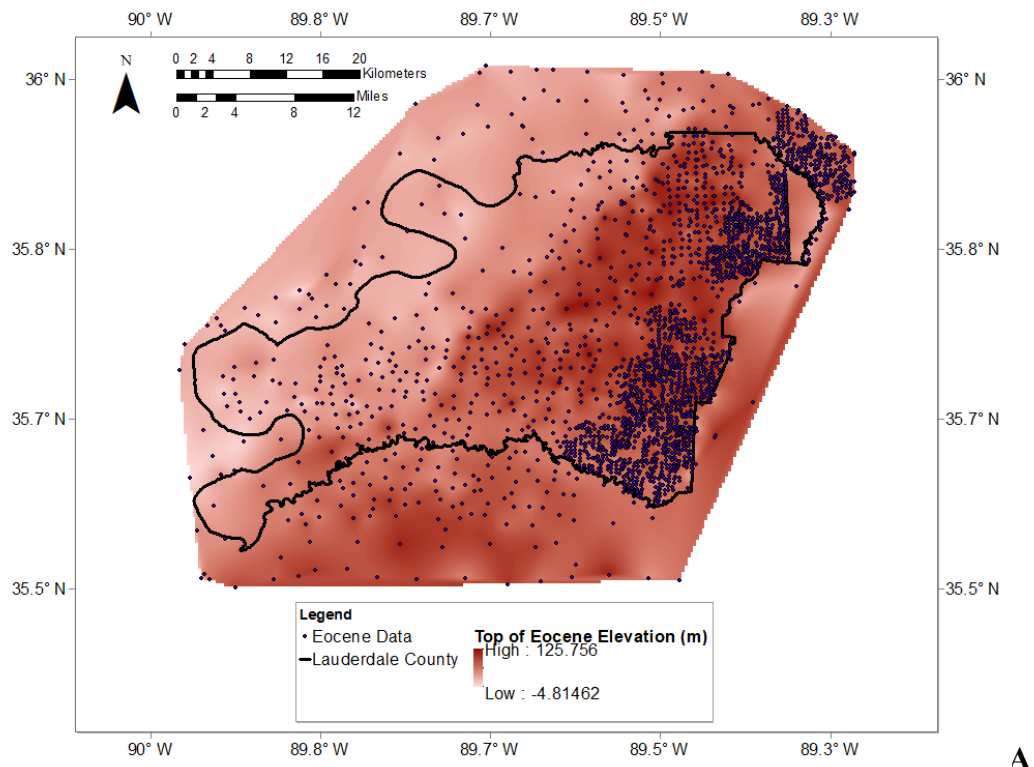
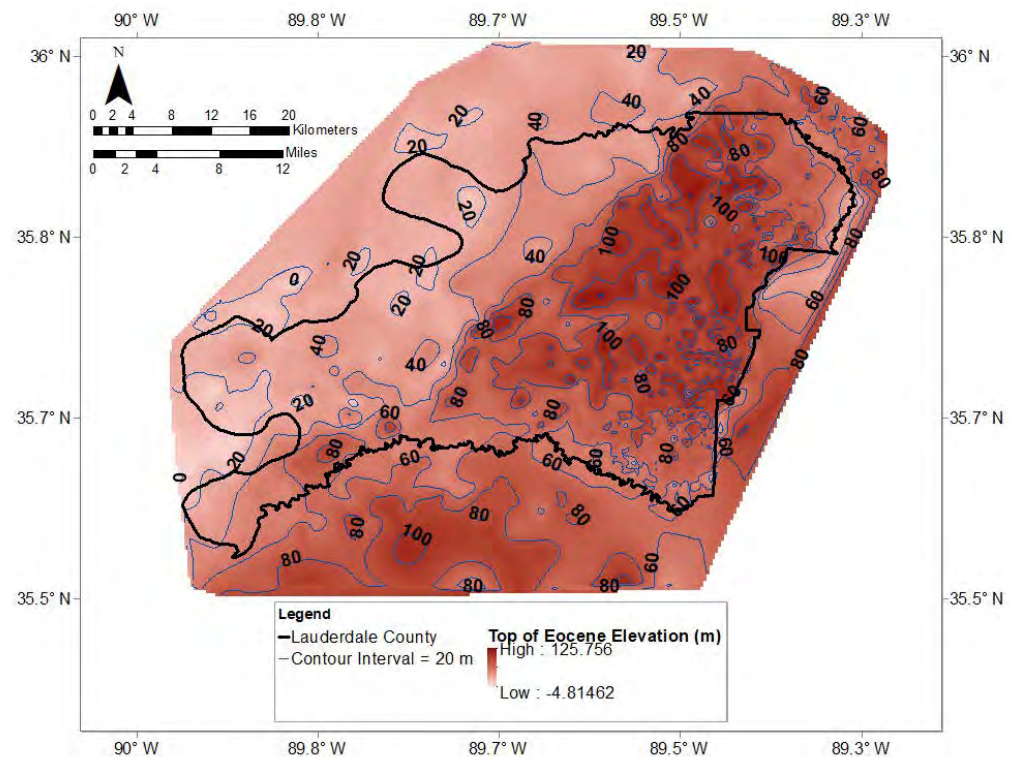


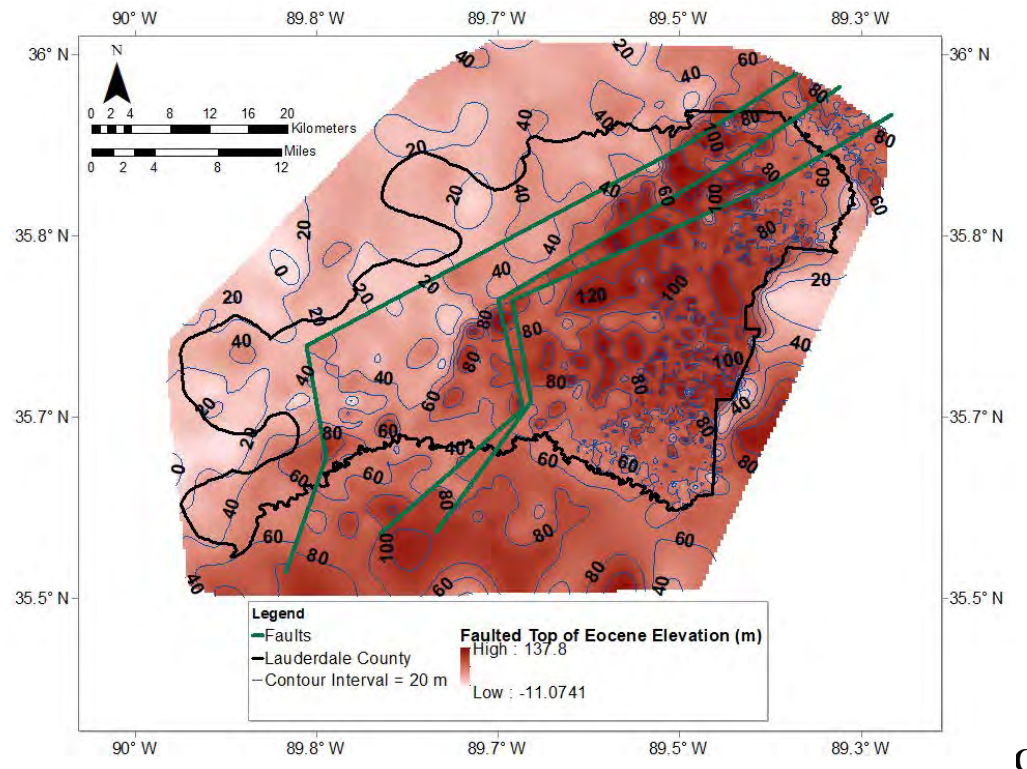
Figure 4: A) Faults mapped in the subsurface of Lauderdale County. Red star is Porter's Gap surface fault location. B) Example of a seismic line and its interpretation used in fault mapping.



A

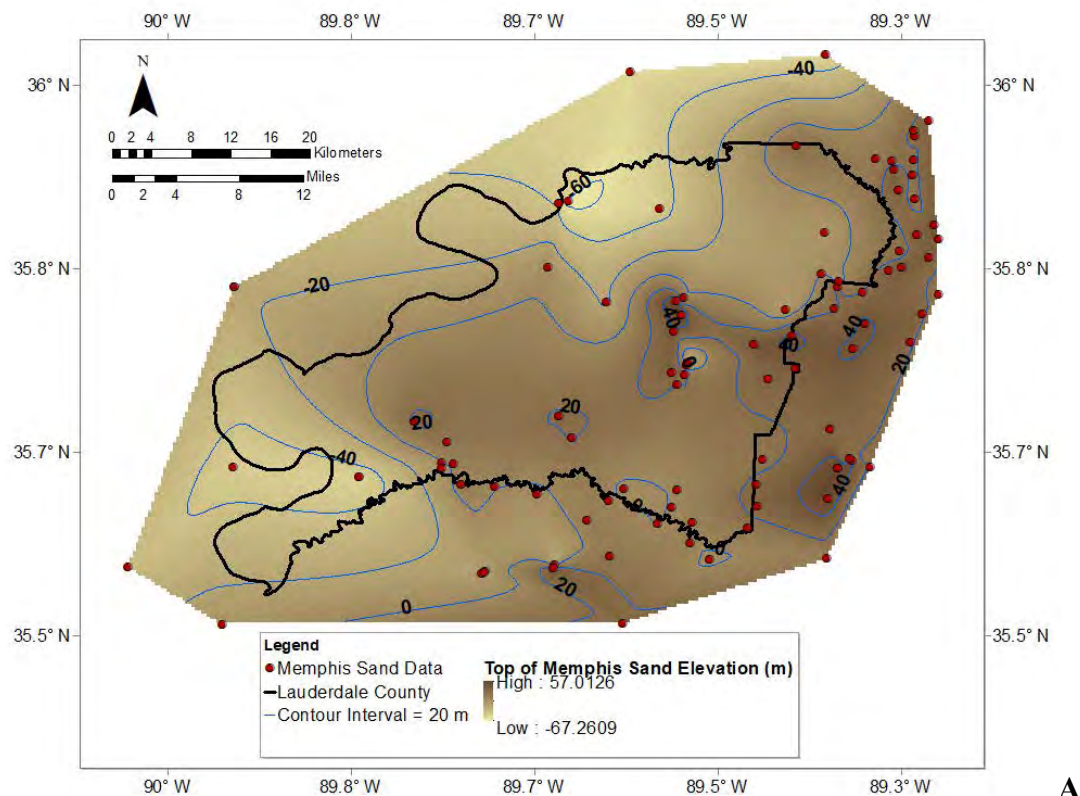


B

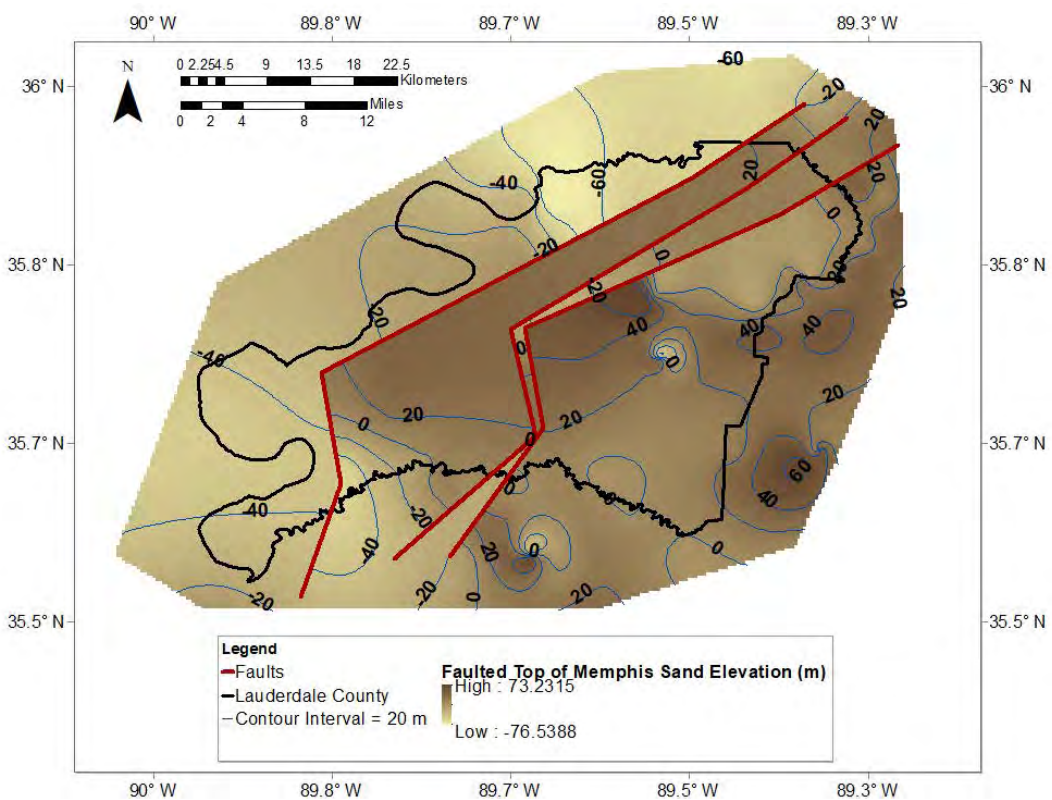


C

Figure 5: A) Drill holes (black dots) used to map top of Eocene strata. B) Structure contour map of the un-faulted top of Eocene strata. (C) Structure contour map of the faulted top of Eocene strata.



A



B

Figure 6: Un-faulted (A) and faulted (B) structure contour maps of the top of the Memphis Sand strata with red dots illustrating drill holes used to make the maps.

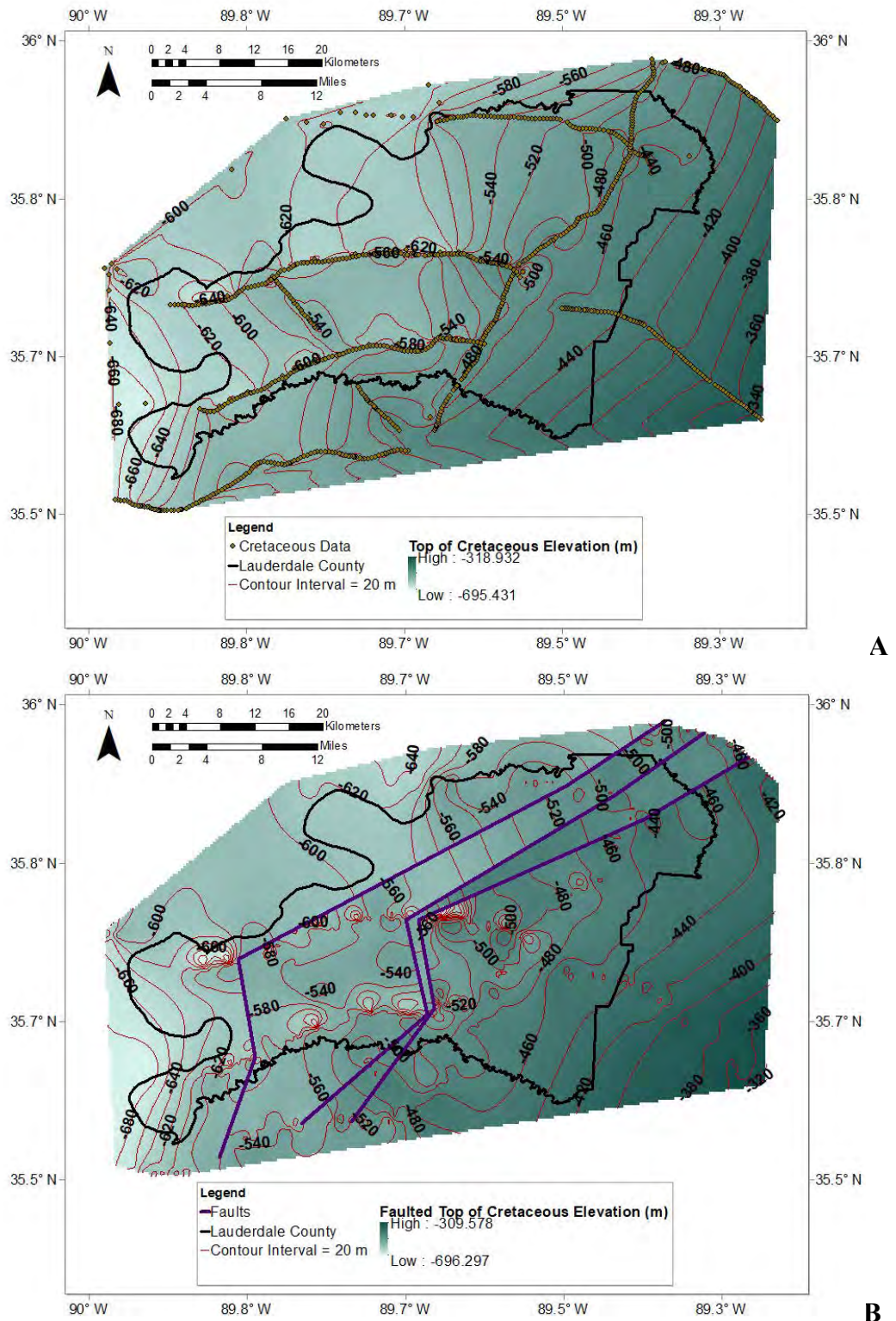


Figure 7: Un-faulted (A) and faulted (B) structure contour maps of the top of the Cretaceous strata with dots illustrating seismic reflection shot points and drill holes used to make the maps.

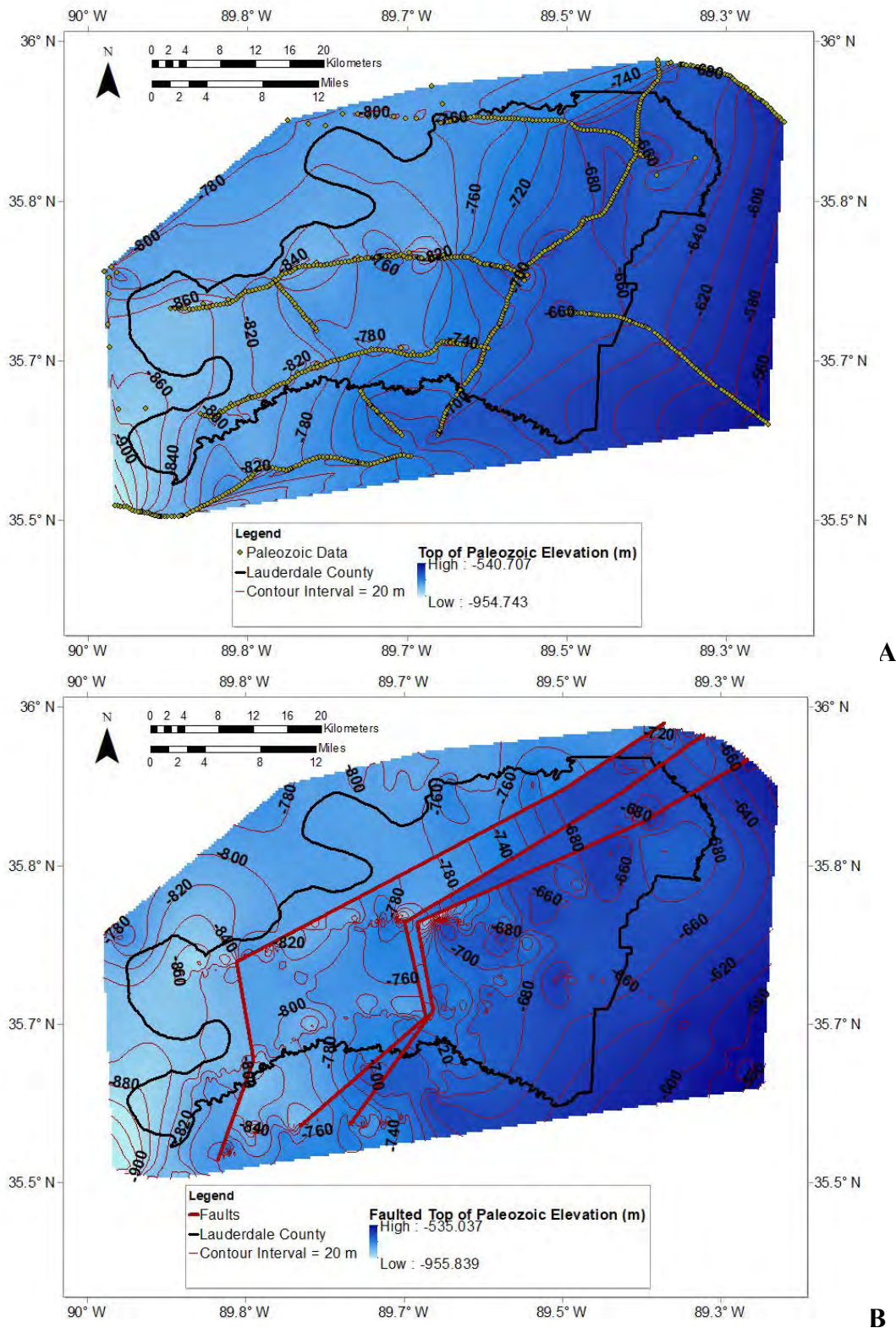


Figure 8: Un-faulted (A) and faulted (B) structure contour maps of the top of the Paleozoic strata with dots illustrating seismic reflection shot points and drill holes used to make the map.

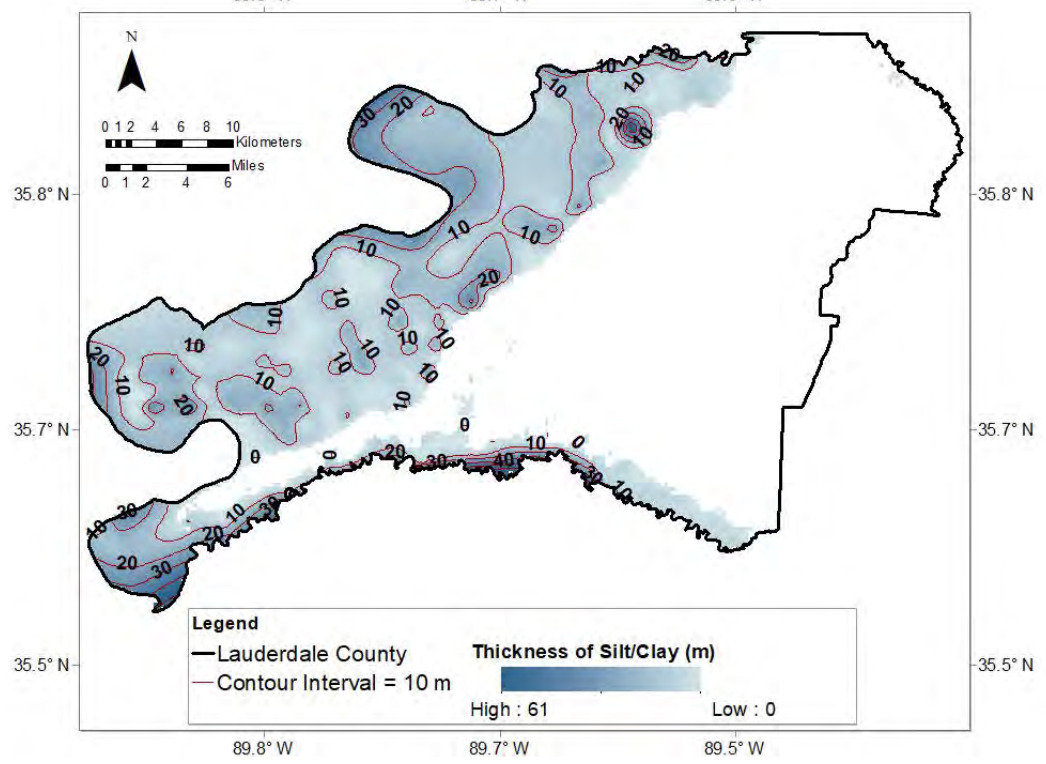
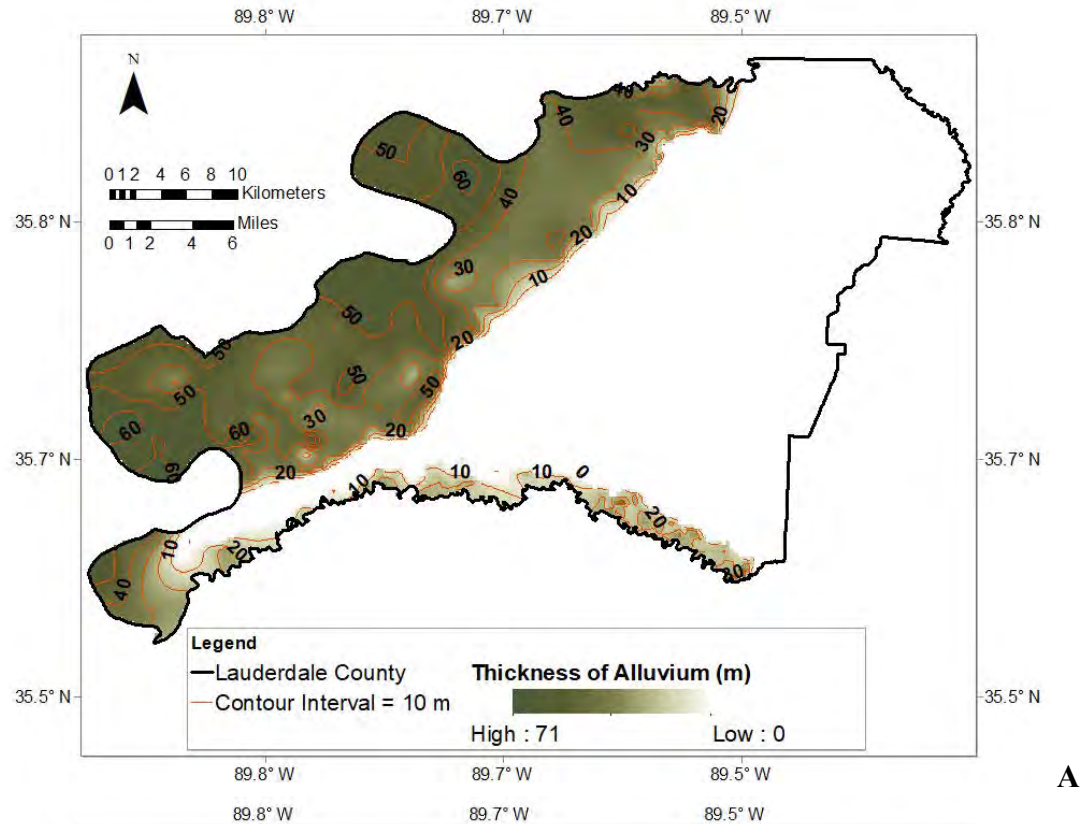


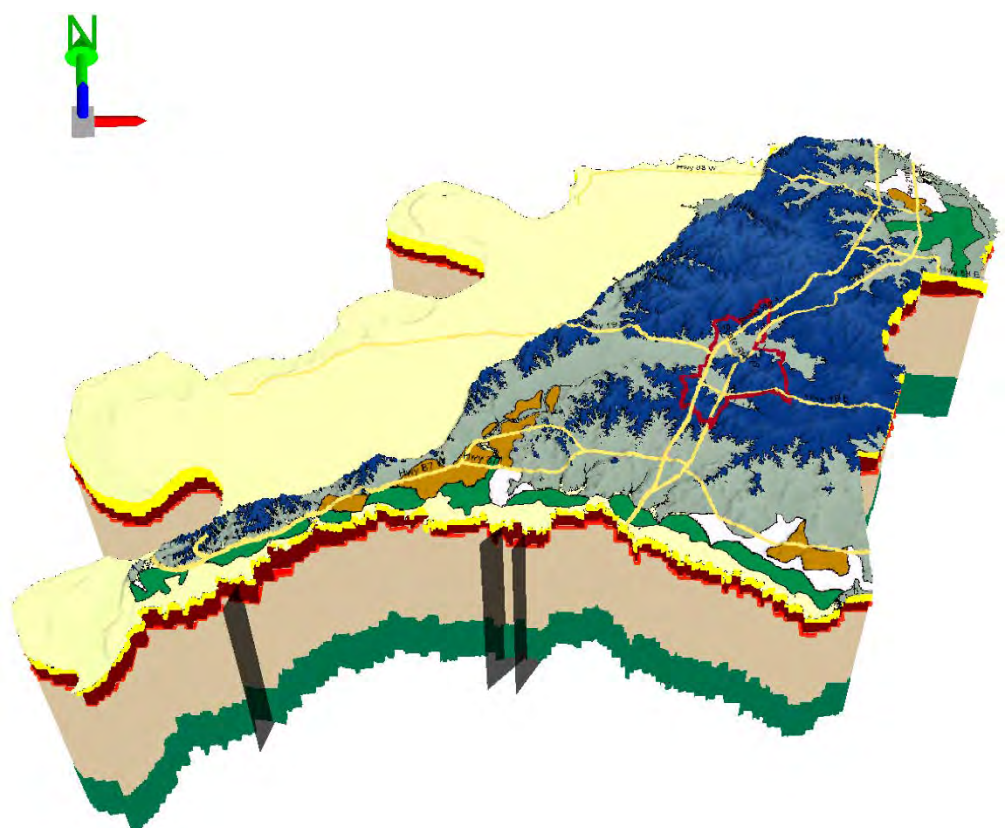
Figure 9: A) Isopach of the Holocene alluvium in Lauderdale County. B) Isopach of the uppermost silt and clay portion of the Holocene alluvium in Lauderdale County.

Geologic Summary

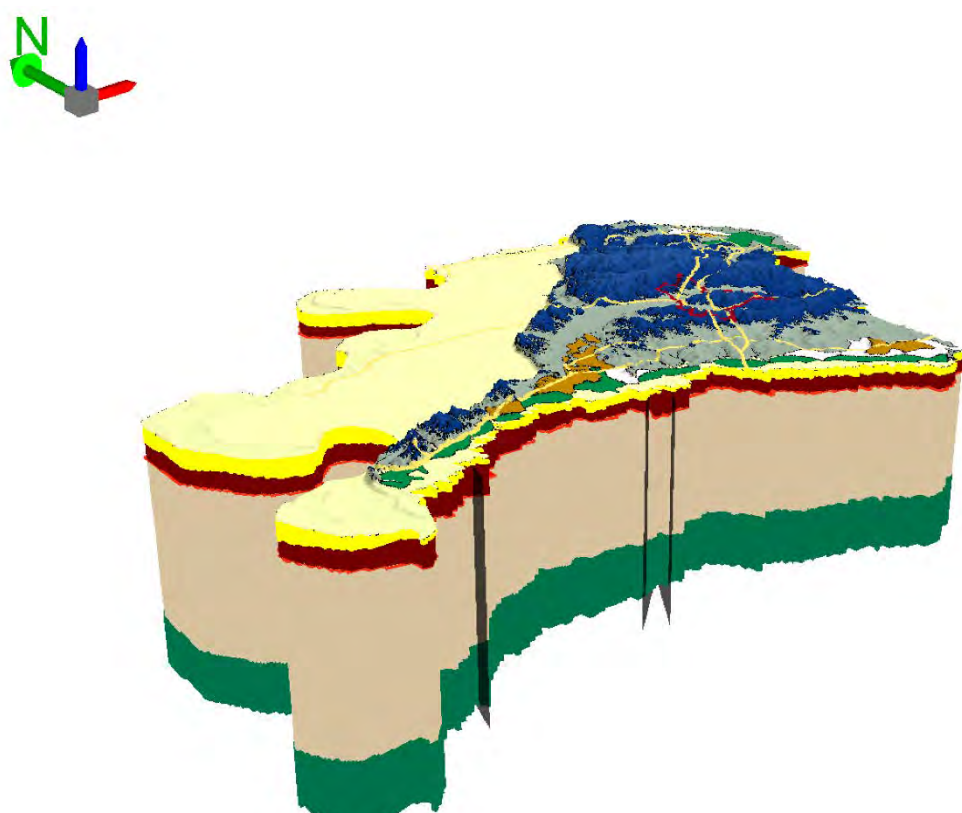
The near-surface geology reveals incision of the ancestral Mississippi/Ohio river system through time. Approximately 3.6 Ma (Odum et al., *in press*) the ancestral Mississippi/Ohio river system (Upland Complex) flowed across a vast floodplain surface that extended beyond Lauderdale County (Van Arsdale et al., 2007; Cupples and Van Arsdale, 2014; Cox et al., 2014). Incision through the Upland Complex throughout the lower Mississippi River system has been proposed to have begun in the early Pleistocene with growth of continental ice sheets and resultant low sea levels (Saucier, 1994; Van Arsdale et al., 2007; 2019). During the Pleistocene up to four layers of loess were deposited in western Tennessee (Markewich et al., 1998). In Lauderdale County, Rodbell (1996) identified Peoria loess (< 12 ka) covering the Upland and Intermediate surfaces with underlying Roxana loess that is > 65 ka on top of the floodplain alluvium of the Humboldt and Hatchie terraces. Based on these observations, we know that in Lauderdale County the ancestral Mississippi/Ohio river system and its tributaries entrenched > 65 ka because the Humboldt terrace alluvium is overlain by the > 65 ka loess (Figure 3). Subsequently, the Mississippi/Ohio river system and its tributaries further intrenched to form the topographically lower Hatchie (also > 65 ka) and then Finley (~ 22 ka) terrace levels. The final entrenchment of the Mississippi River and its Hatchie and South Fork of the Forked Deer river tributaries in Lauderdale County occurred within the last ~ 22 ka resulting in most of the Lowlands being underlain by Holocene (< 12 ka) alluvium.

Three faults have been mapped beneath Lauderdale County. We believe these are reactivated Cambrian Reelfoot rift faults that have displaced the top of the Eocene. Thus, these faults have been active within the last 34 Ma. The fault at Porter's Gap (Figure 4) has 8-15 m of Late Wisconsin/Holocene right-lateral offset (Cox et al., 2001; 2006) and thus is an active fault.

Surface and subsurface geologic mapping of Lauderdale County has provided insight into the three-dimensional geology (Figure 10) and the Quaternary geologic history of the county. Of particular importance to the county's earthquake hazards are the seismic velocity structure of the underlying geologic strata, the recurrence intervals of New Madrid (Tuttle et al., 2002) and Lauderdale County faults (Cox et al., 2001; 2006), and the liquefaction potential of the Holocene floodplain sediments of the Mississippi, Hatchie, and South Fork of the Forked Deer rivers.



A



B

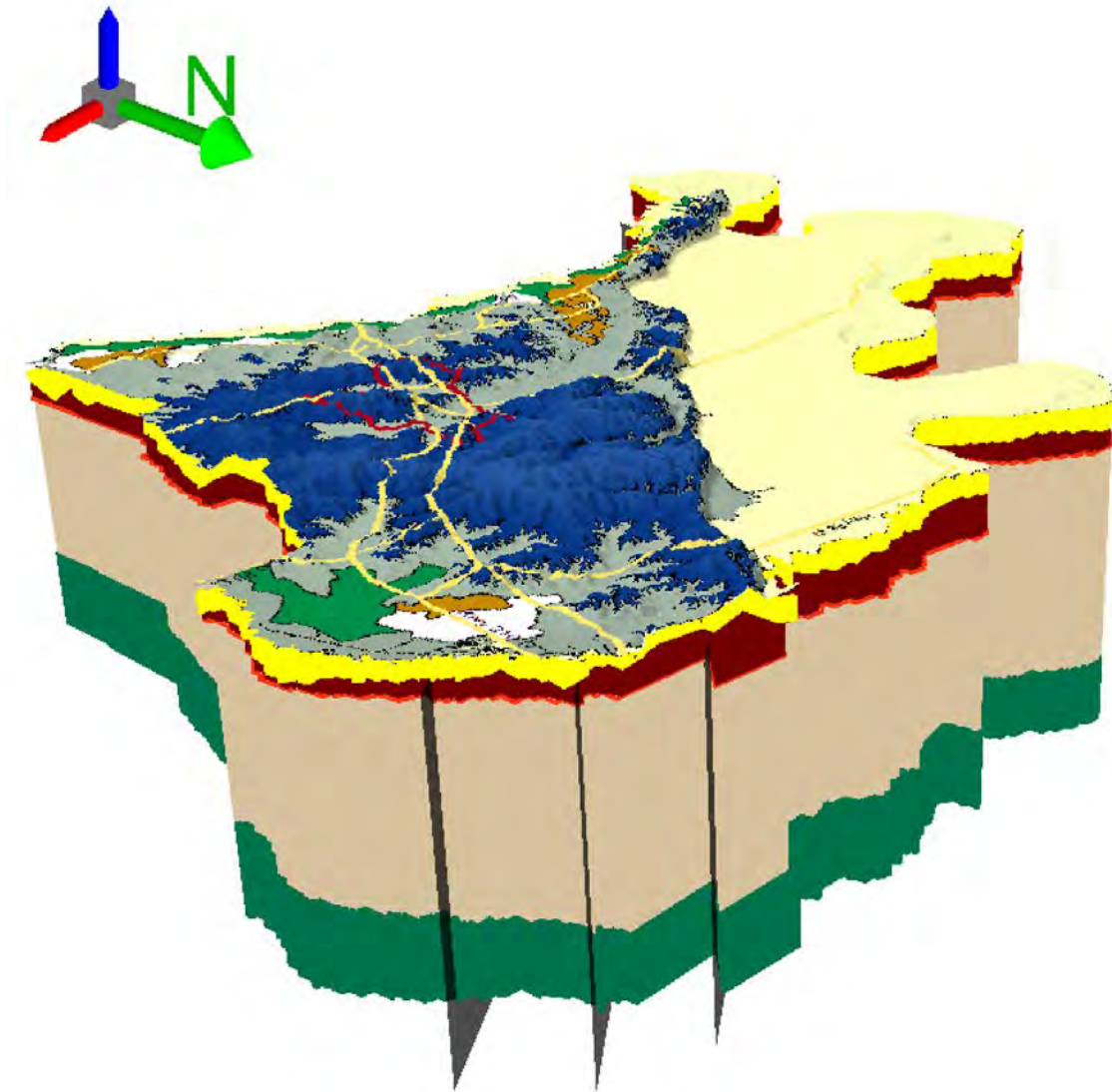


Figure 10: Three-dimensional perspective diagrams of Lauderdale County subsurface geology A) looking north, B) looking northeast, and C) looking southwest. Vertical exaggeration is 15X. The base of the models lay on Paleozoic strata, green is Cretaceous strata, tan is Paleogene strata, red line is top of Memphis Sand (base of Memphis Sand not mapped), brown is Eocene strata, yellow is Pliocene and Quaternary sediment. Gray vertical lines/panels are faults. Surface colors defined in Figure 3A. This model used a Projected Coordinate System for Transverse Mercator - WGS 1984 UTM Zone 16N. See Appendix for 3D video.

Geotechnical Model

Introduction

A summary of the geotechnical engineering investigations and analyses including subsurface data collection and conducted methodologies to develop liquefaction probability curves (LPCs) for Lauderdale County is provided in this section.

Data Collection

To perform liquefaction potential analysis, a series of subsurface data consisted of Standard Penetration Test (SPT) resistance or “N-value” and groundwater level (GWL) data were collected within Lauderdale County. The subsurface data collection process is summarized in the following sections.

SPT Data

A total of 350 SPT soil boring logs were received from the U.S Army Corps of Engineers (USACE) and a total of 250 boring logs from 69 projects were obtained from the Tennessee Department of Transportation (TDOT). To use SPT soil borings in the development of LPCs, specific criteria were utilized for selecting specific boring logs for using in the LPC analysis. The selection procedure for soil boring logs is provided next.

USACE SPT Data

At first, we selected the USACE boring logs based on the selection criteria used in developing the LPCs for the Lake and Dyer counties Seismic and Liquefaction Hazard Maps (Cramer et al. 2019, 2020). The selection criteria are:

- Borings must be at least 20 m (66 ft) deep.
- Borings must be completed with N-values and Unified Soil Classification System (USCS) soil classifications to a depth of 20 m (66 ft).
- The boring locations must have latitude and longitude coordinates.

To add more boring data in the database of developing LPCs, the second criterion was revised as follows:

- Borings with N-values and soil classifications to a depth of at least 15 m (50 ft) instead of the initial 20 m (66 ft) requirement

To extend the N-values and soil classifications to a depth of 20 m (66 ft), the following procedure, which is similar to the procedure used for Lake and Dyer counties, was utilized:

- Missing N-values for any depth at a given boring location was estimated by using the same N-value for a given N-value above or below the depth of the missing N-value if the overlying and underlying soil had the same soil classification.
- If the soil layers above and below the layer of missing N-value did not have the same classification or did not have N-value in a given boring, the N-value was extracted from the closest boring for the same classification and the same depth as classification and depth of the missing N-value.

The above selection criteria yielded data from 71 boring logs out of a total of 350 USACE soil boring logs, and incomplete data from 279 of the USACE boring logs were discarded. Figure 11 indicates the distribution of selected USACE boring logs within Lauderdale County. As shown in Figure 11, most boring locations are along the northwestern and western edge of Lauderdale County.

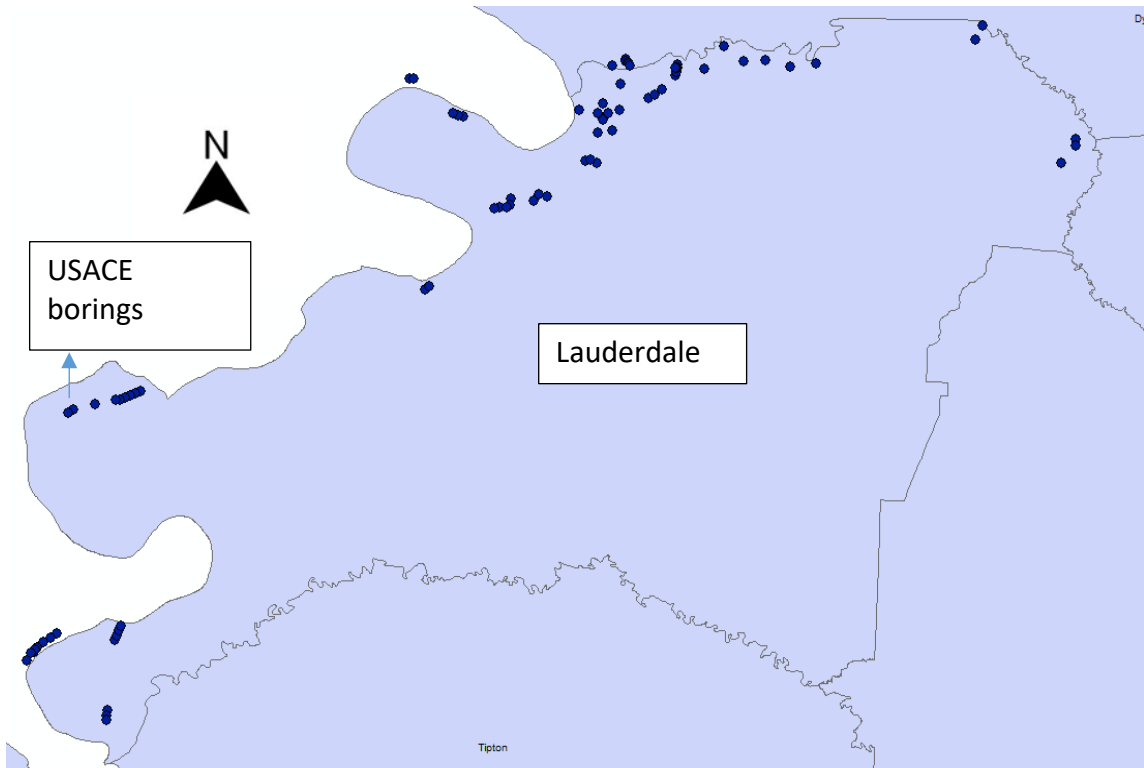


Figure 11: Locations of selected USACE SPT boring logs

TDOT SPT Data

A total of 250 SPT soil boring logs from 69 TDOT projects were received. As in Dyer County, the main issue with the TDOT boring logs in Lauderdale County was the unavailability of specific boring location coordinates. The TDOT projects had only a project general location map (without scale) or general project location description. Based on either the project location map or the general project location description, the coordinates of project locations were estimated using Google Map and Google Earth. The coordinate location of a project was used for all soil borings of a project to find the surface geologic unit of the borings and to estimate the groundwater level (GWL) of each boring based on the GWL contour map which will be discussed later in this report.

The TDOT borings were selected based on the same screening criteria utilized to select the USACE boring logs. A total of 39 TDOT projects that included a total of 138 boring logs were selected and added to the subsurface database of Lauderdale County to develop LPCs. For Lake and Dyer counties the majority of selected boring logs were obtained from the USACE. For Lauderdale County, most of the SPT boring logs were acquired from TDOT. Figure 12 shows the location of the 39 selected TDOT projects within Lauderdale County.

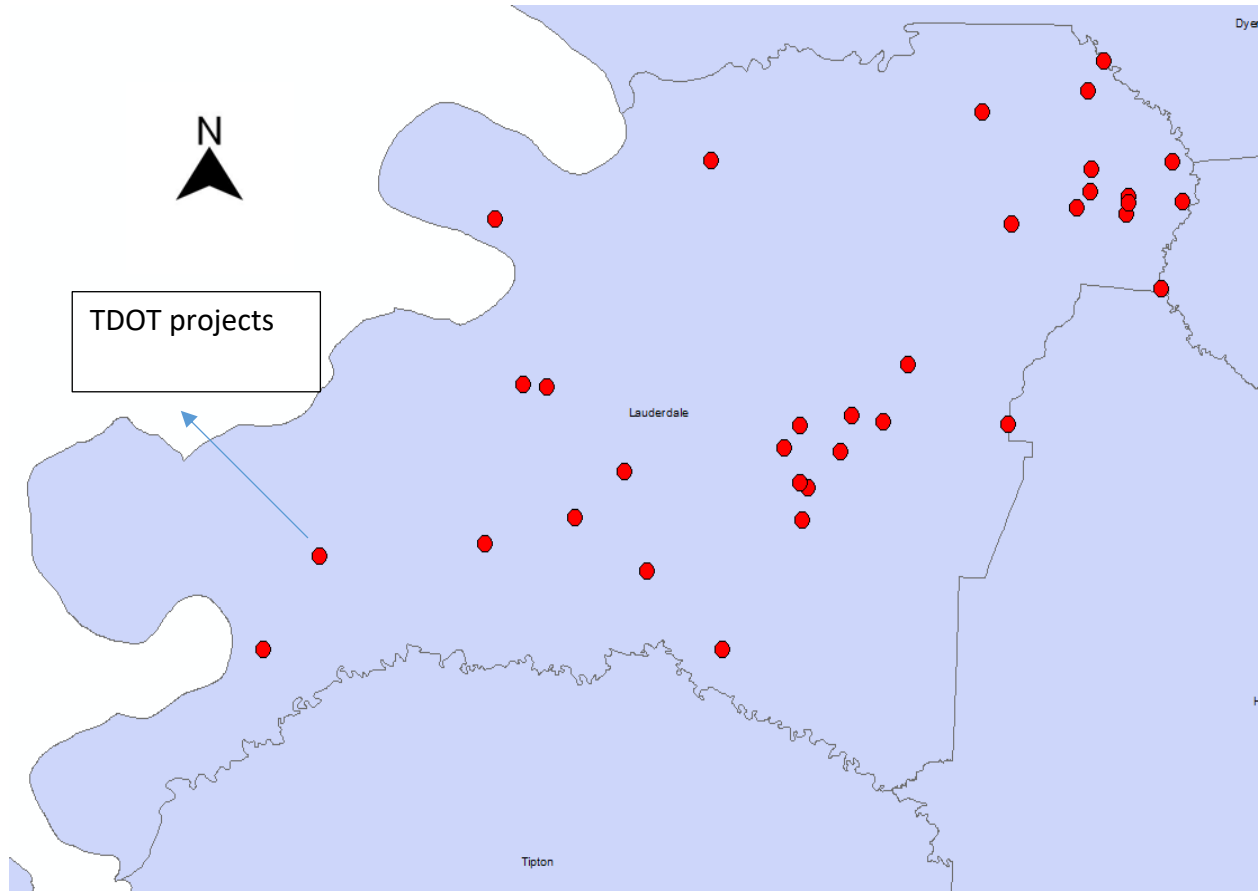


Figure 12: TDOT project locations

Classification of boring logs based on the surficial geologic units

Similar to Dyer County, Lauderdale County also consists of three primary surface geologic units: lowland (elevations below 80 meters), intermediate (elevation between 80 and 107 meters) and, upland (elevations above 107 meters). Figure 13 depicts the surface geology map of Lauderdale County.

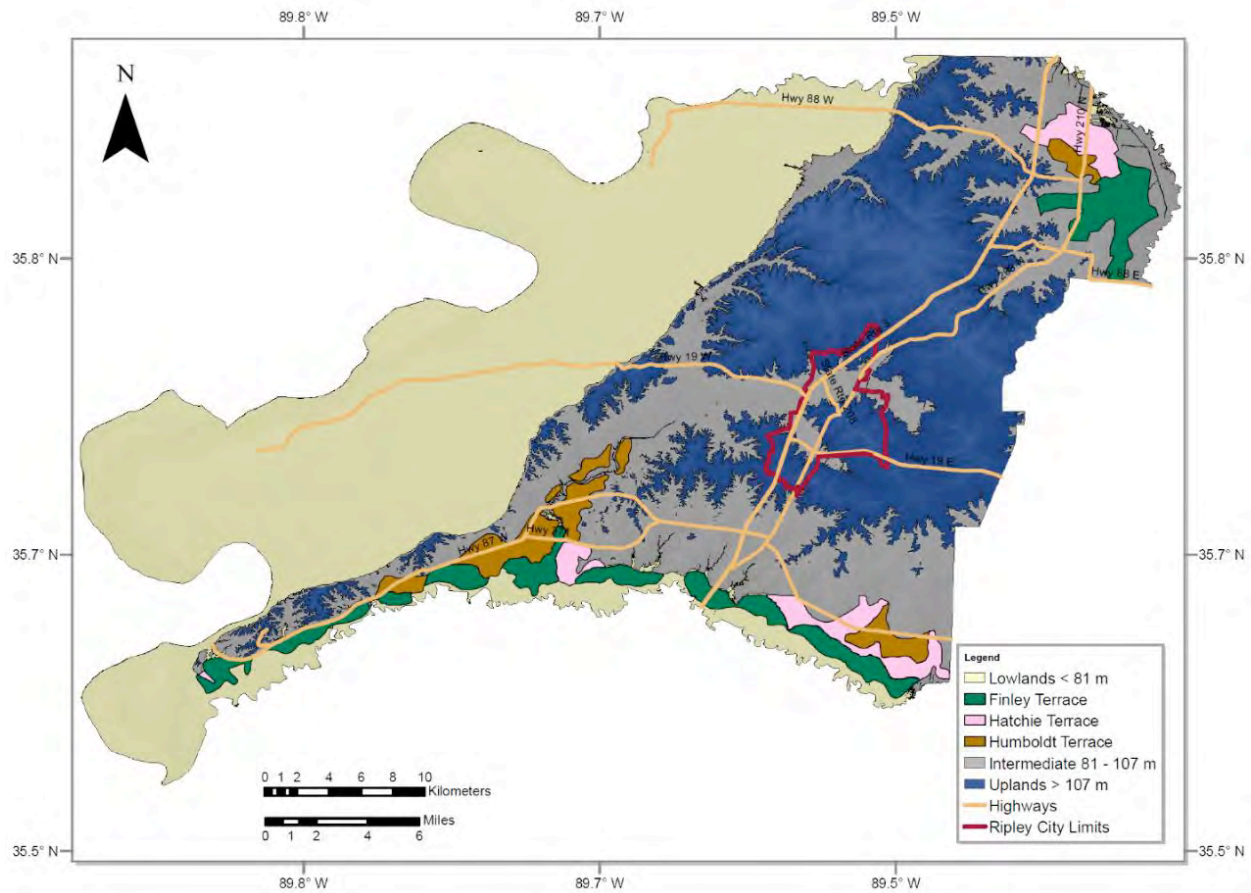


Figure 13: Surface geology map of Lauderdale County

To develop LPCs for each primary surficial geology units separately, the boring logs had to be classified for each surface geologic unit.

The distribution of selected borings from USACE and TDOT on the surface geology map of Lauderdale County is illustrated in Figure 14. Among the total of 209 boring logs selected from USACE and TDOT borings, 153 are in the lowland, 47 are in the intermediate, and 9 are in the upland parts of Lauderdale County. Table 1 provides a summary of the geological classification of boring logs.

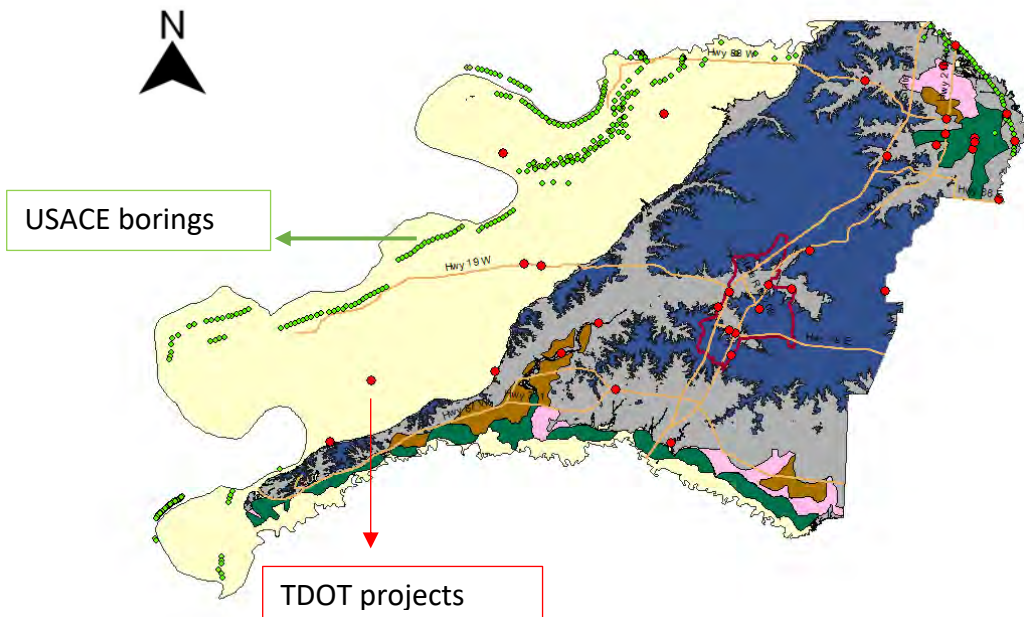


Figure 14: Soil boring logs location on the surface geology map

Table 1: Summary of the number of borings in each geology

	LOWLAND	INTERMEDIATE	UPLAND
TDOT	86	44	8
USACE	67	3	1
TOTAL	153	47	9

Groundwater data

To estimate the GWL at each soil borings location within Lauderdale County, we utilized the same procedure that was used for Lake and Dyer counties (Cramer et al., 2019, 2020). We established a GWL contour map for Lauderdale County based on the groundwater level contour map within the surface alluvial aquifer of the Mississippi Embayment developed by Schrader (2008) and published by USGS shown in Figure 15.

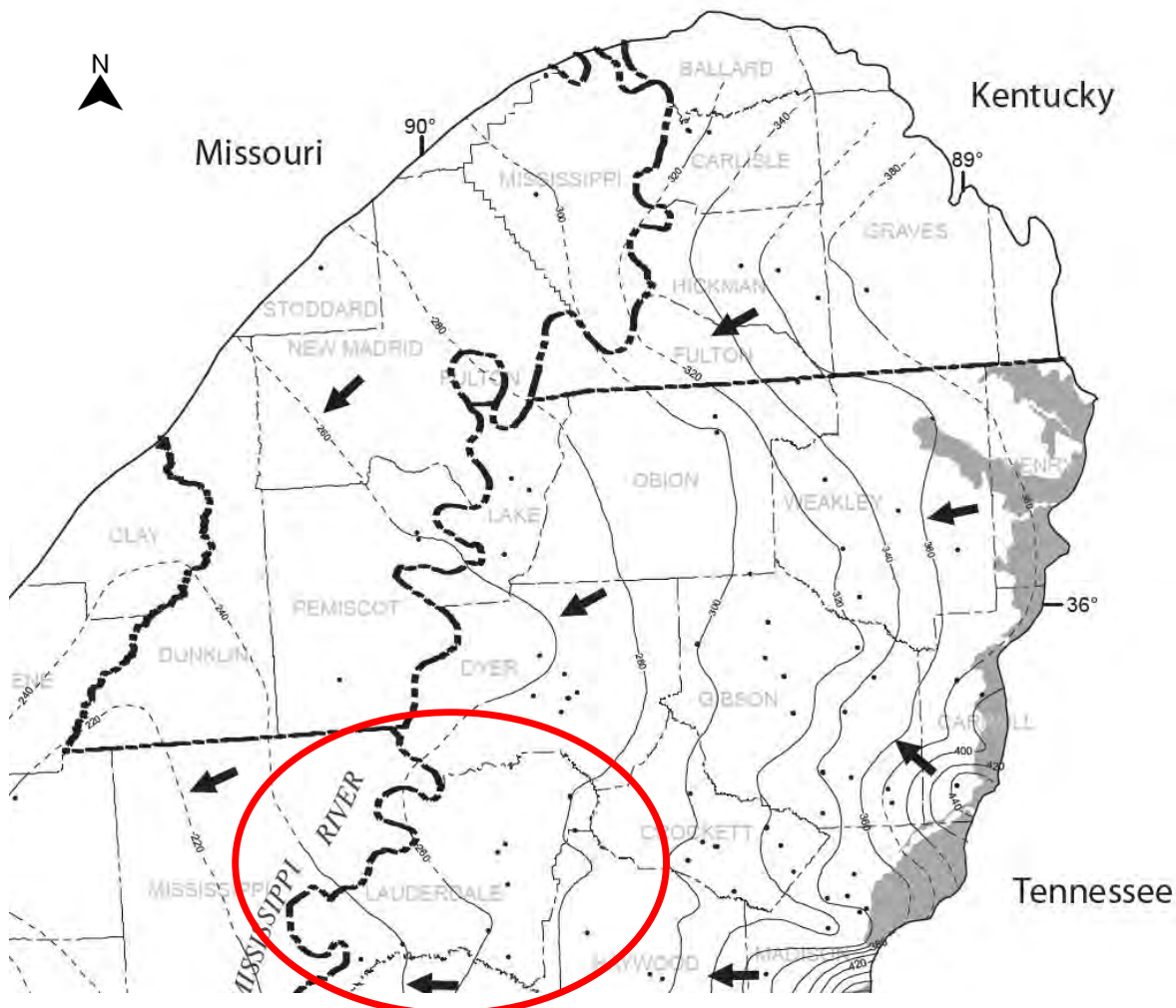


Figure 15: USGS groundwater level contour map (Schrader 2008)

To establish the GWL contour map that covers the entire area of Lauderdale County with an appropriate interval between the contour lines, we utilized the elevation contour lines of 200, 220, 240, 260, 280, and 300 ft from Schrader's map (Figure 15). These elevations are based on the National Geodetic Vertical Datum of 1929 (NGVD 29). The interpolated contour lines were imported in ArcMap and digitized on the 2D boundary shapefile of Lauderdale county. There are various tools to generate a contour map in ArcMap, however, to be consistent with Lake and Dyer counties, the Inverse Distance Weighting (IDW) tool was used to create the GWL contour map of Lauderdale County. Figure 16 indicates the generated GWL contour map of Lauderdale County in the format of a raster file.

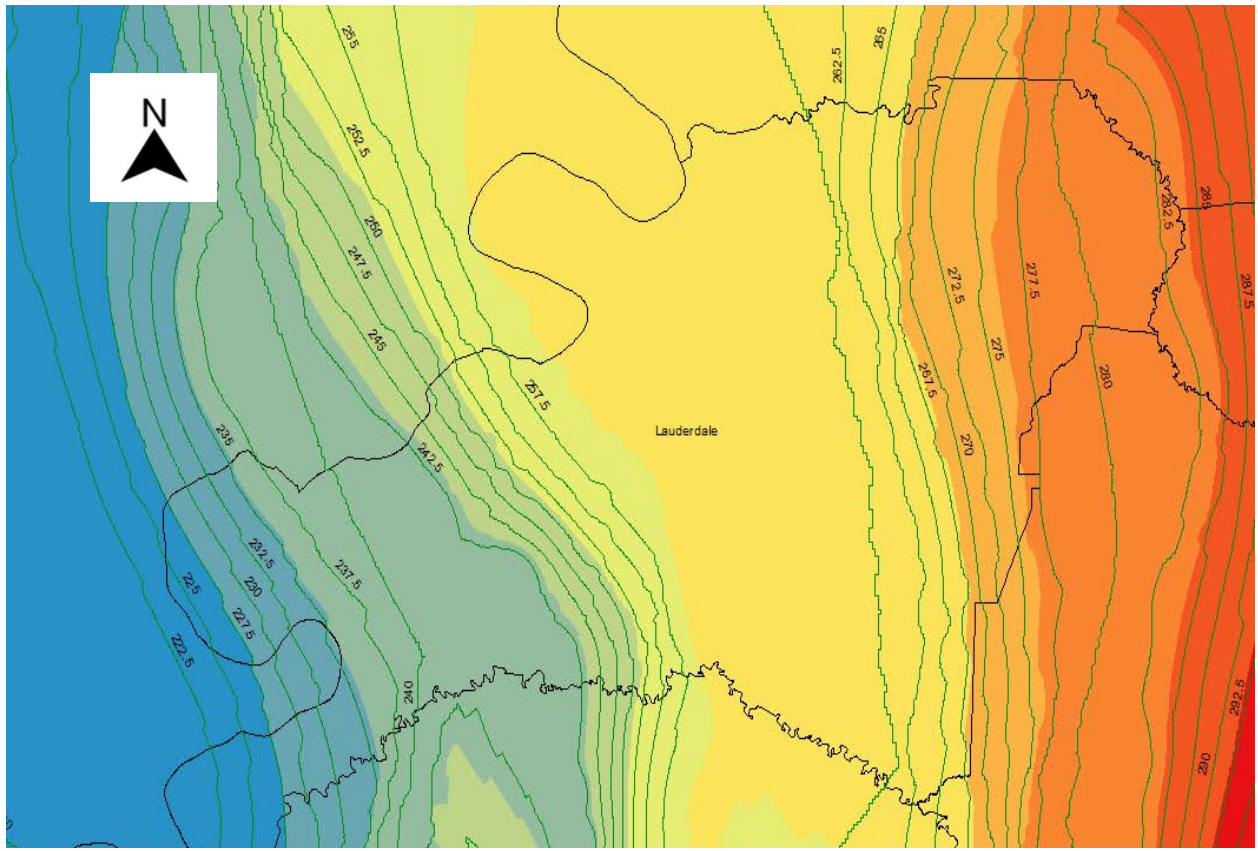


Figure 16: Groundwater level contour map for Dyer County

To verify the accuracy of the GWL contour map, additional groundwater data of nine water wells within Lauderdale County were obtained from the United States Geological Survey (USGS) groundwater data website (<https://maps.waterdata.usgs.gov>). Figure 17 shows the location of the USGS wells on the GWL contour map of Lauderdale County.

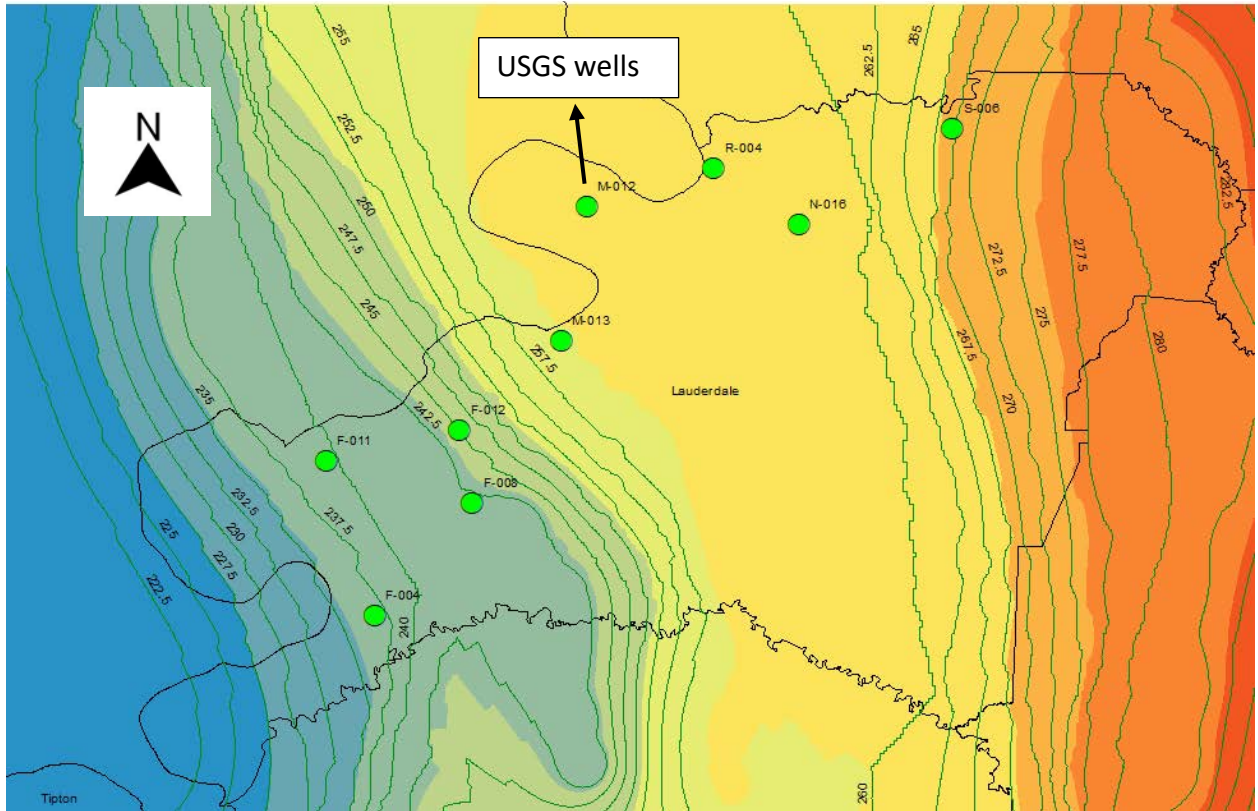


Figure 17: Location of USGS wells on the contour map of Figure 16.

We compared the interpolated GWL of wells from the contour map with the actual groundwater level of wells. As can be seen from Table 2, there is only a 4.5 ft. difference between the overall average of the actual level readings of the wells and the estimated water level obtained from the contour map. The geodetic datum of GWL data of the wells from USGS is NAVD 1988 and GWL contour map is in geodetic datum of NGVD 1929. Thus, the elevation difference between datums may be contributing to the difference between water well readings and the water level estimated from the contour map.

Table 2: Comparison of contour map level for USGS wells and the average of lowest and highest readings of wells

Well ID	Average Readings (ft-NGVD of 1929)	Contour Map (ft-NGVD of 1929)	Difference between contour map and wells readings (ft)
F-009	230	237	+7
F-004	240	237	-3
F-008	236	242	+6
F-011	238	239	+1
F-012	241	245	+4
M-013	252	258	+6
N-016	256	260	+4
M-012	251	260	+9
R-004	258	260	+2
S-006	265	270	+5

Methodologies Used to Develop Liquefaction Probability Curves

Using the same general procedure of developing LPCs used for Lake and Dyer counties (Cramer et al., 2019, 2020), we generated the LPCs of Lauderdale County. To develop the LPCs of Lauderdale County, the following three general main steps were taken:

1. Calculating the factor of safety (FS) against liquefaction at a given depth in the soil profile of each soil boring using the simplified procedure (Seed and Idriss, 1971).
2. Calculating the liquefaction potential index (LPI) of each soil boring location using:
 - o Iwasaki et al. (1978, 1982) method denoted as LPI method or,
 - o Maurer's (2015) framework denoted as LPI_{ISH} method herein.
3. Developing LPCs based on the LPI and the LPI_{ISH} methods for the probability of exceeding LPI of 5 and 15 for each primary surficial geologic unit

Unlike Dyer and Lake counties, the entire process of obtaining shear wave velocity (V_s) field test data could not be completed for Lauderdale County due to the COVID-19 situation. Thus, we did not perform a liquefaction potential analysis based on V_s data and the LPCs of Lauderdale County have been developed based only on SPT field test data. The procedure of developing LPCs based on SPT data for each geologic unit is described in the subsequent section.

Liquefaction Probability Curves Based on the Standard Penetration Test (SPT)

For Lauderdale County, the SPT data were employed to develop LPCs based on the LPI- and LPI_{ISH}-based methods. In both methods, the LPCs were developed for the same 10 earthquake Peak Ground Accelerations (PGA) of 0.1, 0.2, 0.3, 0.4, 0.5, 0.6, 0.7, 0.8, 0.9, and 1.0 and seven earthquake Magnitudes (M_w) of 5, 5.5, 6, 6.5, 7, 7.5, and 8 that we used in the Dyer County

study (Cramer et al., 2020). Thus, we determined the distribution of LPI and LPI_{ISH} for each of the 70 possible combinations of PGA and M_w using the same methodologies and equations that we utilized for Dyer County (Cramer et al., 2020).

Furthermore, using the same procedure as Lake County and Dyer County studies (Cramer et al., 2019, 2020), we computed the probability of exceeding liquefaction potential indices of 5 and 15, which are the lower bounds of “moderate” and “severe” liquefaction, respectively, based on the results of Iwasaki et al. (1978, 1982) and Toprak and Holzer (2003).

LPI-Based LPCs

Initially, the LPCs were developed based on the LPI approach in which it is assumed that all liquefiable layers contribute to the surficial manifestation of liquefaction without considering the impact of the non-liquefiable cap on liquefiable layers. LPI-based LPCs were generated for three surface geology units of lowland, intermediate and upland. For the lowland part of Lauderdale County, LPCs were developed based on SPT data of 153 soil borings while for the intermediate and upland the number of utilized soil borings was 47 and 9, respectively. Figures 18, 19 and 20 show the LPCs for lowland, intermediate and upland of the probability of exceeding LPI of 5 and 15 denoted as $P[LPI>5]$ and $P[LPI>15]$ versus the ratio of PGA over magnitude scaling factor (MSF).

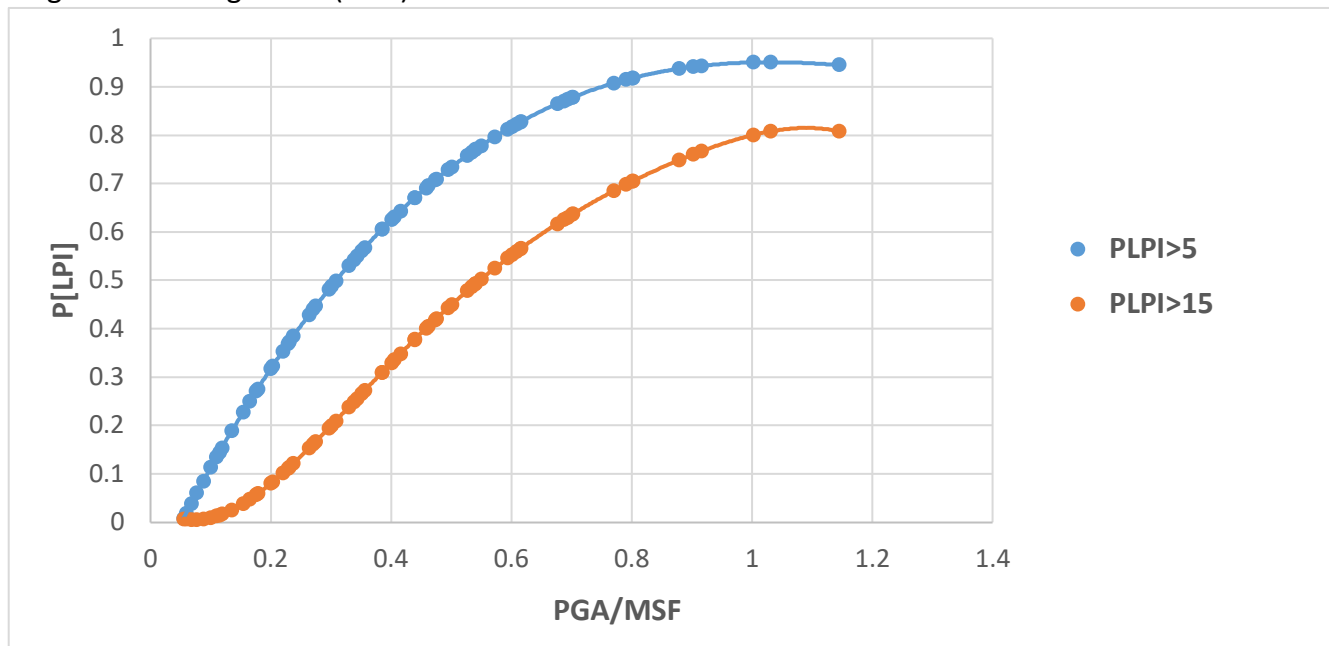


Figure 18: LPI-based lowland LPCs from SPT data

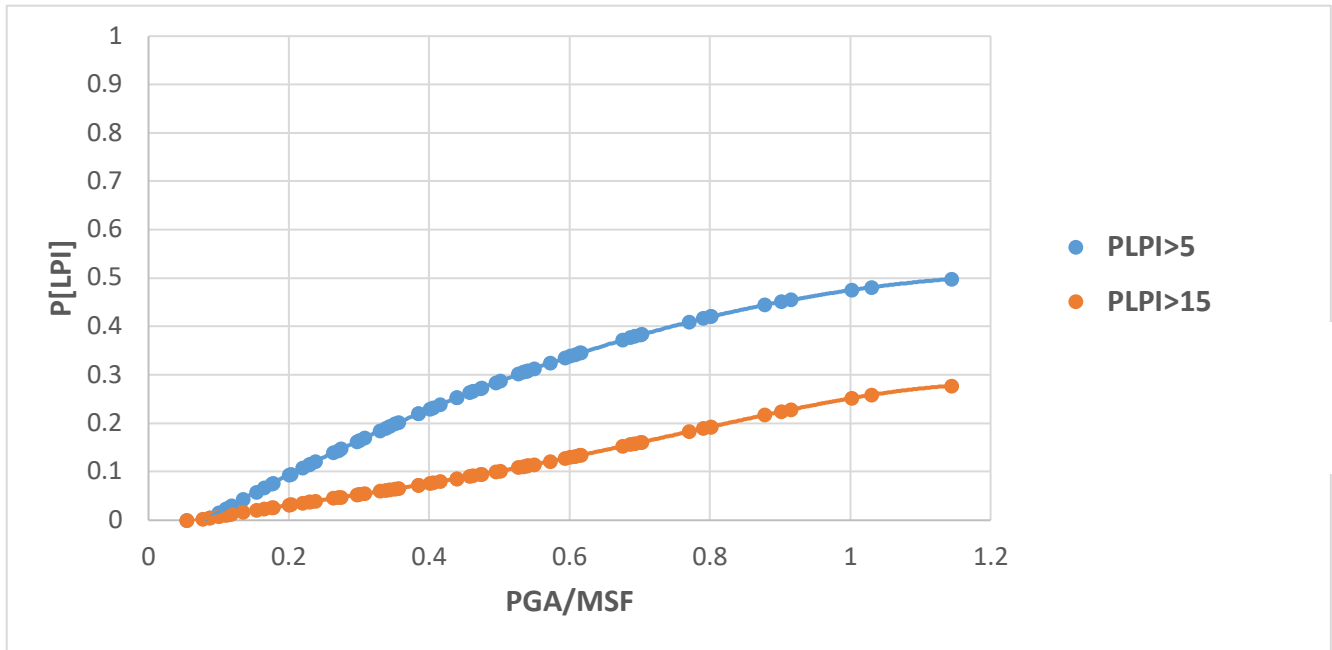


Figure 19: LPI-based intermediate LPCs from SPT data

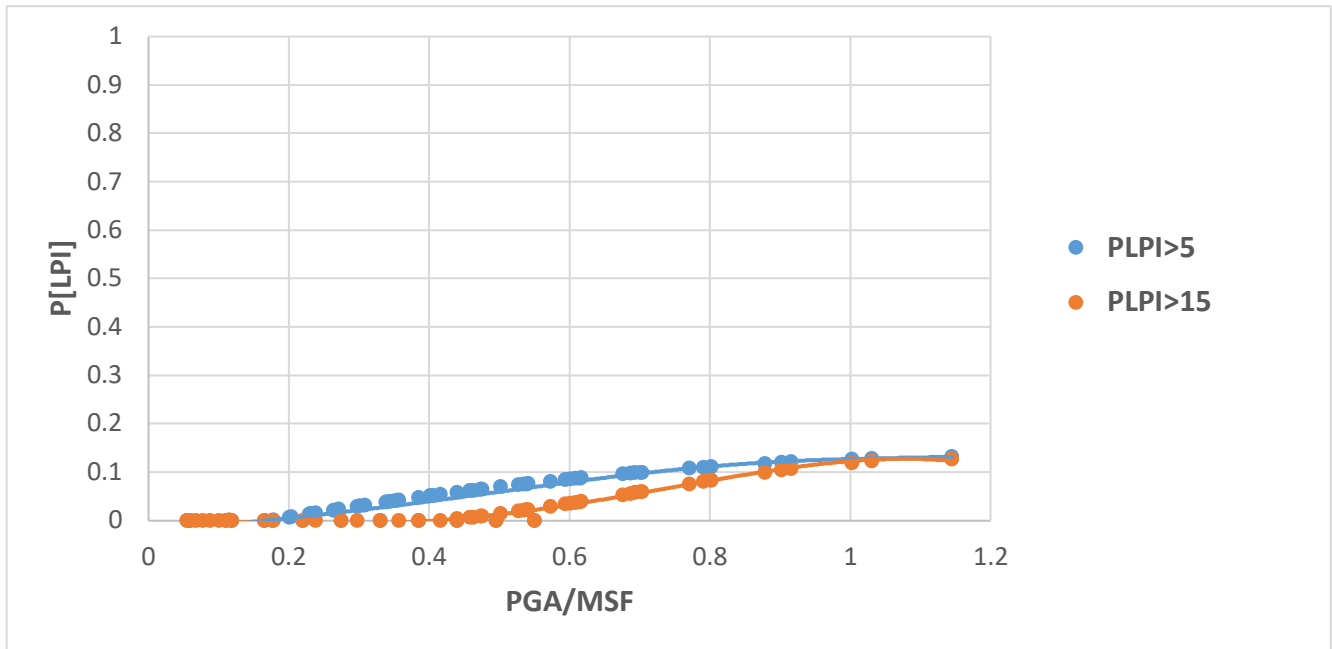


Figure 20: LPI-based upland LPCs from SPT data

As it was expected, the lowland LPCs are significantly higher than the intermediate and upland LPCs for both $P[\text{LPI}>5]$ and $P[\text{LPI}>15]$. Table 3 provides the maximum probability of exceeding $\text{LPI}>5$ and $\text{LPI}>15$ for each geologic unit that was observed from the LPCs at the highest ratio of PGA/MSF.

Table 3: the maximum probability of exceeding LPI>5 and LPI>15 at each geologic unit

The maximum probability of exceeding	Lowland	Intermediate	Upland
P[LPI>5]	0.94 (94%)	0.49 (49%)	0.13 (13%)
P[LPI>15]	0.8 (80%)	0.27 (27%)	0.12 (12%)

For Dyer County due to lack of having enough soil boring data within the intermediate and upland, the LPCs were developed for the lowland and non-lowland which was the combination of the intermediate and upland. For Lauderdale county also the boring log data of intermediate (47 borings) and upland (9 borings) were combined to develop the LPCs for the non-lowland parts of the county as shown in Figure 21. The maximum probability of exceeding LPI>5 and LPI>15 at the highest ratio of PGA /MSF for the non-lowland is 0.43 (43%) and 0.24 (24%), respectively. Therefore, compared to the intermediate only, the probability decreases and compared to the upland only the probability increases for both LPI>5 and LPI>15 when the soil boring data of intermediate and upland are combined.

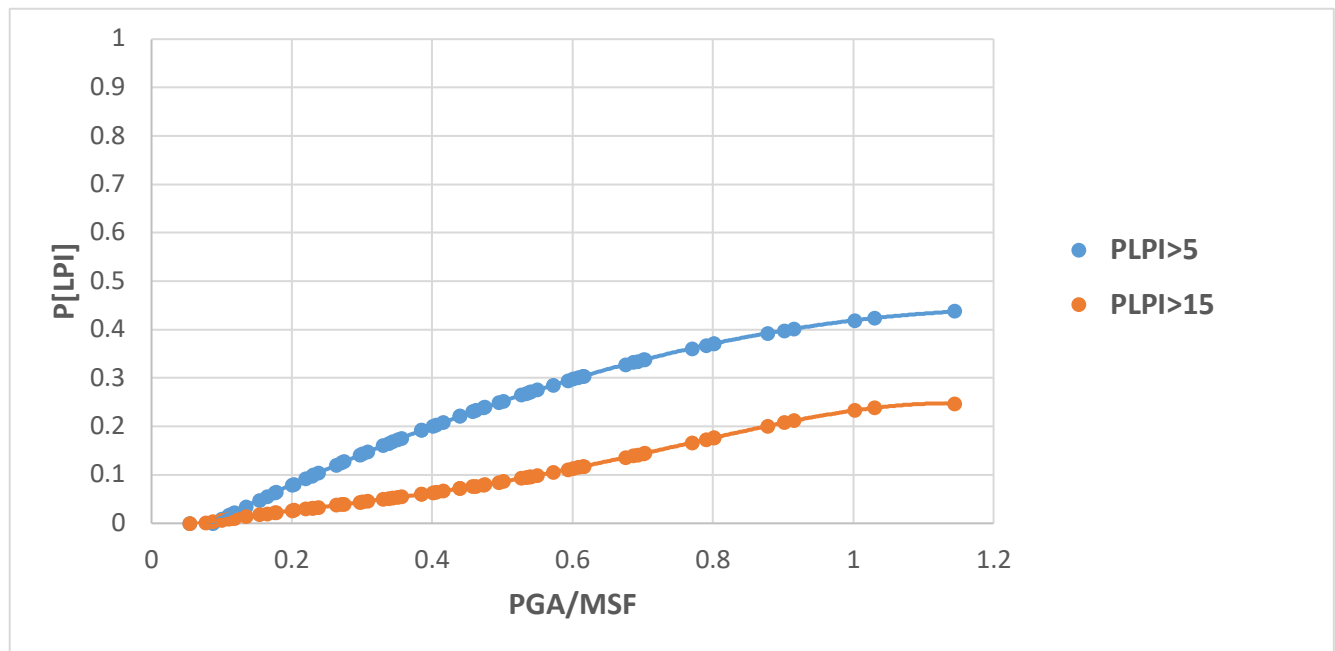


Figure 21: LPI-based non-Lowland LPCs from SPT data

LPI_{ISH}-Based LPCs

In addition to the LPI-based method of developing LPCs, the Maurer's (2015) framework which employs LPI of Ishihara (1985) (LPI_{ISH}) has been utilized to develop LPCs. Maurer's framework considers the influence near ground surface non-liquefiable layers on the surface manifestation of liquefaction. The detail of Maurer's framework is provided in the Seismic and Liquefaction Hazard Mapping of Dyer County report (Cramer et al., 2020).

Using Maurer's framework LPCs were generated for both lowland and non-lowland parts of Lauderdale County as they are shown in Figures 22 and 23, respectively.

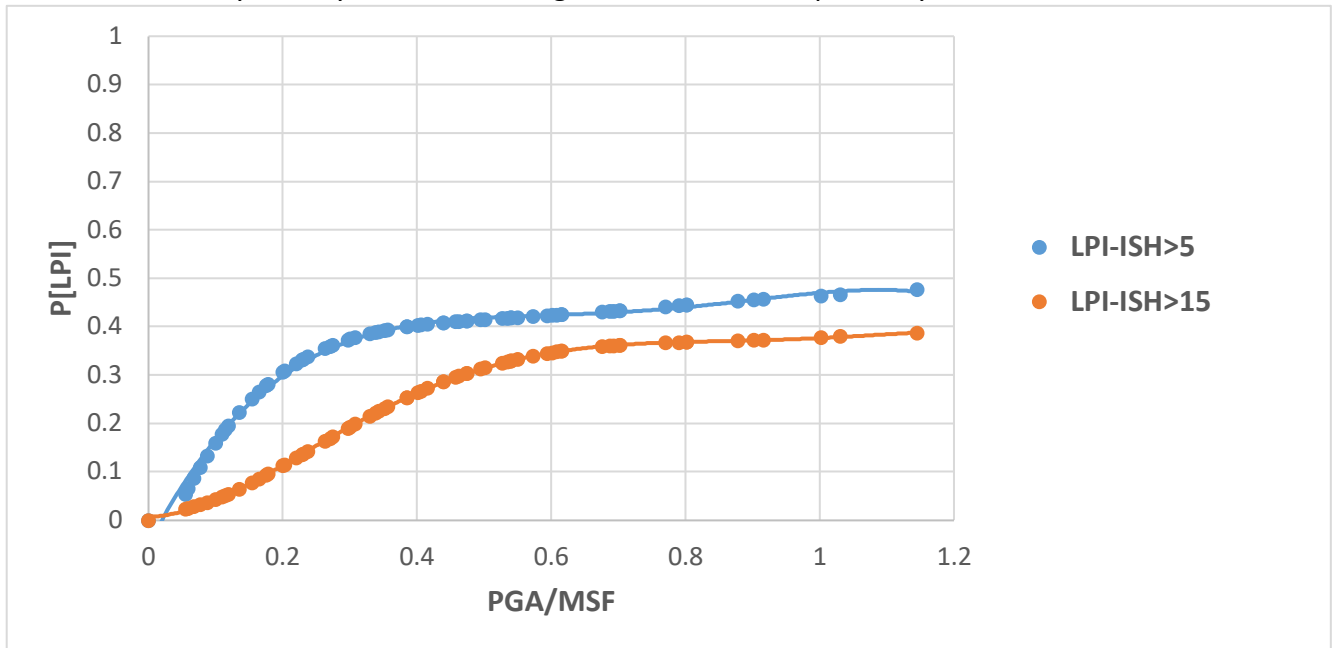


Figure 22: LPI_{ISH} based LPCs of lowland from SPT data

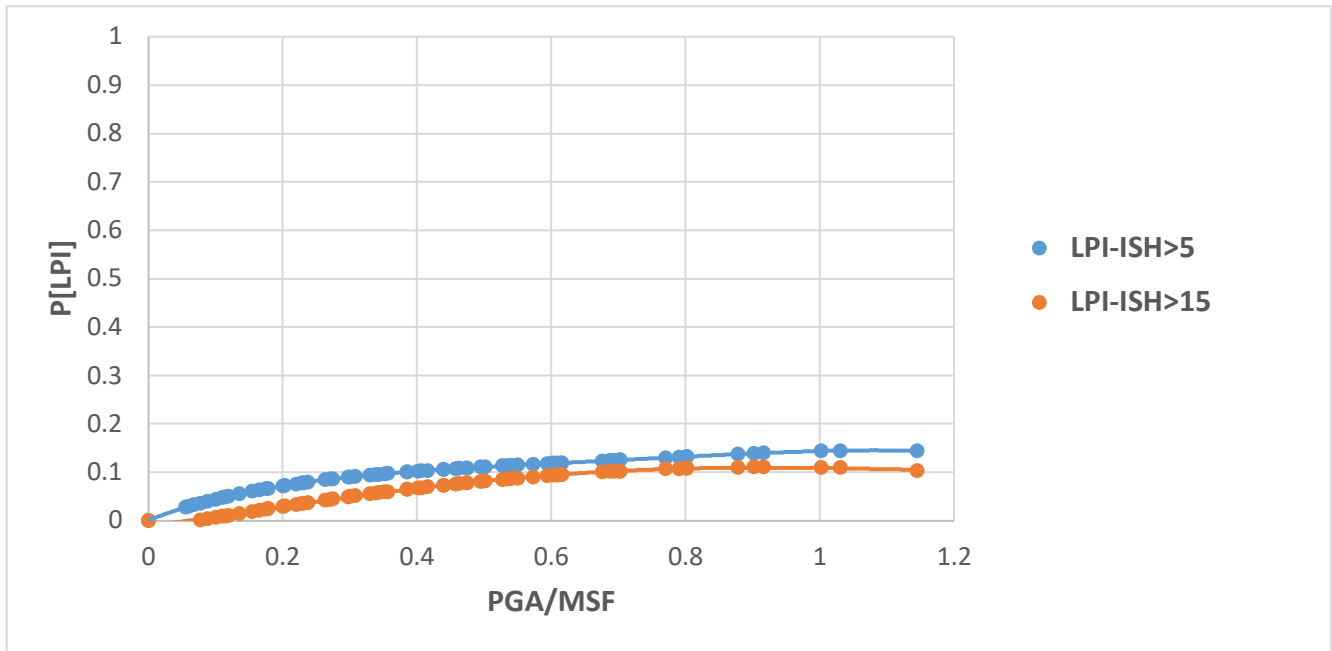


Figure 23: LPI_{ISH} based LPCs of non-Lowland from SPT data

Lowland LPI_{ISH}-based LPCs show higher trend than non-lowland LPI_{ISH}-based LPCs for both P[LPI>5] and P[LPI>15].

The results of the LPI- and LPI_{ISH}- based methods are compared and discussed in the next section.

Comparison of LPI- and LPI_{ISH}-based LPCs

For the lowland and non-lowland areas of Lauderdale County, the LPI- and LPI_{ISH}- based LPCs are compared in this section. Figures 24 and 25 provide a comparison of LPI- and LPI_{ISH}-based lowland LPCs for P[LPI>5] and P[LPI>15], respectively.

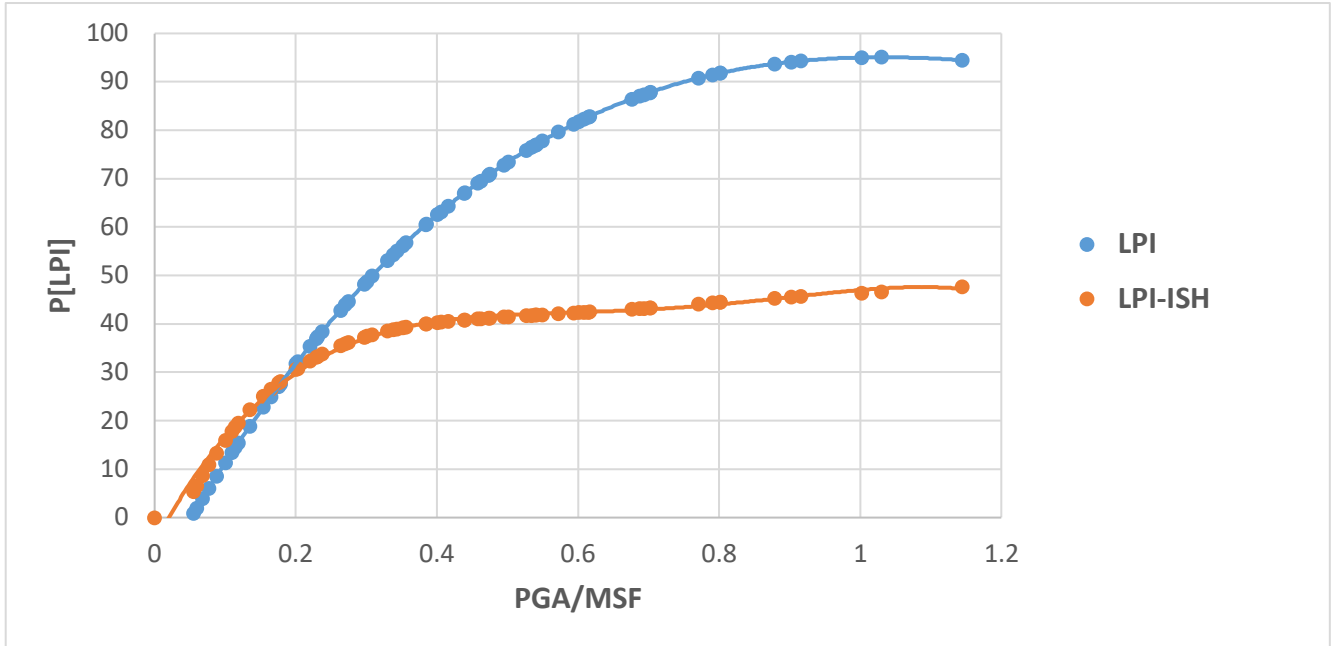


Figure 24: LPI- and LPI_{ISH}-based lowland LPCs for P[LPI>5]

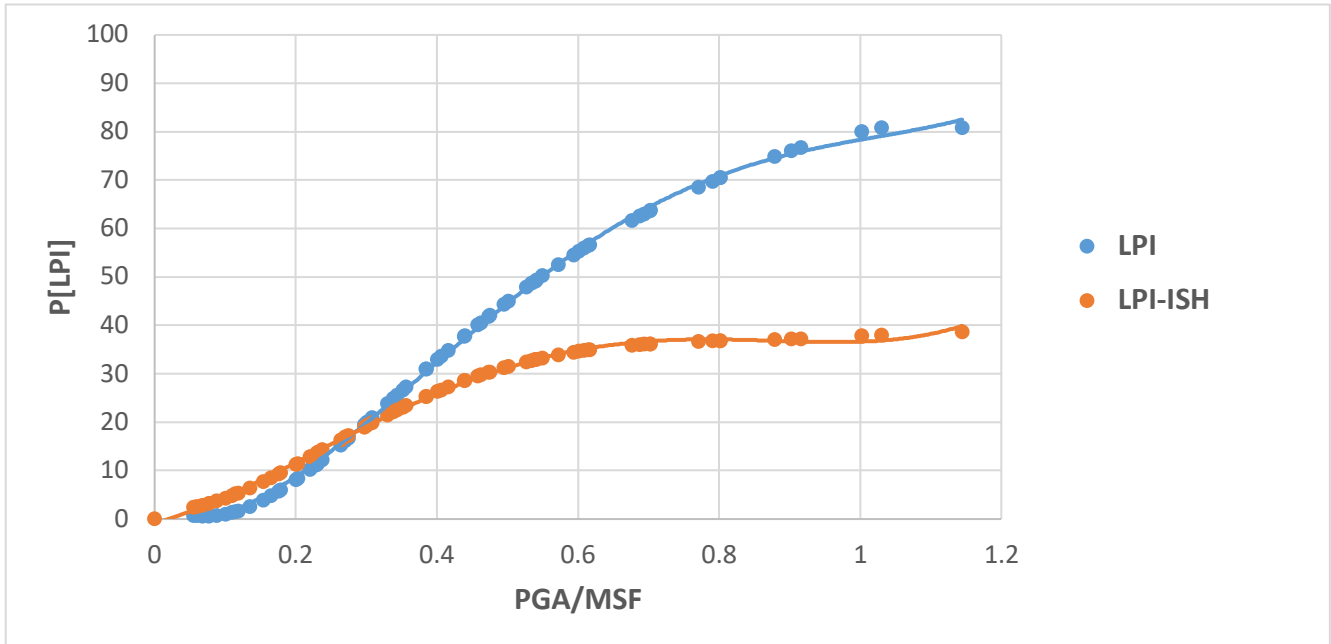


Figure 25: LPI- and LPI_{ISH}-based lowland LPCs for P[LPI>15]

Figure 24 indicates that the LPI_{ISH}-based LPC is significantly lower than LPI-based LPC especially for PGA/MSF ratios of higher than 0.25 and the maximum difference is about 45% for PGA/MSF

in the range of 0.6 to 1.2. For the severe probability of liquefaction ($P[LPI>15]$) as shown by Figure 25, the gap between LPI and LPI_{ISH} based LPC for PGA/MSF ratios of higher than 0.35 reaches to a maximum for PGA/MSF of 1.2 at which the LPI based LPC shows 80% probability of liquefaction while LPI_{ISH} based LPC shows 40% probability of liquefaction.

For the non-lowland parts of the county, the comparison between LPI and LPI_{ISH} based LPCs is shown in Figures 26 and 27. Similar to the results of the lowland areas, for the non-lowland areas the LPI_{ISH} based LPCs show lower probabilities than LPCs from the LPI method. However, the amount of difference between the LPCs of the two frameworks is less for the non-lowland than the lowland.

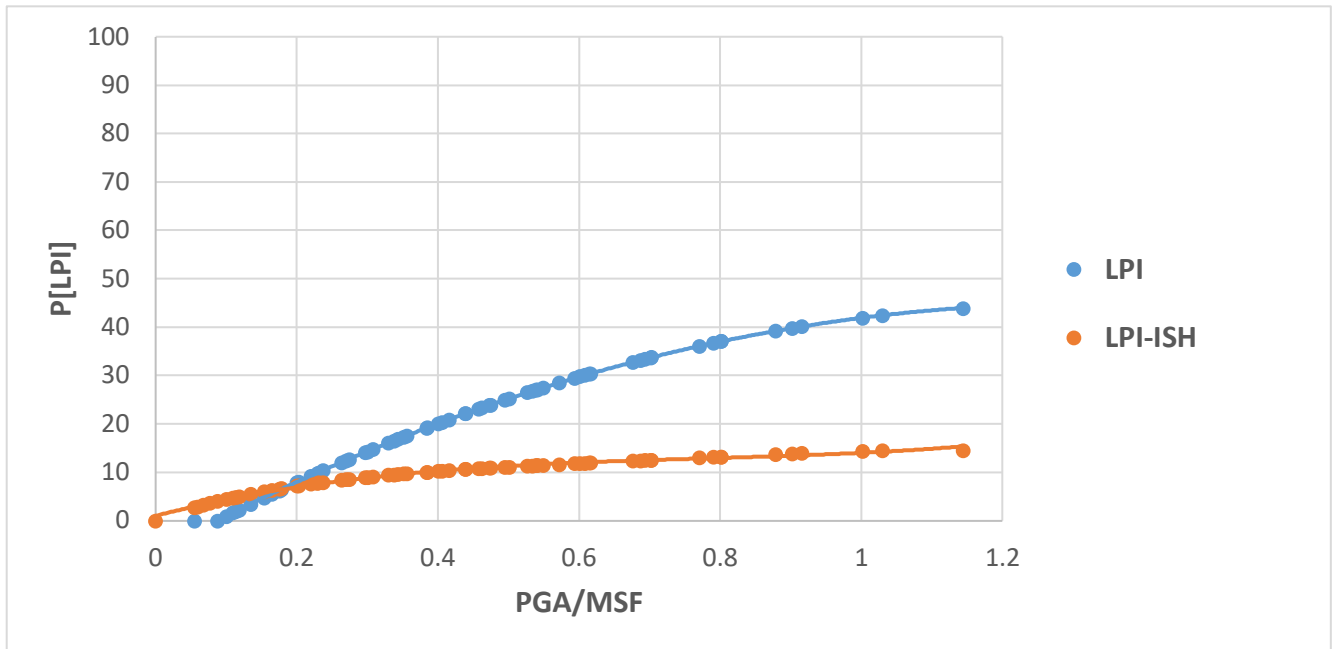


Figure 26: LPI- and LPI_{ISH} -based non-lowland LPCs for $P[LPI>5]$

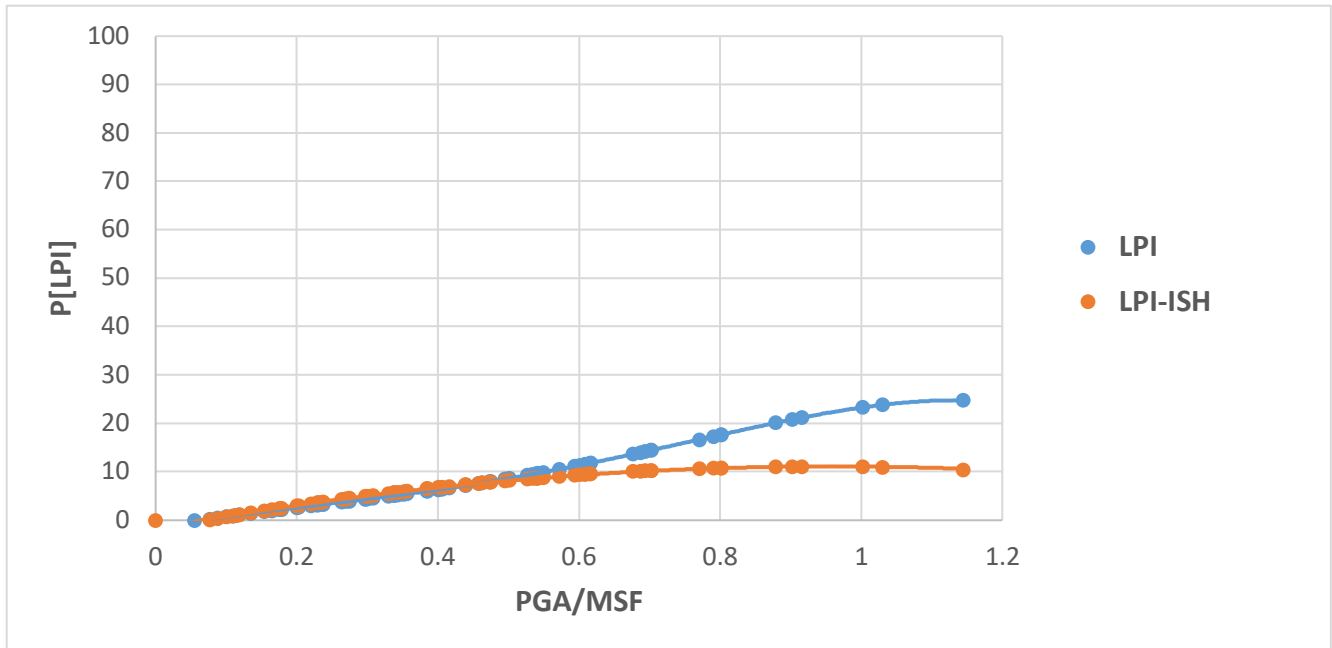


Figure 27: LPI- and LPI_{ISH}-based non-lowland LPCs for P[LPI>15]

Figure 26 depicts that both LPCs are showing the same probability in the range of 0 to 0.2 PGA/MSF while for PGA/MSF higher than 0.2, LPI-based LPC reaches to 45% probability for PGA/MSF of 1.2 for which the LPI_{ISH} LPC is showing a probability of 15%.

The least amount of difference between the LPCs of two methods is for the non-lowland severe probability of liquefaction as shown in Figure 27. For 0 to 0.6 PGA/MSF both LPCs show the same probability and they have a different trend of probabilities of liquefaction for the range of 0.6 to 1.2 PGA/MSF ratios. The maximum amount of difference is for PGA/MSF of 1.2 that LPI LPC shows 25% probability of liquefaction and LPI_{ISH} LPC shows a 10% probability of liquefaction.

In summary, the LPCs based on the LPI_{ISH} method provide lower probabilities for liquefaction than the LPCs based on the LPI method because the LPI_{ISH} method incorporates the effect of near ground surface non-liquefiable layers on liquefaction surface manifestation and the LPI method does not.

Liquefaction Probability Curves Based on the Shear Wave Velocity (Vs)

For Lauderdale County, due to time overlap with COVID-19 situation, the geophysics team was not able to conduct shear wave velocity tests at more than three sites, hence, we could not perform liquefaction potential analysis based on Vs data.

LPCs for liquefaction hazard maps of Dyer County

This section discusses the recommended LPCs for lowland and non-lowland parts of Lauderdale County that are utilized to generate liquefaction hazard maps. For Lauderdale County, because

there was not enough V_s profile data available within lowland and non-lowland geologic units, the LPCs were developed only based on the SPT borings data of USACE and TDOT.

Lowland LPCs Recommendation

For the lowland surface geology part of Lauderdale County, the LPCs were developed using SPT data of 153 borings based on Iwasaki's LPI method and LPI_{ISH} of Maurer's framework for $P[LPI>5]$ and $P[LPI>15]$. As described in the Comparison of LPI- and LPI_{ISH} -based LPCs section of this report, because Maurer's framework considers the impact of non-liquefiable layers on the surficial manifestation of liquefaction, the Maurer's framework-based LPCs show significantly lower probability of liquefaction than LPI-based LPCs. Therefore, it is suggested that the liquefaction hazard maps of the lowland part of Lauderdale County be based on the LPCs of both frameworks of Iwasaki and Maurer as presented in Figures 18 and 22, respectively.

Non-lowland LPCs Recommendation

For the non-lowland surface geology part of Lauderdale County, the LPCs were developed using SPT data of 56 borings based on Iwasaki's LPI method and LPI_{ISH} of Maurer's framework for $P[LPI>5]$ and $P[LPI>15]$. Similar to the lowland part of the County, for the non-lowland parts, it is suggested that the liquefaction hazard maps of the lowland part of Lauderdale County be based on the LPCs of both frameworks of Iwasaki and Maurer as presented in Figures 21 and 23, respectively.

Geotechnical summary

We used the same general procedure to develop LPCs that we utilized to develop the Dyer County LPCs (Cramer et al., 2020). However, unlike Dyer County where the LPCs were developed based on SPT-N as well as V_s profile data, in Lauderdale County due to the COVID-19 situation the procedure of conducting V_s tests could not be completed and the LPCs were developed based only on the SPT-N data.

Similar to Dyer County, the surficial geology of Lauderdale County consists of three primary units of lowland, intermediate, and upland. The LPCs of Lauderdale County were developed based on Iwasaki's LPI methodology that was utilized to develop the LPCs of Shelby County (Cramer et al., 2015; Cramer et al., 2018a) as well as Lake County (Cramer et al., 2019) and Dyer County (Cramer et al., 2020). The LPI-based LPCs of lowland, intermediate and upland parts of the county are provided in Figure 18, 19, and 20, respectively. For each geologic unit, the LPCs are shown for $P[LPI>5]$ and $P[LPI>15]$ which represents the "moderate to severe" and "severe" probability of liquefaction, respectively.

For Dyer County, because the most SPT-N boring data was available from the lowland and insufficient boring data to develop LPCs was available from the intermediate and upland parts of the County, we combined the boring data of these two geologic units to represent the non-lowland parts of Dyer County. Therefore, to be consistent with Dyer County, we also combined

the SPT data from intermediate and upland areas to represent the non-lowland parts of Lauderdale County. The LPCs of non-lowland for $P[LPI > 5]$ and $P[LPI > 15]$ are provided in Figure 21.

Similar to Dyer County (Cramer et al., 2020), the LPCs of Lauderdale County were also developed based on Maurer's (2015) framework which employs the procedure of Ishihara (1985) referred herein as LPI_{ISH} method. The Maurer framework includes the impact of near ground surface non-liquefiable layers on liquefaction manifestation at the ground surface. Figures 22 and 23 illustrate the LPCs obtained using the LPI_{ISH} method and based on the SPT boring data for the lowland and non-lowland areas, respectively. For both the lowland and non-lowland areas of Lauderdale County, the probability of liquefaction provided by the LPCs based on the LPI_{ISH} framework are lower than the LPCs based on the LPI framework especially at higher ratios of PGA/MSF as shown in Figures 24-27 because the LPI_{ISH} method incorporates the effect of near ground surface non-liquefiable layers on liquefaction surface manifestation and the LPI method does not.

For the lowland parts of Lauderdale County, it is suggested that the liquefaction hazard maps be based on both LPI- and LPI_{ISH} -based LPCs developed from SPT data of 153 soil borings. For the lowland parts of Lauderdale County, the LPI- and LPI_{ISH} -based LPCs are presented in Figures 18 and 22, respectively. For the non-lowland it is recommended that the LPCs of LPI and LPI_{ISH} based approaches that were developed based on the SPT data of 56 boring logs within the intermediate and upland parts of the county be used to develop liquefaction hazard maps. The non-lowland LPI- and LPI_{ISH} -based LPCs are provided in Figures 21 and 23, respectively.

Seismic Measurements

Introduction

Multichannel Analysis of Surface Waves (MASW) is a geophysical exploration technique that measures shear-wave velocity of underground layers using the dispersion of surface waves along an array of geophones. The MASW seismic survey obtains velocity structure of the layers using surface waves.

The seismic refraction method is sensitive to low velocity layers. If low velocity layers are not detected, the results of seismic refraction may be compromised, while seismic reflection can detect geological features not seen in refraction tests. Geophysical exploration at shallow depths (less than 50 meters) can be a challenge. Invasive procedures such as downhole and crosshole seismic surveys can be expensive. Non-invasive procedures such as MASW can be advantageous and economical and can be a viable alternative.

In the MASW method, an array of geophones captures the surface waves that are generated by an energy source such as a sledgehammer or a heavier source (Figure 28). The changes in amplitude and arrival times are measured using a post-processing software at different

frequencies (e.g., SurfSeis, developed by Kansas Geological Survey, KGS). These “changes” are associated with the dispersion of surface waves. Complicated propagation of surface waves has unique characteristics that can relate the amplitude of surface waves with shear-wave velocity, depth, and frequency. In a few words, amplitude (and consequently, velocity) of a certain frequency of surface waves (phase velocity) is affected by the shear-velocity structure of the ground down to certain depths. This combination provides us with valuable information called dispersion curves, which is a plot of phase velocity versus frequency. Figure 29 shows the amplitude variation of surface waves with respect to wavelength, which is the normalized depth on the vertical axis and normalized motion (amplitude at depth z over amplitude at surface) on the abscissa. As shown in Figure 30, longer wavelength (or lower frequencies) can sample larger depths.

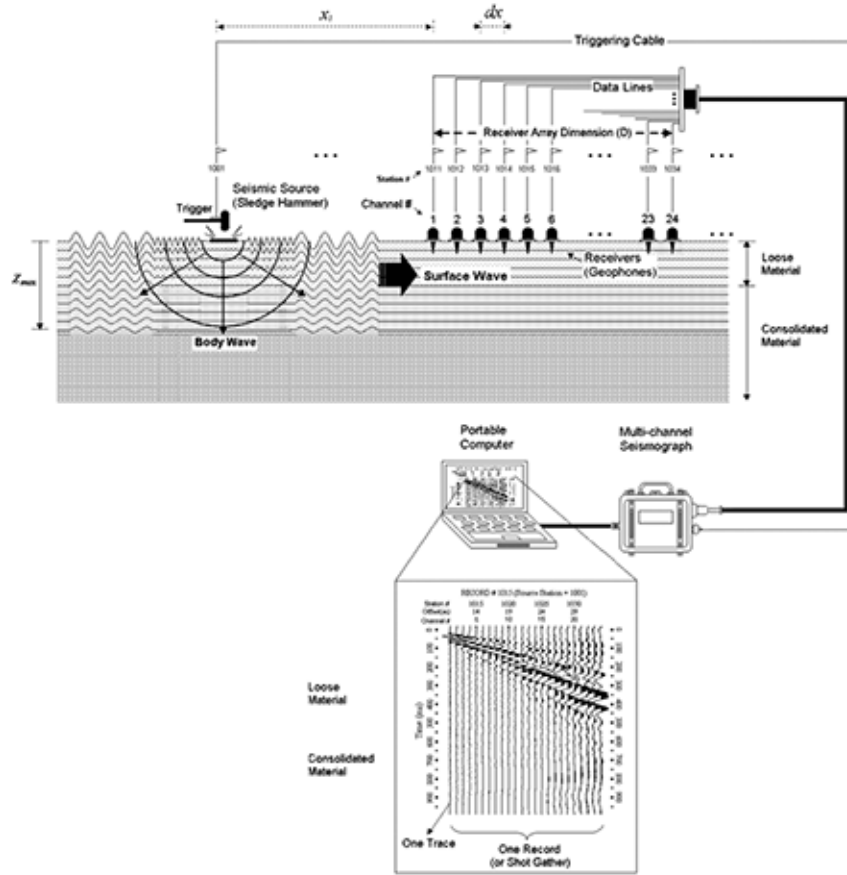


Figure 28: Active MASW test setup. (from KGS.ku.edu).

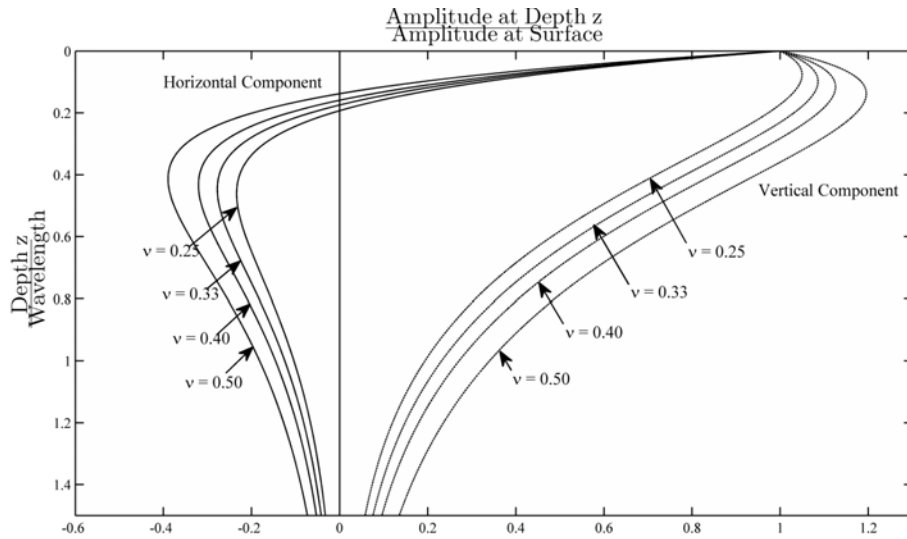


Figure 29: Variation of horizontal and vertical normalized components of displacements induced by Rayleigh waves with normalized depth in a homogeneous isotropic, elastic half-space.

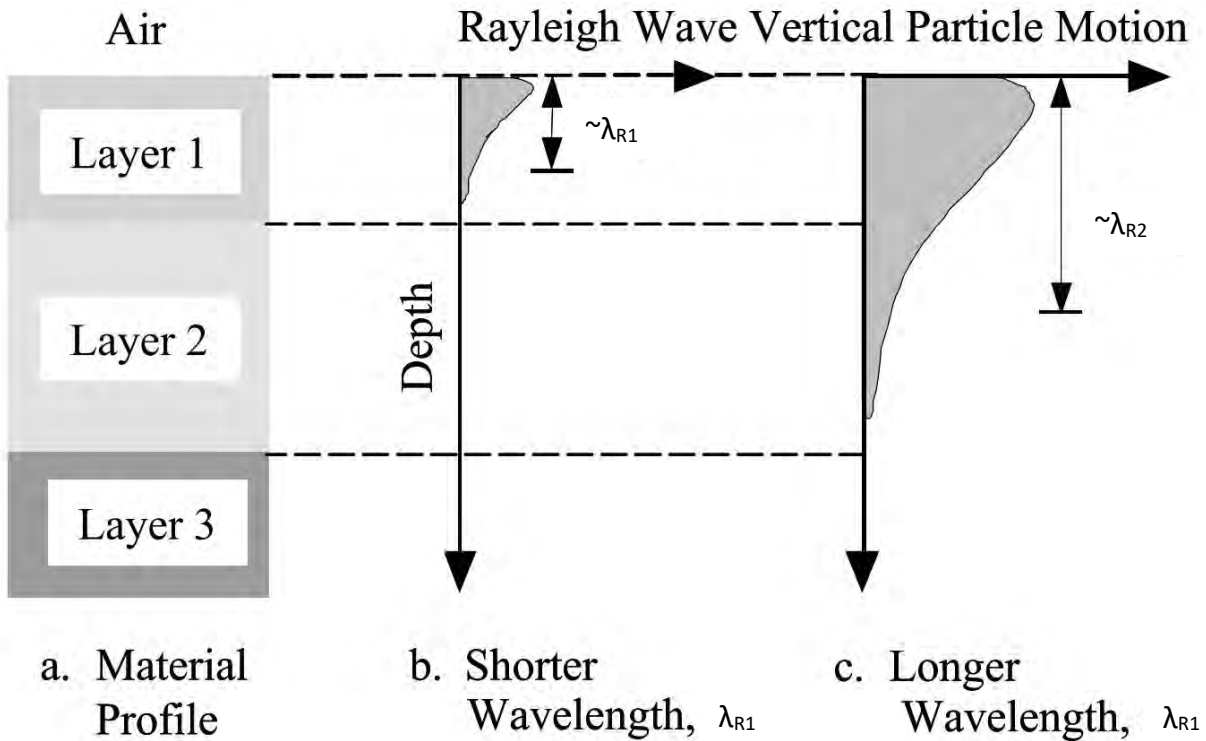


Figure 30: Depth sampled by Rayleigh waves with different wavelengths (Stokoe II and Santamarina, 2000).

Finally, through an iterative inversion process using the SurfSeis software, the best matching velocity profile is obtained. It is important to mention that the inversion process may produce

several shear-wave velocity profiles with similar dispersion curves matching the experimental dispersion curve which is referred to as the non-uniqueness of the inversion process. There are some provisions embedded in the software that can remove irrelevant velocity profiles. Also, geological studies and prior expert knowledge can help mitigating the non-uniqueness issue.

MASW Equipment and Testing procedure

In all the sites that we performed MASW survey in 2019 (6 in the Lauderdale County and 3 in Dyer County), we used a 144 m linear array of 72 4.5 Hz geophones with 2 meters of spacing between geophones. Our active energy source was a Propelled Energy Generator (PEG – Figure 31). This device has a 40 kg mass that is driven down using an elastic band, which is stretched using the motor mounted on the device. The energy produced by quick drop of the weight was experimentally considered enough for the entire length of the array plus a 16m offset from the first geophone.

We started shooting at a 16 m offset from the first geophone and advanced every 4 meters through the middle of the spread. Each location was shot three times. Several shots per location can help reduce the effects of noise by stacking the records. Stacking will average out the noise and enhance the main signal, to reach a higher signal to noise ratio.

To obtain deeper velocity structures (e.g., lower frequency range) we recorded ambient noise using the Refraction Microtremor (ReMi) seismic survey. An array of 24 geophones with 10 ft spacing was placed at the same location and several 32s second records of data was acquired multiple times. The dispersion curve obtained using the MASW seismic survey was augmented with the dispersion curve points obtained by the ReMi procedure to better estimate the shear-wave velocity of deeper layers of the soil structure. We used the SeisOpt ReMi software to process data collected using the ReMi seismic survey.



Figure 31: Propelled Energy Generator used as an Active Source.

Data Processing

Data processing is performed using the SurfSeis software. The recordings were analyzed to obtain the “Overtone Images” (Figure 32). In Figure 32 and 33, the vertical axis is the phase velocity in m/sec and the horizontal axis is the frequency. The dispersion curves were automatically picked, and visually checked. Furthermore, the dispersion curve obtained using the ReMi procedure were combined with the MASW dispersion curve as shown in Figure 33. In some cases, dispersion curves from MASW is augmented with ReMi at low frequencies to obtain information at greater depths. Then, the dispersion curves were inverted to obtain the shear-wave velocity profile associated with the site. In Figure 33, the orange curve is the high energy (the middle of the overtone image from ReMi analysis) and the gray curve is the lower energy curve (the lower margin of the overtone image). The lower limit of the apparent phase velocities can be recognized as the true phase velocities (Louie, 2001).

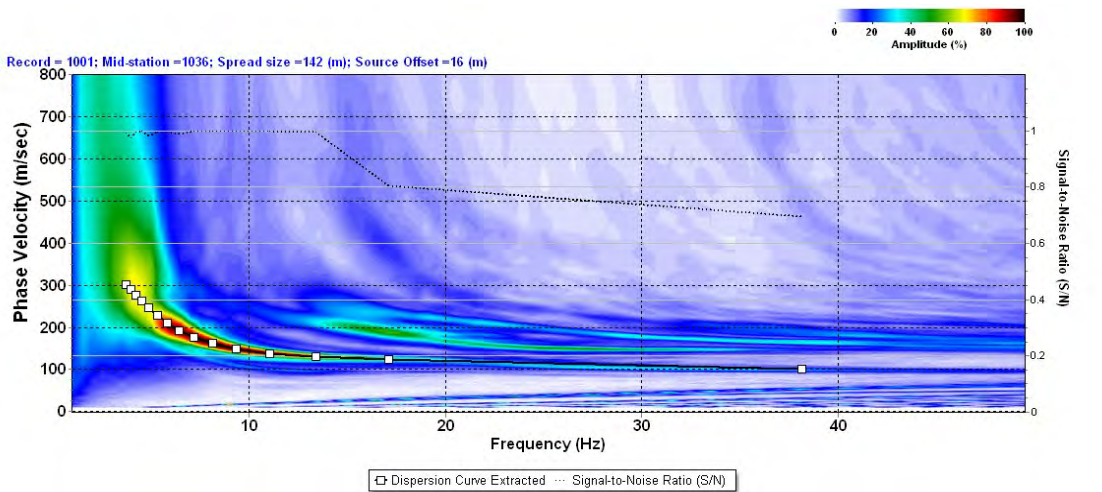


Figure 32: A sample of the dispersion curve obtained by the Surfseis Software.

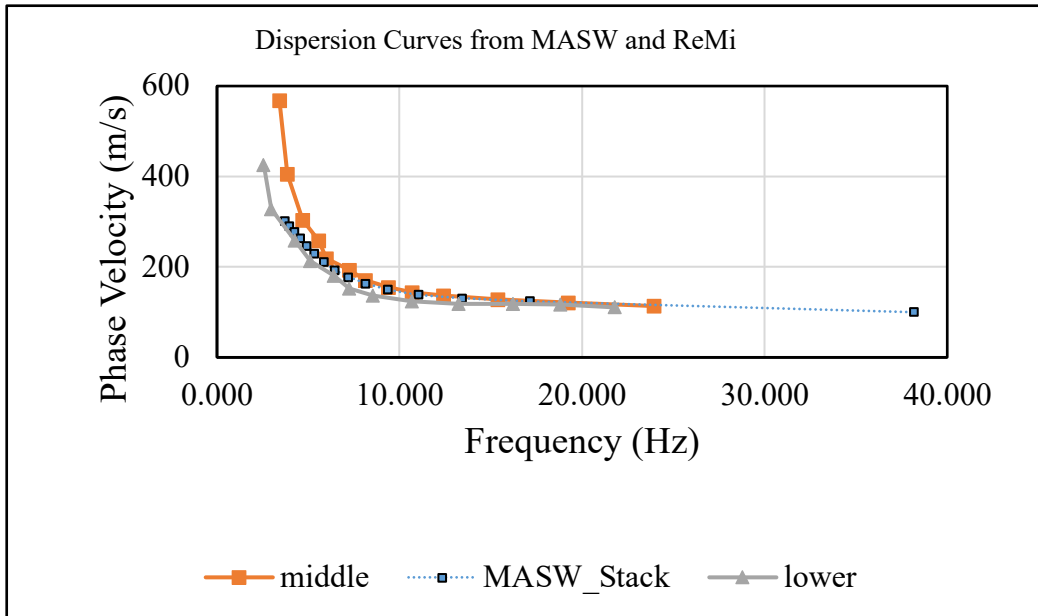


Figure 33: Comparison of dispersion curves obtained with MASW and ReMi.

Depth of investigation is proportional to the largest wavelength captured by the instruments (Schuler, 2008).

$$\text{Depth of Investigation} = 0.4 \times \text{Wavelength} = 0.4 \times \text{Velocity} / \text{frequency}$$

Depth of investigation depends on a few parameters.

- Corner frequency of the geophones, which was 4.5Hz in our case that is a widely and practically used device for surface exploration methods.
- Energy source. The energy source should be strong and capable of generating enough low frequencies.
- Velocity of subsurface soil. The faster the velocities, the greater depth we can measure.
- Noise in the area. A noisy location can obscure wave motion at long distances, where the wave has attenuated.

Results

The final results of the 9 MASW and ReMi 2019 seismic surveys (Figure 34) in Lauderdale and Dyer Counties are summarized in this section (Figure 35). We were able to obtain shear-wave velocity profiles to depths of about 30m to 70m. Previously we developed a representative non-lowlands velocity profile with depth from 12 MASW profiles recorded in 2018 (Cramer et al., 2020). Our studies in Lake (Cramer et al., 2019), Dyer (Cramer et al., 2020), and Lauderdale (this

report) Counties confirms that the MASW procedure can estimate down to 50m depth with acceptable accuracy. Data quantity does not support the reliability and accuracy at depths higher than 50m. In general, uncertainty increases with depth. In some cases, we included higher modes into our inversion process to enhance the resolution of the velocity profiles. Although, the estimated depth of the velocity profile is only dependent on the wavelength (frequency) of the modes, meaning that including higher modes does not increase the depth of conversion. Yet, the benefit of recognizing higher modes is to increase the resolution of the profile and decreasing the uncertainty of the inversion process.

Figure 36 presents the mean and standard deviation of the velocity profiles with depth at 20 MASW non-lowlands measurement sites in Dyer and Lauderdale Counties (see Cramer et al., 2020 for details concerning the Dyer County MASW measurements). The 20 measurements were broken down into 8 intermediate, 7 terrace, and 5 uplands sites and average velocity profiles determined separately for each group of MASW profiles. In Figure 36 it is clear that these three non-lowlands group average profiles cluster close together and seem distinct from the Lake County representative lowlands profile (Cramer et al., 2019). The representative Dyer County non-lowlands profile is also shown following the intermediate, terrace, and uplands average velocity profiles. Thus, only a lowlands and non-lowlands representative profile, with their uncertainties, are needed for seismic hazard calculations in Lauderdale County.

We compare in Figure 37 the two Lauderdale County representative velocity profiles with the uplands average profile of Romero and Rix (2001) and a representative uplands site velocity profile for Shelby County. At shallower depths less than 20 m, the uplands profiles agree quite well. In Lauderdale County the top of the faster velocity Eocene sediments can be as shallow as 20 m or less, which can start biasing the MASW profiles to faster velocities especially below 30 m. In Lauderdale County in the non-lowland areas, the top of the Eocene is typically 30 m. A check of the estimated depth to the top of the Eocene at MASW sites from the geology model with the depth at which the V_s exceeds 500 m/s (estimated Eocene V_s) in the MASW profiles shows a fairly good correlation both in Dyer and Lauderdale Counties.

Lauderdale Co MASW Sites

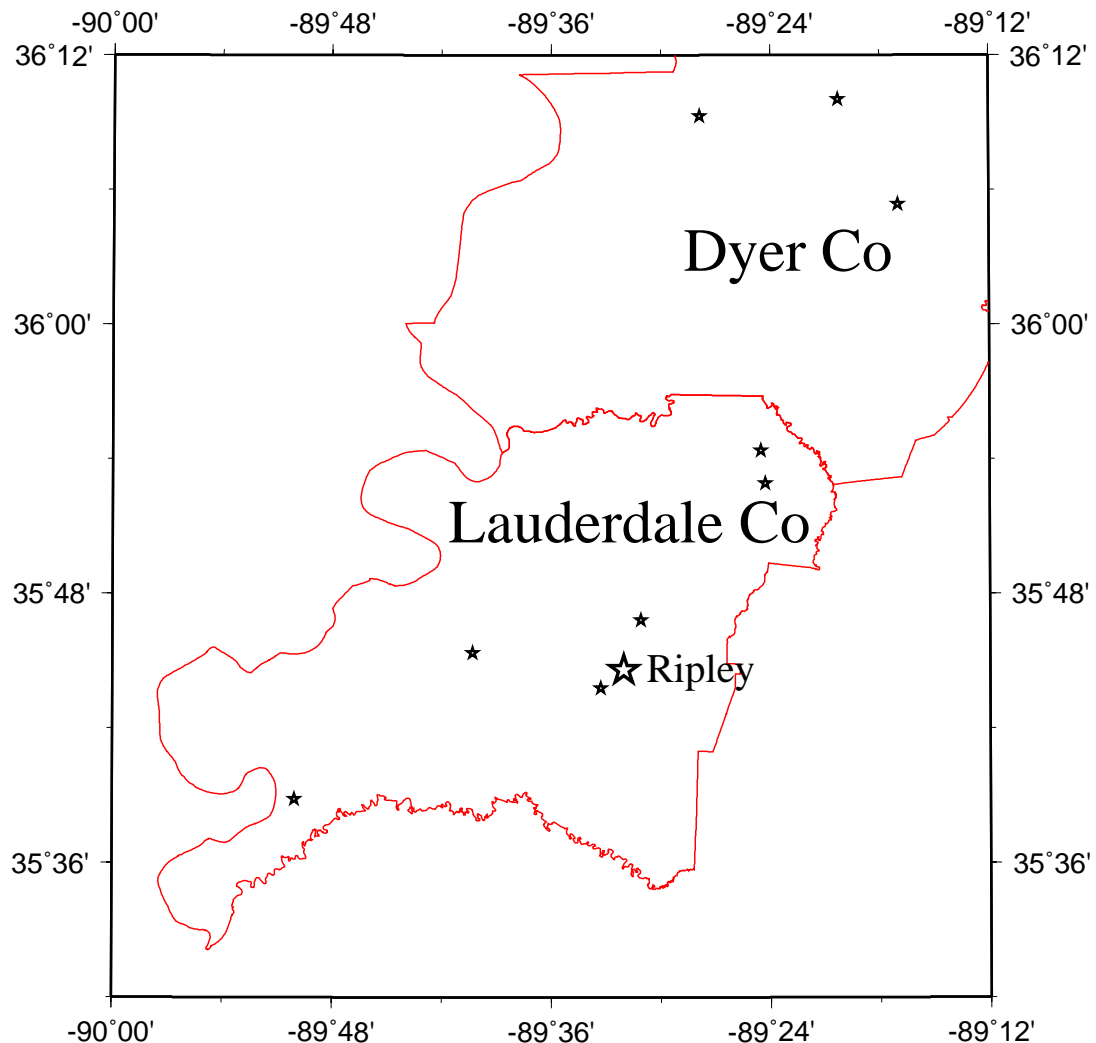


Figure 34: Location of MASW measurements (filled stars) in Lauderdale and Dyer Counties (red outline).

Lauderdale Co Vs Profiles

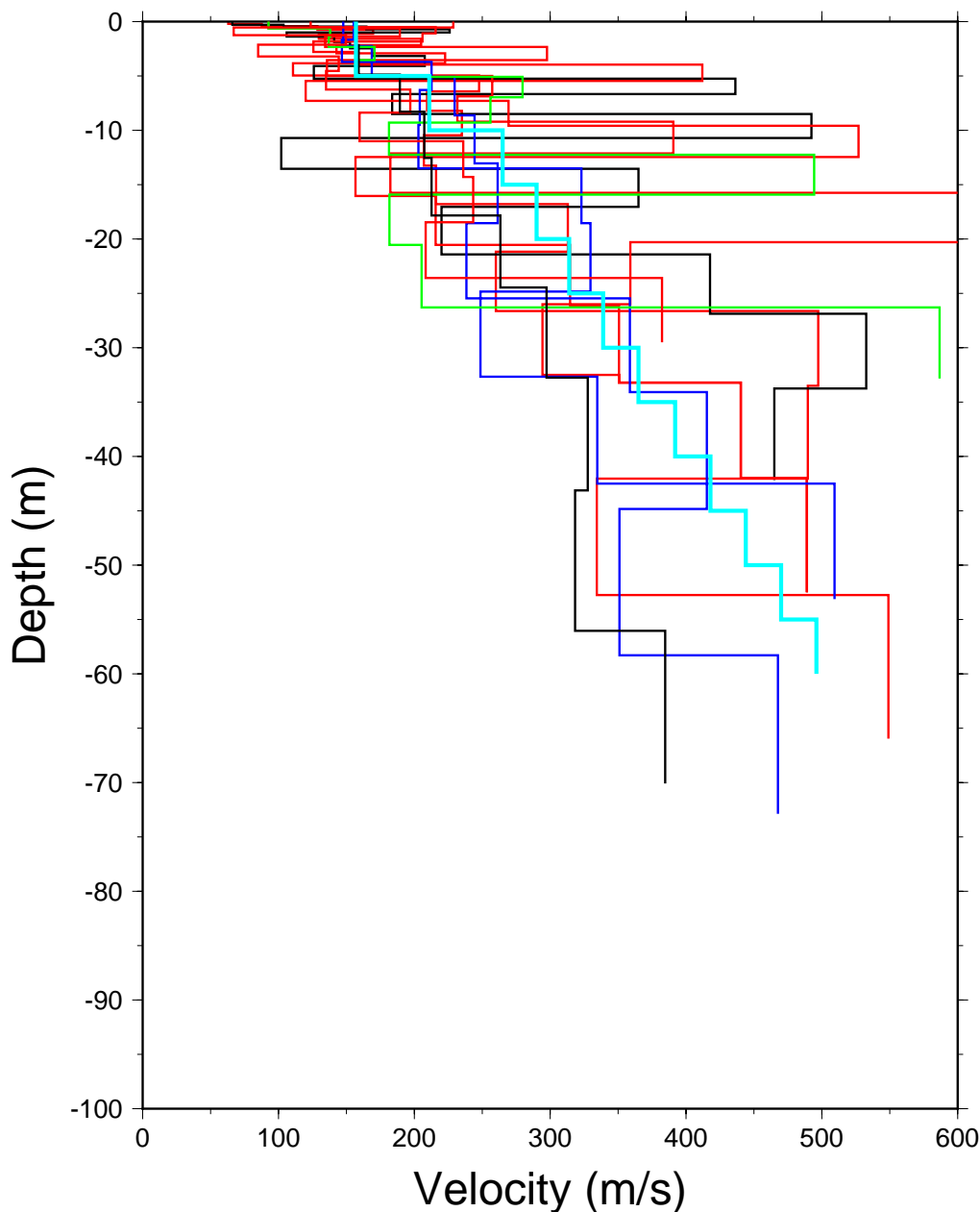


Figure 35: Comparing the velocity profiles obtained via testing at 6 Lauderdale County sites and 3 Dyer County sites. The thick cyan (light blue) line is the non-lowlands profile developed from the Lauderdale and Dyer County non-lowlands MASW profiles as representative of the velocity gradient in the Quaternary soils.

DyLa Co Vs Profiles

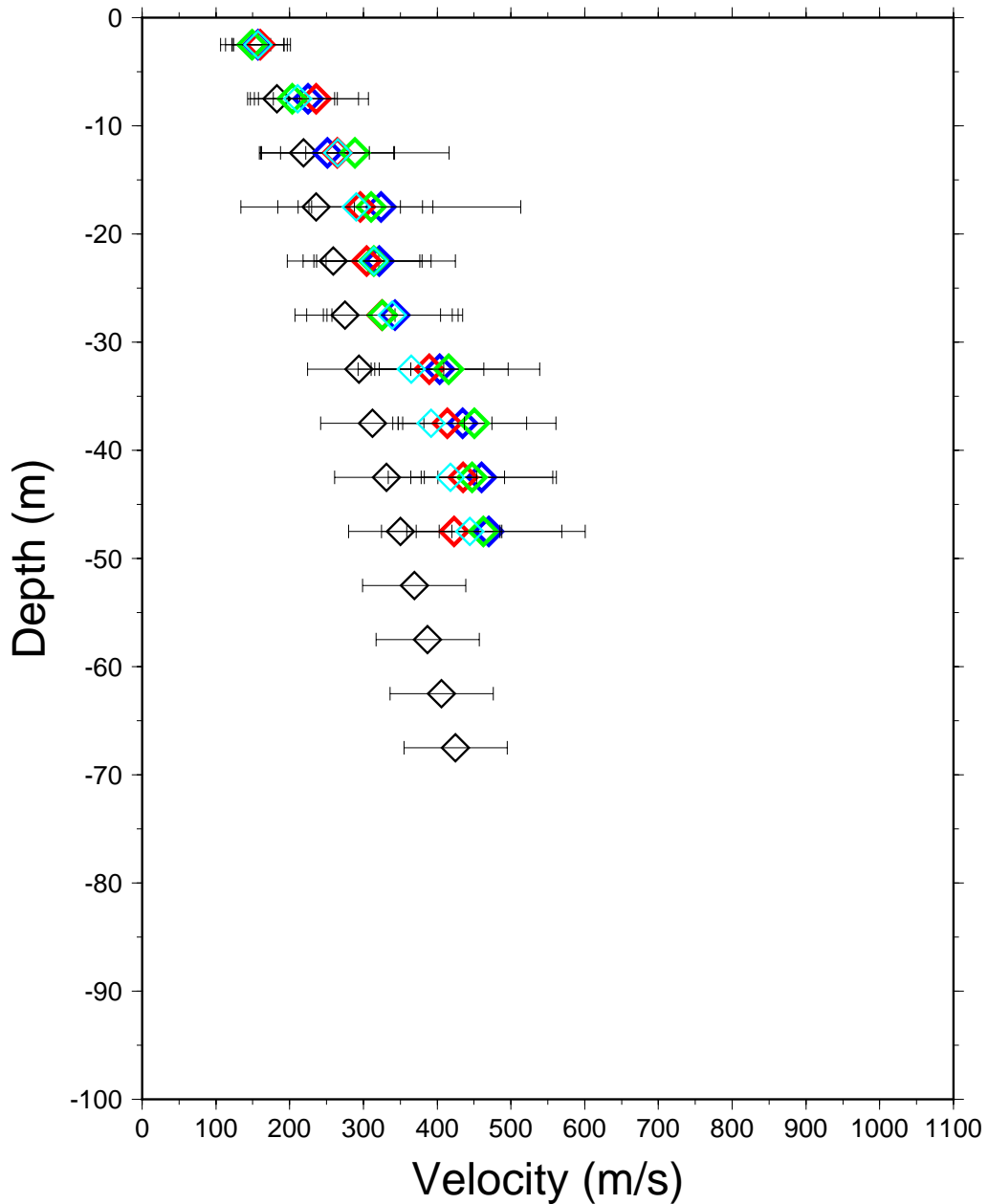


Figure 36: Mean and standard deviation of 8 intermediate (blue), 7 terrace (red), and 5 uplands (green) velocity profiles in Dyer and Lauderdale Counties. Also shown are the adopted velocity profiles (with uncertainties) for non-lowlands in Lauderdale County (cyan) and lowlands in Lauderdale, Dyer, and Lake Counties (black).

DyLa Co Vs Profiles

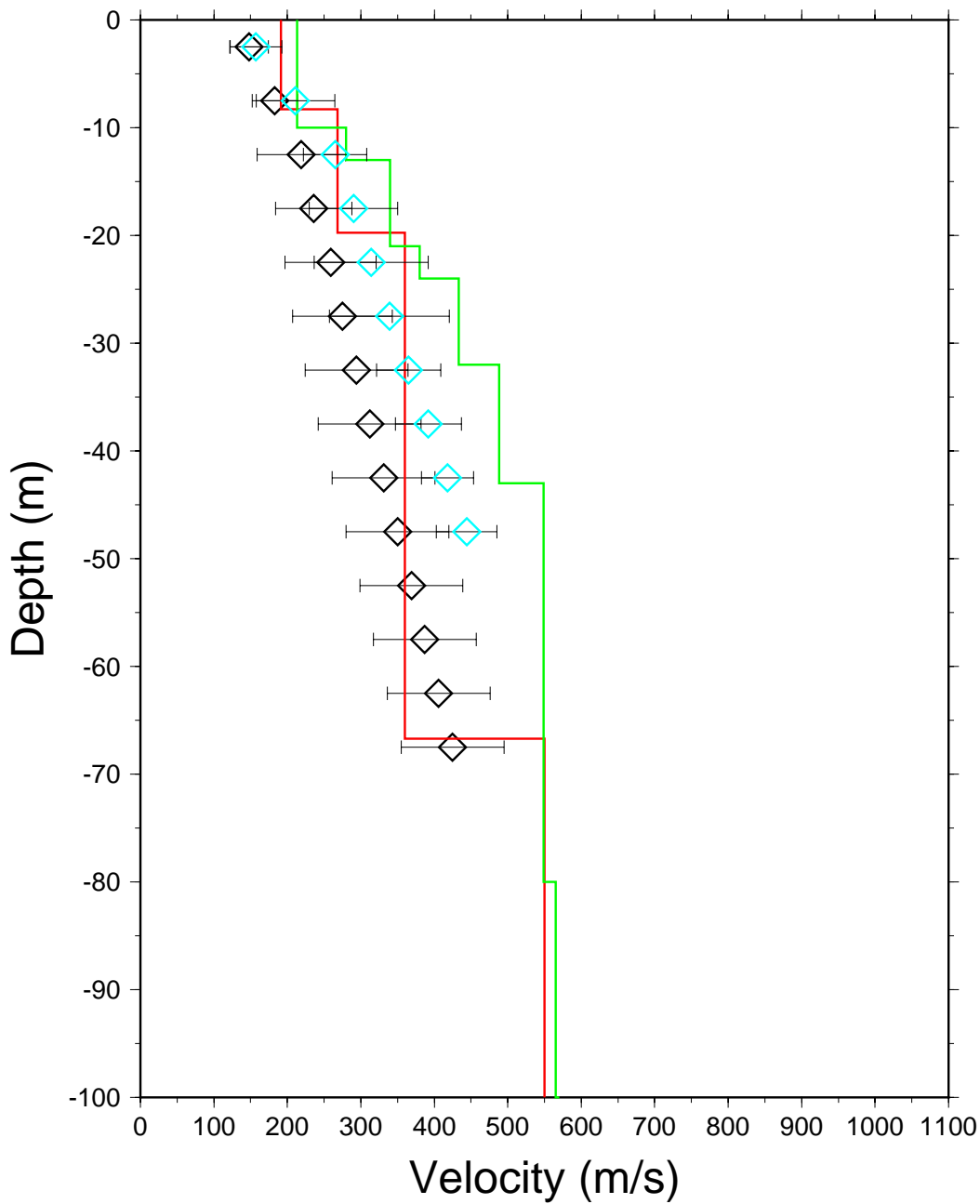


Figure 37: Comparison of adopted lowlands (black) and non-lowlands (cyan) velocity profiles for Lauderdale County with the Romero and Rix (2001) uplands average profile (green line) and typical velocity profile (red line) in Shelby County.

Hazard Maps Development

Methodology

A standard methodology for including the effects of local geology in seismic and liquefaction hazard estimates was used in this study. We followed the approach of Cramer et al. (2006, 2008, 2014, 2017, and 2018a) of developing site amplification distributions on a grid, applying those distributions to modify hard rock hazard curves to geology-specific hazard curves and develop seismic hazard maps, and then applying geology-specific liquefaction probability curves to develop liquefaction hazard maps. The site amplification distributions are based on the 3D geological, geotechnical, and seismological models developed above for Lauderdale County. The 2014 U.S. Geological Survey (USGS) National Seismic Hazard Project's seismic hazard model (seismic sources and ground motion attenuation model of Petersen et al., 2014) for hard rock was modified using our Lauderdale County site amplification distributions. Probabilistic seismic hazard maps were generated from the USGS probabilistic model and scenario (deterministic) seismic hazard maps were generated using selected scenario fault ruptures (earthquakes) and the USGS ground motion attenuation model. The resulting peak ground acceleration (PGA) seismic hazard maps were then modified using appropriate Lauderdale County liquefaction probability curves (discussed above) to generate liquefaction hazard maps (both probabilistic and scenario).

Lauderdale County Shear-wave Velocity Model

Seismic hazard maps with the effects of local geology depend on developing site amplification distributions on a grid for the 3D geology of the study area. The 3D geology is converted to geologic (sediment) profiles on a uniform grid. The geology layers are converted to shear-wave velocity (V_s) profiles at each grid point and input to a geotechnical soil response program (SHAKE91), along with appropriate geotechnical properties, to develop site response distributions at each grid point using the University of Memphis High Performance Computing (HPC) facility. The site amplification distributions model frequency and amplitude dependent amplification/deamplification at the surface of hard rock ground motions input at the bottom of the sediment profile.

The Lauderdale County representative velocity models used were developed from published and measured V_s profiles in and near the county as described above. Three separate models were developed for Lauderdale County, two for the Quaternary sediments above the top of the Eocene deposits and one for the geologic layers from the Eocene to the Paleozoic. The two Quaternary representative velocity models were divided between lowlands and non-lowlands as shown in Figures 36 and 37 above.

The Quaternary V_s models are a step-wise gradient model developed from the shallow V_s observations with different gradients for lowlands and non-lowlands models. The depth to the top of the Eocene layer varies for each profile between less than 30 m and 70 m depth so the gradient trend was projected downward from the all Quaternary sediment trend above 30 m to

50 -70 m in 5 m depth steps. The Eocene Vs jumps to 515 m/s at the top of that layer. Appropriate uncertainties based on the statistics (standard deviation) of the profile averaging at each depth interval were developed and applied in the sediment profile randomization process employed in the development of the site amplification distributions at each grid point.

The Eocene to Paleozoic Vs model is the same as developed for Lake County (Cramer et al., 2019). It was developed from the CUSSO deep hole site in Kentucky (Woolery et al., 2016) and published deeper embayment measurements in and near Lake County plus Vs models from Shelby County (Cramer et al., 2006). The borehole geological information mainly constrained the depths to the top of the Eocene, Cretaceous, and Paleozoic (bedrock) layers. In Lake County, very limited observations were available for other intermediate geological layers such as the top of the Memphis Sand, Flour Island clay, Fort Pillow sand, and Old Breastworks clay. The depth to the top of these four geological layers are needed to define the geology and Vs profiles beneath Dyer County. Using the limited observations in Lake County for these four layers and the better constrained isopachs for the top of the Eocene and Cretaceous, we developed a scheme to estimate the depth to the tops of the four intermediate layers between the Eocene and Cretaceous layers. Taking the depth difference between the tops of the Eocene and Cretaceous layers as unity, statistical estimates (average and standard deviation) were determined from the few available measurements for the depth difference between the top of the Eocene and the tops of each intermediate layer. The results in Table 4 are in fraction of the distance between the tops of the Eocene and Cretaceous. We then used these averages and standard deviations to estimate the depth with uncertainty to the top of the intermediate layers at each grid point. Vs values and uncertainties assigned to each intermediate layer was determined from the CUSSO Vs profile and checked and adjusted with available deeper Vs profile observations in Lake County and from the Shelby Co model. Figure 38 and Tables 5 and 6 show the resulting deeper Vs model and uncertainties used in the site amplification distribution calculations at each grid point for lowlands and non-lowlands, respectively.

As a further check on the intermediate Vs profile model developed for Lake County, we compared our model and available observations with the Vs profile from ambient noise (surface-waves) based Vs profile by Chunyu Liu (Figure 39). Liu's results are from the Non-Volcanic Tremor (NVT) L-shaped array of 19 broadband stations with a 60m spacing (600 m on a side). The NVT array was located near Mooring in Lake County. Clearly in Figure 39 below 150 m depths the Liu profile agrees with our model and other observations within the uncertainty. Above 150 m the Liu profile estimates of Vs are lower, but still within uncertainty, although with a loss of resolution in Liu's profile above 50 m. Liu did find an Vs anisotropy between 100 and 140 m depths.

Grids

There is one grid size used in our Lauderdale County study. The 3D geology for the depth to the top of the Eocene, Cretaceous and Paleocene layers where provided on a 0.005-degree grid (~500 m). These geology inputs were combined using the Quaternary and deeper Vs models

discussed above for site amplification distribution and seismic hazard calculations. The final seismic and liquefaction hazard maps use this 0.005-degree grid spacing.

Lake Co Vs Profiles

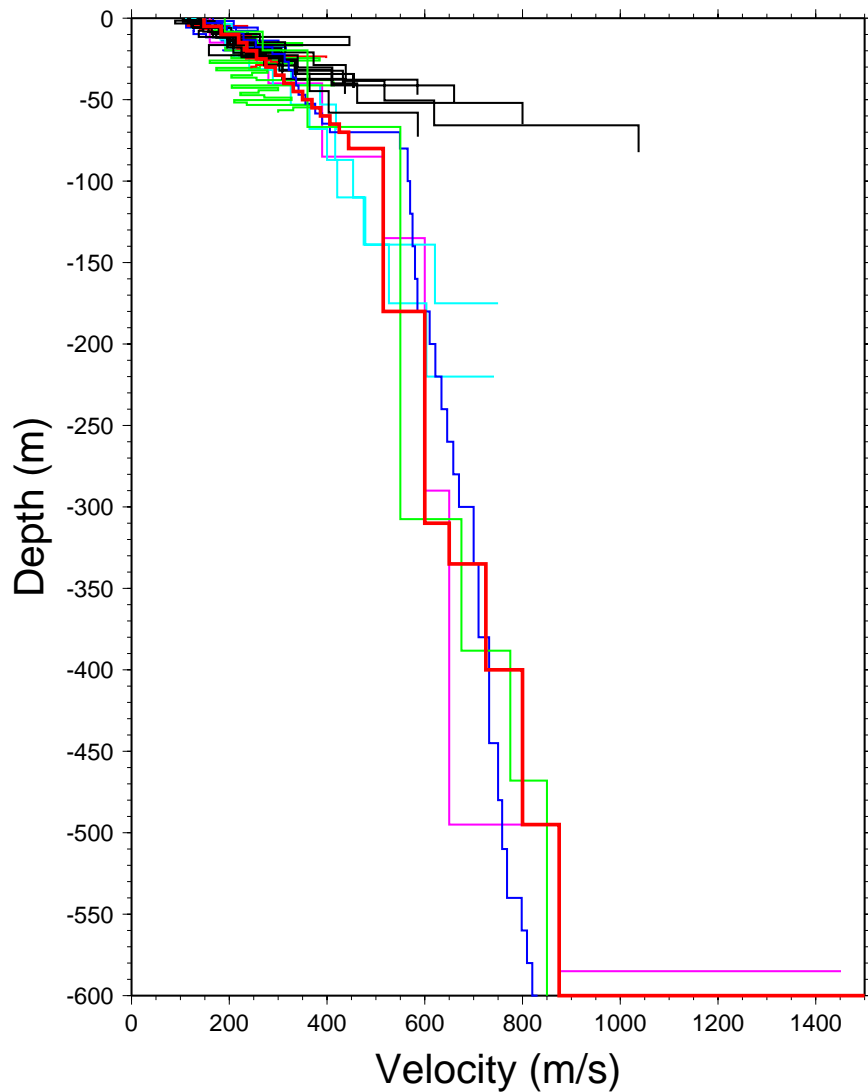


Figure 38: Vs profiles down to 600 m depth with Lake County Quaternary Vs model shown in heavy red line. Thin colored lines are published Vs profiles. Thin black lines are MASW profiles measured as a part of the Lake County study. The magenta profile is the CUSSO (Kentucky) deephole profile. The deeper green profile is the Shelby County reference profile. The blue profile is the Romero and Rix (2001) profile.

Table 4: Intermediate layer statistics in fraction of Cretaceous-Eocene depth difference.

Top of Formation	Fractional Distance	Fractional Std. Deviation	# of Observations
Memphis Sand	0.234	± 0.029	6
Flour Island (clay)	0.546	± 0.034	6
Fort Pillow (sand)	0.611	± 0.048	5
Old Breastworks (clay)	0.771	± 0.035	5

Table 5: Lowlands geotechnical profile used in 3D geology hazard model. Uncertainties are one std. deviation.

Formation	DepthToTop(m)	Damping	Density(g/cc)	Velocity(m/s)
Alluvium	0.	0.05	2.00	148 ± 13
	5 ± 0.75	0.05	2.00	183 ± 15
	10 ± 0.75	0.03	2.00	219 ± 30
	15 ± 0.75	0.03	2.00	236 ± 26
	20 ± 0.75	0.03	2.00	259 ± 31
	25 ± 0.75	0.03	2.00	275 ± 34
	30 ± 0.75	0.02	2.00	294 ± 35
	35 ± 0.75	0.02	2.00	312 ± 35
	40 ± 0.75	0.02	2.00	331 ± 35
	45 ± 0.75	0.02	2.00	350 ± 35
	50 ± 0.75	0.02	2.00	369 ± 35
	55 ± 0.75	0.02	2.00	387 ± 35
	60 ± 0.75	0.02	2.00	406 ± 35
	65 ± 0.75	0.02	2.00	425 ± 35
	70 ± 0.75	0.02	2.00	444 ± 35
Eocene	80 ± 1.00	0.02	2.00	515 ± 127
Memphis Sand	180 ± 12	0.02	2.00	600 ± 50
Flour Island	310 ± 7.5	0.02	2.00	650 ± 25
Fort Pillow	335 ± 15	0.01	2.00	725 ± 15
Old Breastworks	400 ± 13	0.01	2.00	800 ± 25
Cretaceous	495 ± 13	0.01	2.50	875 ± 63
Paleozoic	600 ± 13	0.001	2.80	2800

Table 6: Non-lowlands geotechnical profile used in 3D geology hazard model. Uncertainties are one std. deviation.

Formation	DepthToTop(m)	Damping	Density(g/cc)	Velocity(m/s)
Alluvium	0.	0.05	2.00	157±13
	5.±0.75	0.05	2.00	211±15
	10.±0.75	0.03	2.00	265±30
	15.±0.75	0.03	2.00	290±26
	20.±0.75	0.03	2.00	314±31
	25.±0.75	0.03	2.00	339±34
	30.±0.75	0.02	2.00	365±35
	35.±0.75	0.02	2.00	392±35
	40.±0.75	0.02	2.00	418±35
	45.±0.75	0.02	2.00	444±35
Eocene	50.±0.75	0.02	2.00	470±35
	55.±0.75	0.02	2.00	496±35
Memphis Sand	70.±1.00	0.02	2.00	515±67
Flour Island	180±12	0.02	2.00	600±50
Fort Pillow	310±7.5	0.02	2.00	650±25
Old Breastworks	335±15	0.01	2.00	725±15
Cretaceous	400±13	0.01	2.00	800±25
Paleozoic	495±13	0.01	2.50	875±63
	600±13	0.001	2.80	2800

Lake Co Vs Profiles

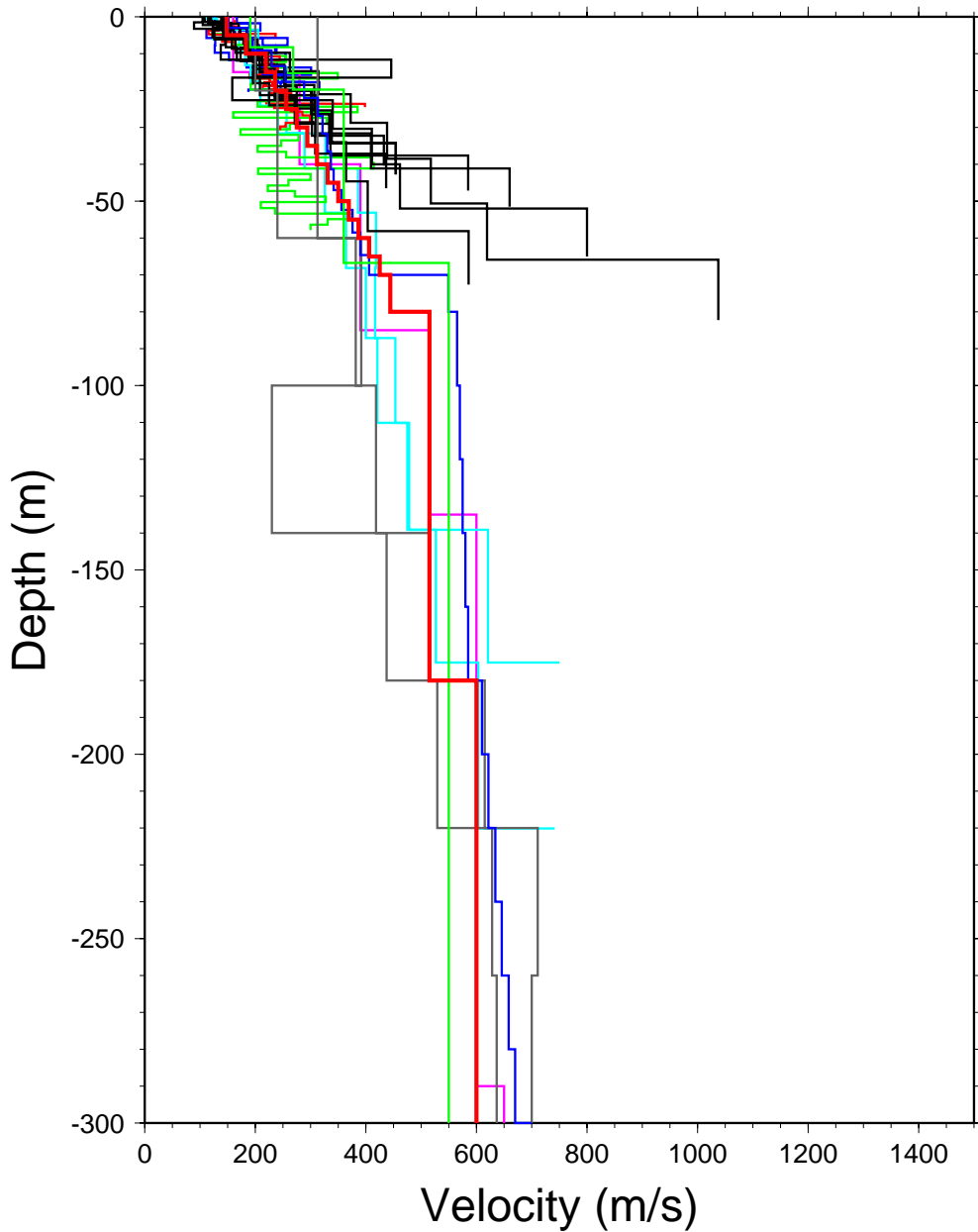


Figure 39: Vs profiles down to 300 m depth with Lake County Quaternary Vs model shown in heavy red line. The grey lines are Chunyu Liu's NVT profiles. The other profiles are colored as indicated in Figure 38.

Time History Database

The site amplification distribution calculations use a suite of input time histories (seismograms) at the bedrock/sediment interface to estimate sediment response. Time histories are required by soil response computer programs to estimate site response. The time histories used are listed in Table 7 and have been used by Cramer et al. (2006, 2017, and 2018) in similar seismic hazard analyses. At each grid point, the time history used is randomly selected for each iteration in the soil profile randomization to properly include uncertainty in the site amplification distribution calculations.

Table 7: Strong motion time series on rock used in the analysis (Cramer, 2006).

Earthquake	Station	Components
1989 M 6.9 Loma Prieta, California	G01	E, N
1992 M 7.1 Cape Mendocino, California	CPM	E, N
1992 M 7.3 Landers, California	JOS	E, N
1995 M 6.9 Kobe, Japan	KJM	E, N
1999 M 7.4 Kocaeli, Turkey	GBZ	W
	IZT	S
1999 M 7.6 Chi-Chi, Taiwan	TCU	N, W
1999 M 7.1 Duzce, Turkey	1060	E, N
Atkinson and Beresnev (2002)	M 7.5 and M 8.0 at Memphis, Tennessee	

Hazard Maps

Seismic and liquefaction hazard maps have been developed for both probabilistic and scenario cases. Probabilistic hazard maps have been generated for 10%, 5%, and 2% probability of exceedance in 50 years. The 2%-in-50-year maps correspond to current building code standards and represent up to the 80 percentile New Madrid seismic ground motions. 5%-in-50-year maps are similar to median scenario ground motion maps for the **M7** earthquakes in the New Madrid seismic zone and represent up to 60 percentile ground motions. The 10%-in-50-year maps correspond to an older design standard and only represent up to 35 percentile ground motions from the New Madrid seismic zone (NMSZ) sources. The 10%-in-50-year maps do not adequately represent expected median ground motions from New Madrid 1811-1812 earthquakes, are no longer recommended for design purposes by regulatory agencies, and are not presented here.

Median ground motion scenario (deterministic) hazard maps have been generated for seven scenario earthquakes (Table 8 and Figure 40A,B) and represent median expected ground motions from those earthquakes. The scenarios are for the largest earthquakes from the 1811-1812 New Madrid sequence, a **M6** earthquake in 1843, and for a hypothetical **M5.8** earthquake in Lauderdale County near Ripley. Because of its distance from Lauderdale County and low expected ground motions, the historical **M6** in 1895 earthquake is not included in our collection

of scenarios for Lauderdale County. The **M**5.8 scenario represents the effects of recent **M**5.5-6.0 Central and Eastern North American earthquakes if a similar size earthquake were to occur in Lauderdale County.

The ground motion periods represented in the Lauderdale County seismic hazard maps are peak ground acceleration (PGA), 0.2 s, and 1.0 s. 0.3 s maps have also been generated for compatibility with HAZUS, a risk and loss assessment package commonly used in loss analysis. The 0.2 and 0.3 s hazard maps are similar so the 0.3 s hazard maps are not shown in this report.

Table 8: Scenario earthquakes used in Lauderdale County study.

- M** 7.7 on the Reelfoot Thrust (central segment)
- M** 7.5 on the Cottonwood Grove Fault (SW segment)
- M** 7.3 on the New Madrid North Fault (NE segment)
- M** 6.9 “Dawn” Aftershock (2 alternatives)
- M** 6.2 near Marked Tree, Arkansas (1843 earthquake)
- Hypothetical **M** 5.8 earthquake near Ripley (recent CEUS earthquakes)

Lauderdale Co Scenario Eqks

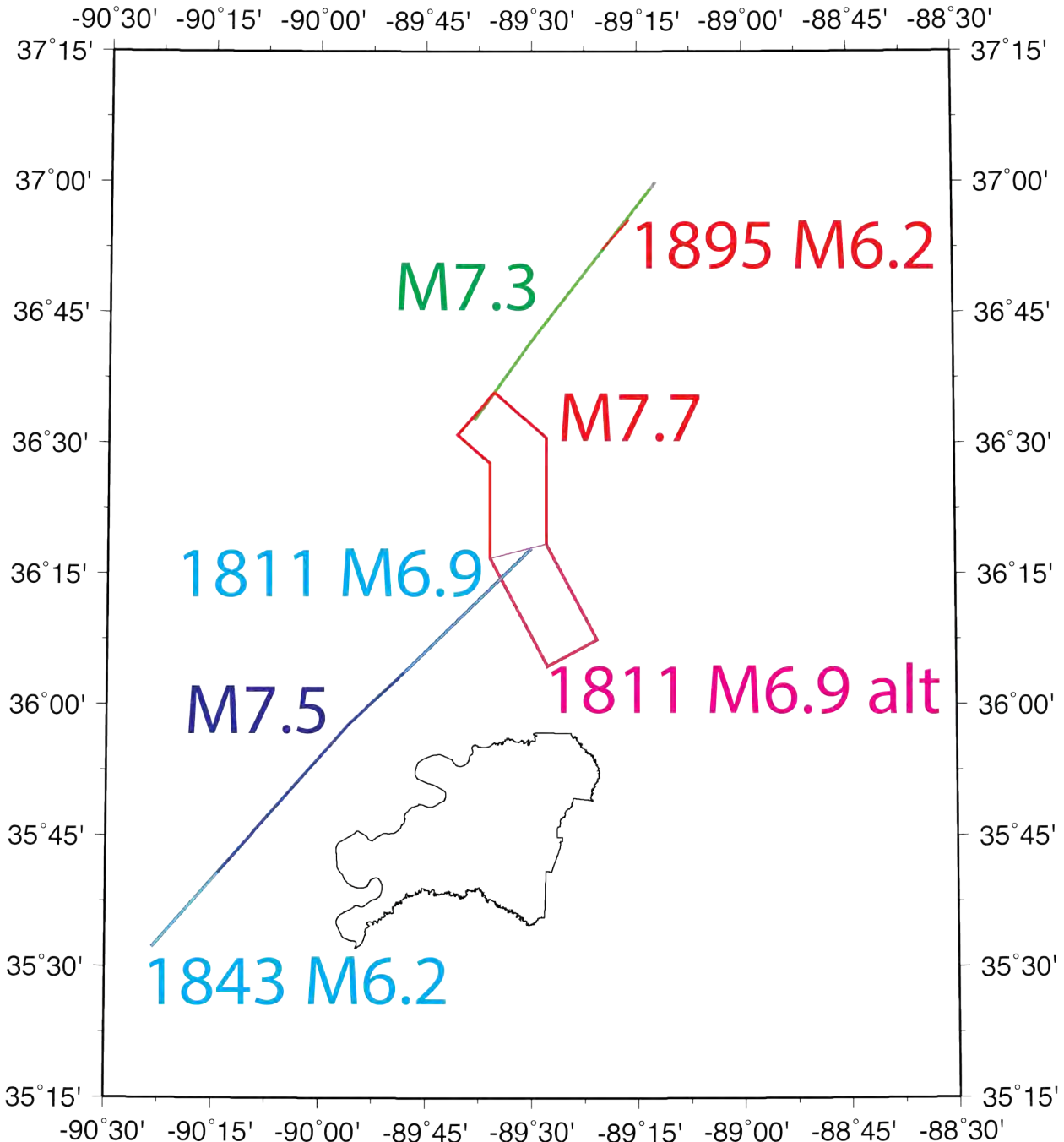


Figure 40A: Potential scenario ruptures for Lauderdale County. 1811–1812 **M7** ruptures indicated by **M7.5**, **M7.3**, and **M7.7**. 1811 **M6.9**s indicate two alternative “Dawn” aftershock ruptures. 1843 and 1895 **M6.2**s indicate historic end of seismic zone ruptures.

Lauderdale Co Scenario Eqks

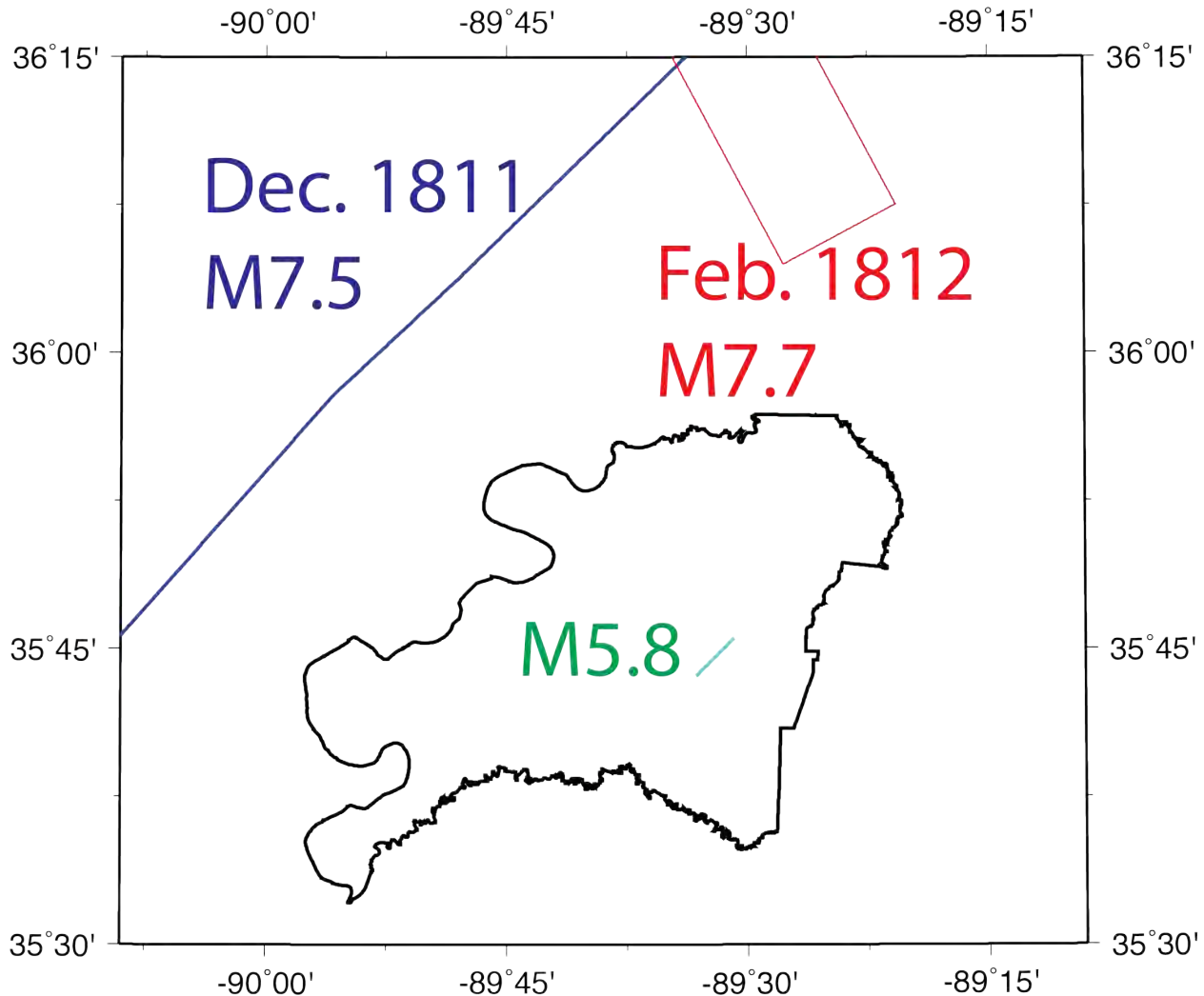


Figure 40B: Scenario ruptures close to Lauderdale County. The Dec. 1811 is strike-slip mainshock rupture extending out of the map view. The Feb. 1812 is thrust mainshock rupture mostly out of map view. The **M5.8** is a hypothetical earthquake in Lauderdale County.

Seismic Hazard Maps

Figures 41 - 43 show the 5%-in-50-year probabilistic seismic hazard maps for Lauderdale County for PGA, 0.2 s, and 1.0 s. The background maps are the equivalent USGS national seismic hazard maps for B/C boundary conditions ($V_{s30} = 760 \text{ m/s}$). At short periods (PGA and 0.2 s) the Lauderdale County range of values is 0.4 – 0.9 g (g is the acceleration of gravity at the earth's surface – 9.80665 m/s). At long periods (1.0 s) the range is 0.4 – 0.6 g. Short period seismic hazard is for 1-2 story buildings, while long period hazard is for ~10 story buildings.

Lauderdale Co PGA Hazard

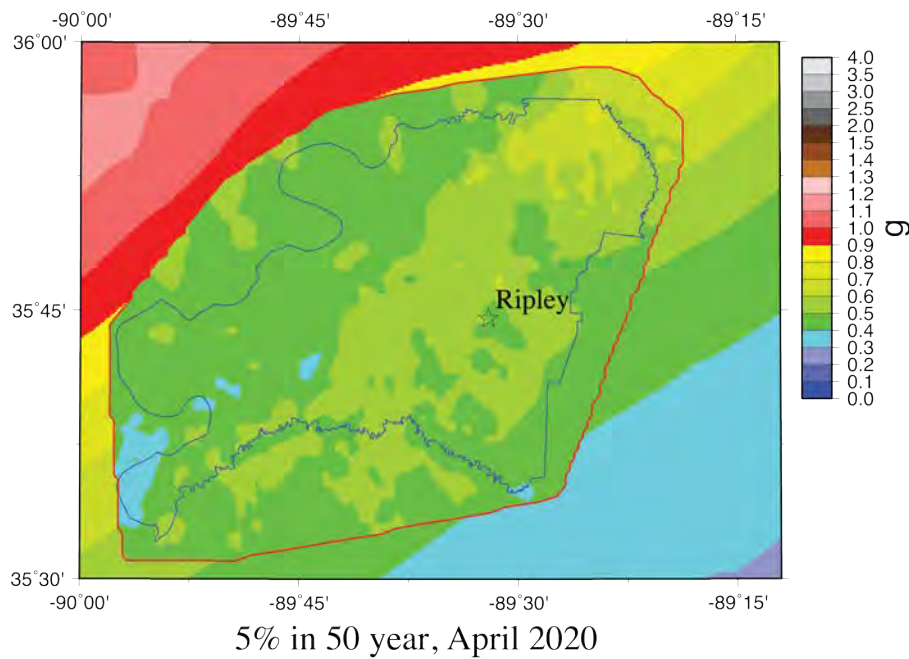


Figure 41: 5%-in-50-year PGA hazard map for Lauderdale County with the effects of local geology inset on the U.S. Geological Survey's national seismic hazard map for BC boundary conditions.

Lauderdale Co 0.2s Hazard

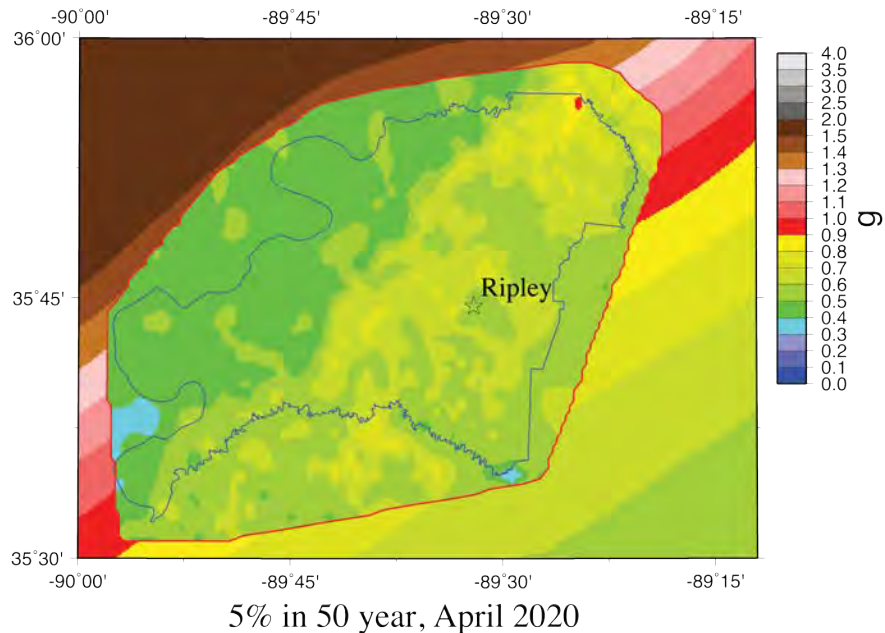
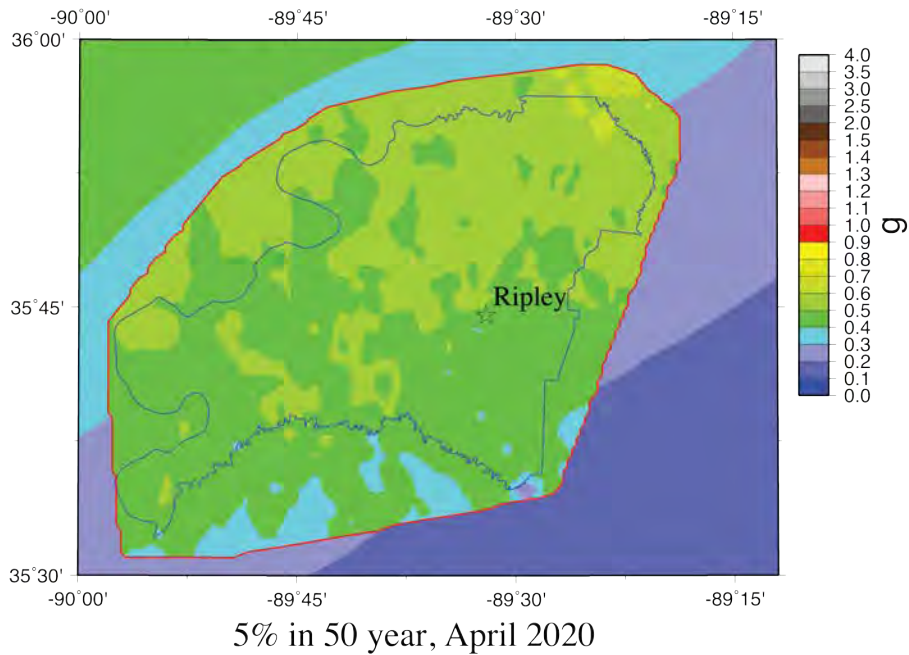


Figure 42: 5%-in-50-year 0.2 s hazard map for Lauderdale County with the effects of local geology inset on the U.S. Geological Survey's national seismic hazard map for BC boundary conditions.

Lauderdale Co 1.0s Hazard



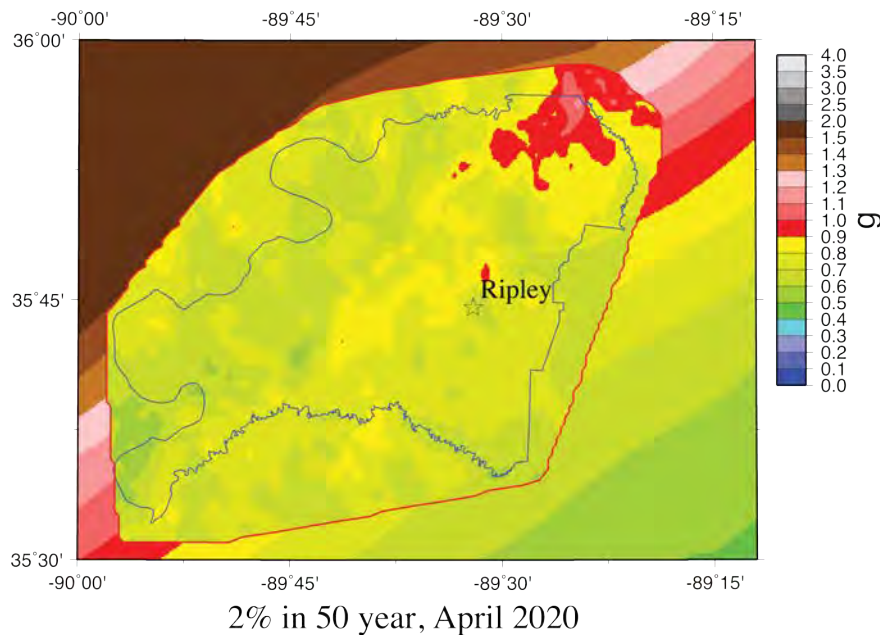
5% in 50 year, April 2020

Figure 43: 5%-in-50-year 1.0 s hazard map for Lauderdale County with the effects of local geology inset on the U.S. Geological Survey's national seismic hazard map for BC boundary conditions.

Figures 44 - 46 show the 2%-in-50-year probabilistic seismic hazard maps for Lauderdale County. The hazard range is higher than the 5%-in-50-year maps: 0.6 – 1.1 g for PGA, 0.6 – 1.3 g for 0.2 s, and 0.6 – 1.1 g for 1.0 s.

The probabilistic seismic hazard maps with the effect of local geology show a short period reduction of 10% to 70% and a long period amplification of 10% to 100% relative to the USGS national seismic hazard maps at the same periods. The short period reduction is due to estimated ground motion nonlinear soil effects strongly reducing the high ground motions expected near the earthquake sources. The long period amplification is due to the reduced nonlinear effects and increase dominance of soil column resonant effects amplifying ground motions. As we progress further from the earthquake sources the ground motion level decreases, the nonlinear effects decrease, and the dominance of resonance effects increases. In Shelby County, about 50 km from the New Madrid earthquake sources, Cramer et al. (2018a) show Shelby County seismic hazard maps with 40 – 60% decreases at short period and 50 – 100 % increases at long period over the USGS national seismic hazard maps. Another feature of the probabilistic seismic hazard maps is the high ground motion estimates in the northern portion of the county. These high estimates are due to most of Lauderdale County being in the uplands, which has thinner Quaternary sediments than the lowlands and hence less nonlinear deamplification. This northern county region is also closer to the earthquake sources in the model.

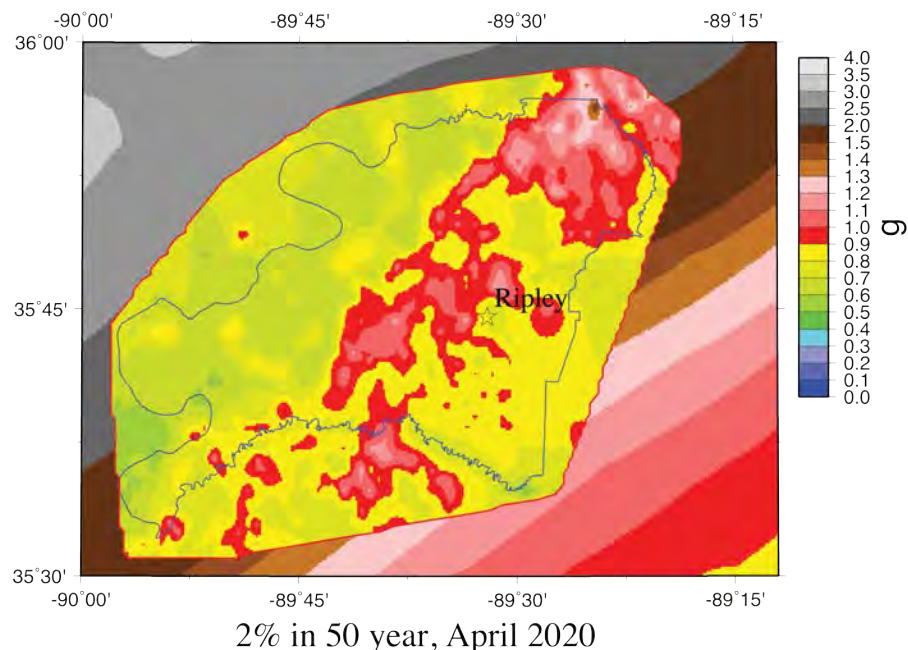
Lauderdale Co PGA Hazard



2% in 50 year, April 2020

Figure 44: 2%-in-50-year PGA hazard map for Lauderdale County with the effects of local geology inset on the U.S. Geological Survey's national seismic hazard map for BC boundary conditions.

Lauderdale Co 0.2s Hazard



2% in 50 year, April 2020

Figure 45: 2%-in-50-year 0.2 s hazard map for Lauderdale County with the effects of local geology inset on the U.S. Geological Survey's national seismic hazard map for BC boundary conditions.

Lauderdale Co 1.0s Hazard

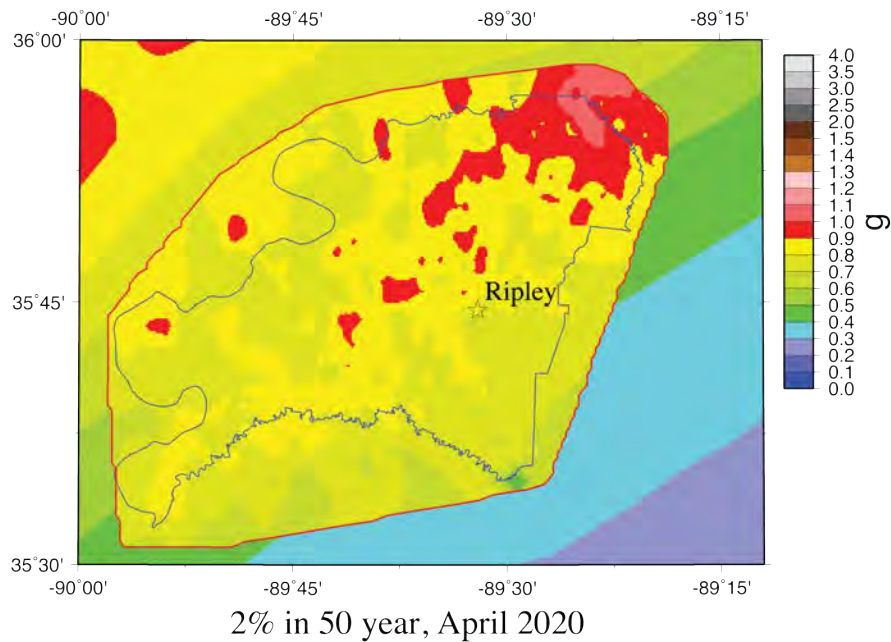


Figure 46: 2%-in-50-year 1.0 s hazard map for Lauderdale County with the effects of local geology inset on the U.S. Geological Survey's national seismic hazard map for BC boundary conditions.

Figures 47 - 53 present the PGA, 0.2 s, and 1.0 s seismic hazard maps for the seven scenarios of Table 8. There are no equivalent comparisons to the USGS probabilistic maps for these scenarios. At all periods shown, the M7 New Madrid scenario hazard maps range from 0.2 to 0.7 g for a repeat of the M7.7 February 1812 earthquake, from 0.2 to 0.5 g for the repeat of the M7.5 December 1811 earthquake, and 0.1 to 0.4 g for the repeat of the M7.3 January 1812 earthquake. The M6.9 largest aftershock hazard map alternatives range from 0.1 to 0.4 g if on the northern end of the SW arm and 0.1 to 0.6 g if on the east end of the Reelfoot thrust. The M6.2 1843 scenario ground motions are 0.1 to 0.3 g, and the M5.8 hypothetical Lauderdale County earthquake ground motions ranges from 0.1 – 0.7 g. Thus, both the scenario and probabilistic seismic hazard maps show similar ground motion levels at short and long periods due to the close proximity of ruptures and the effect of soils of the Mississippi embayment. These scenarios continue to show the higher hazard in the northern portion of the county seen in the probabilistic hazard maps, due to the thinner upland Quaternary sediment along with the proximity to seismic sources in several cases. For the M6.2 Marked Tree scenario and at 1.0 s for the M7.5 SW arm scenario, the higher ground motions are in the western portion of the county.

Lauderdale Co PGA Hazard

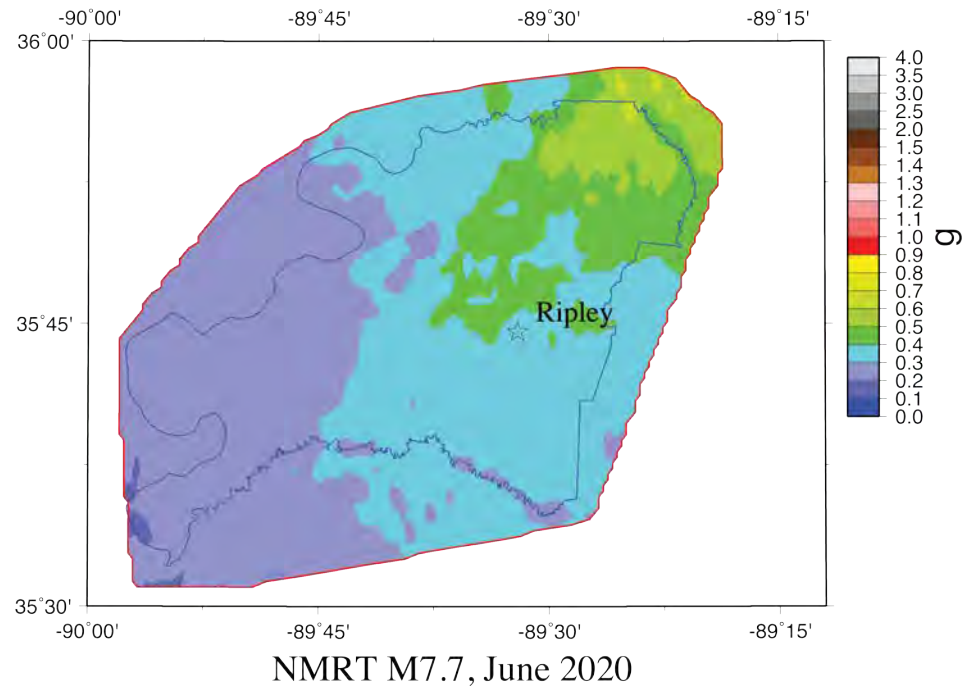


Figure 47A: Scenario PGA hazard map for a M7.7 earthquake on the Reelfoot Thrust (central segment of NMSZ) for Lauderdale County with the effects of local geology.

Lauderdale Co 0.2s Hazard

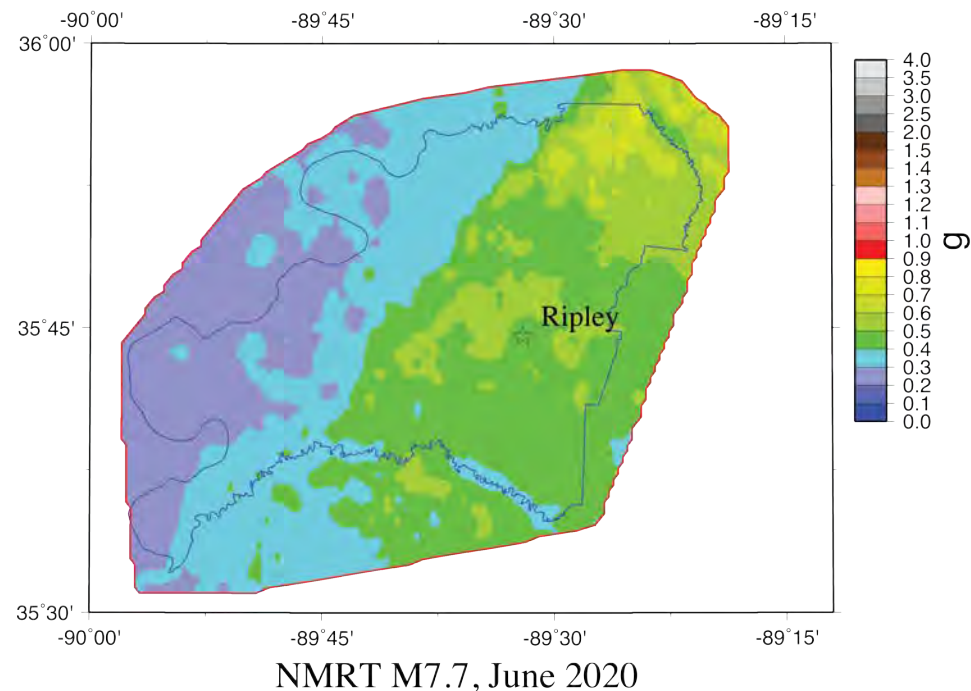


Figure 47B: Scenario 0.2 s hazard map for a M7.7 earthquake on the Reelfoot Thrust (central segment of NMSZ) for Lauderdale County with the effects of local geology.

Lauderdale Co 1.0s Hazard

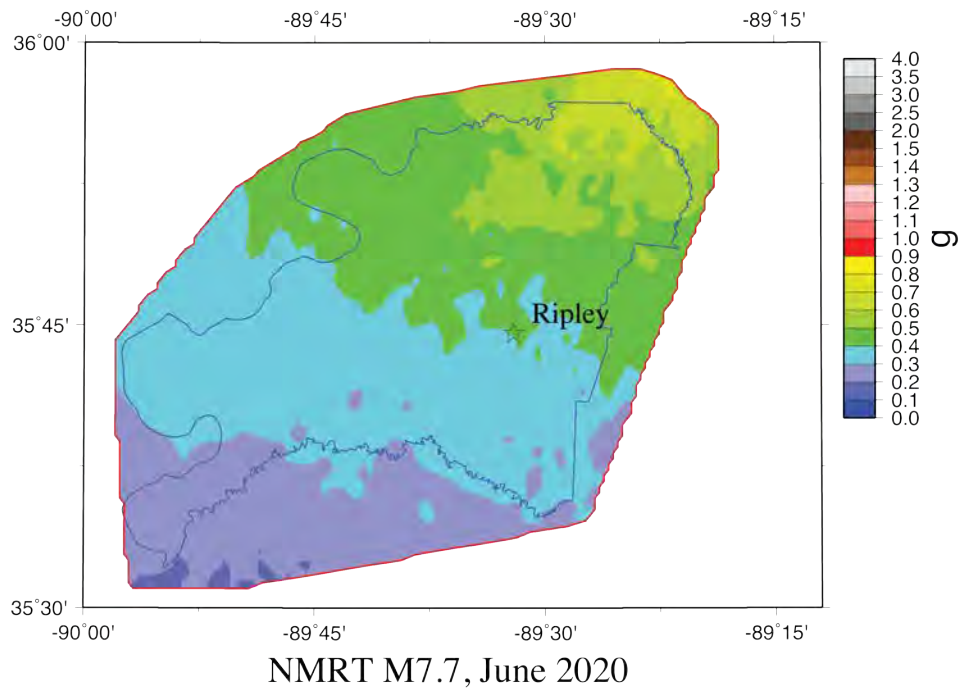


Figure 47C: Scenario 1.0 s hazard map for a M7.7 earthquake on the Reelfoot Thrust (central segment of NMSZ) for Lauderdale County with the effects of local geology.

Lauderdale Co PGA Hazard

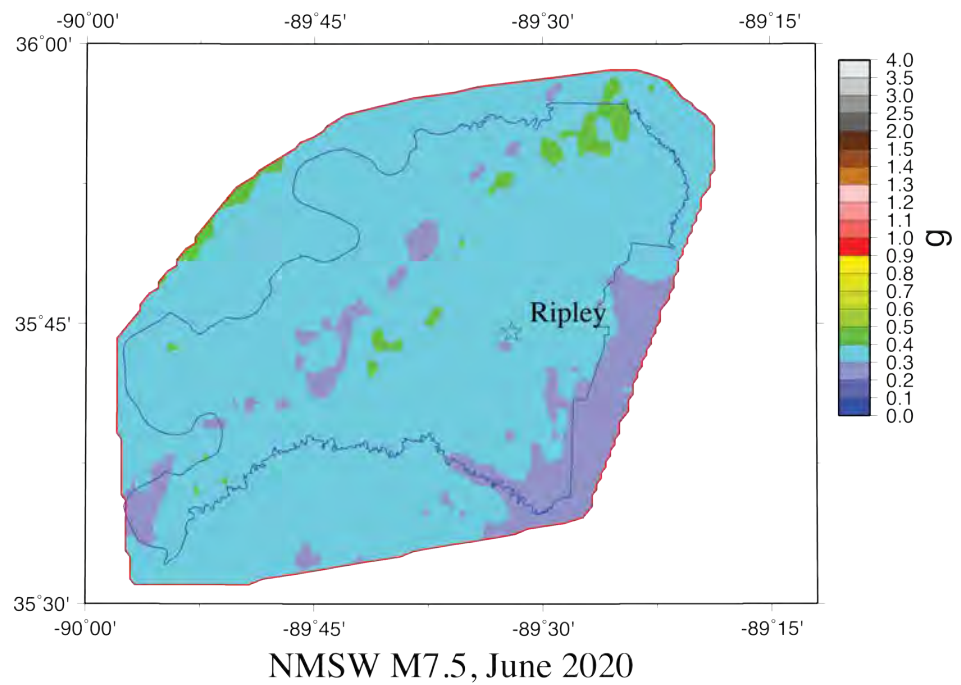
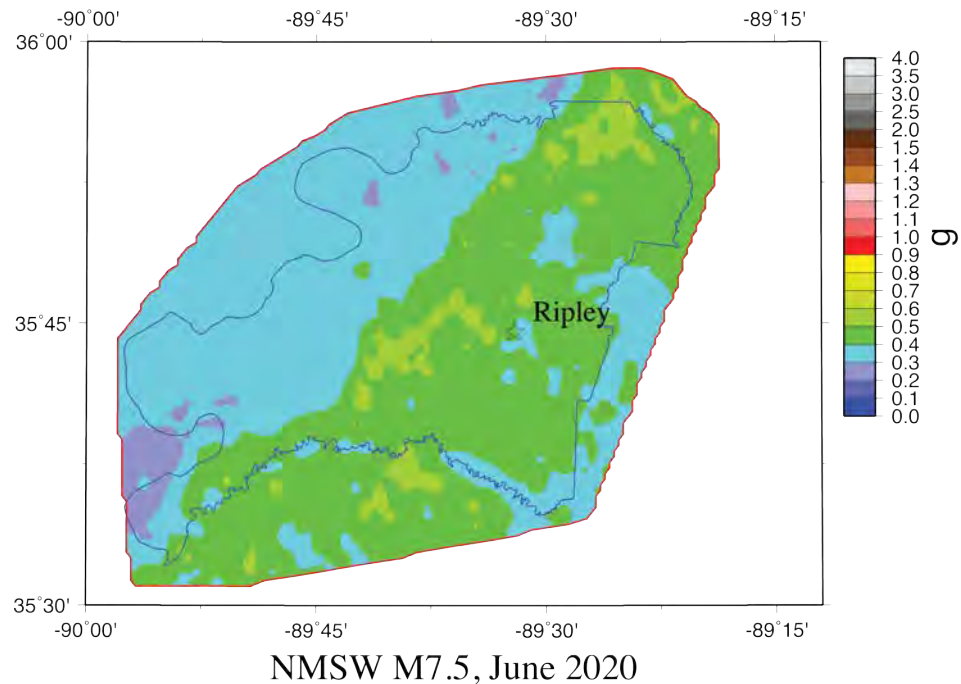


Figure 48A: Scenario PGA hazard map for a M7.5 earthquake on the Cottonwood Grove Fault (SW segment of NMSZ) for Lauderdale County with the effects of local geology.

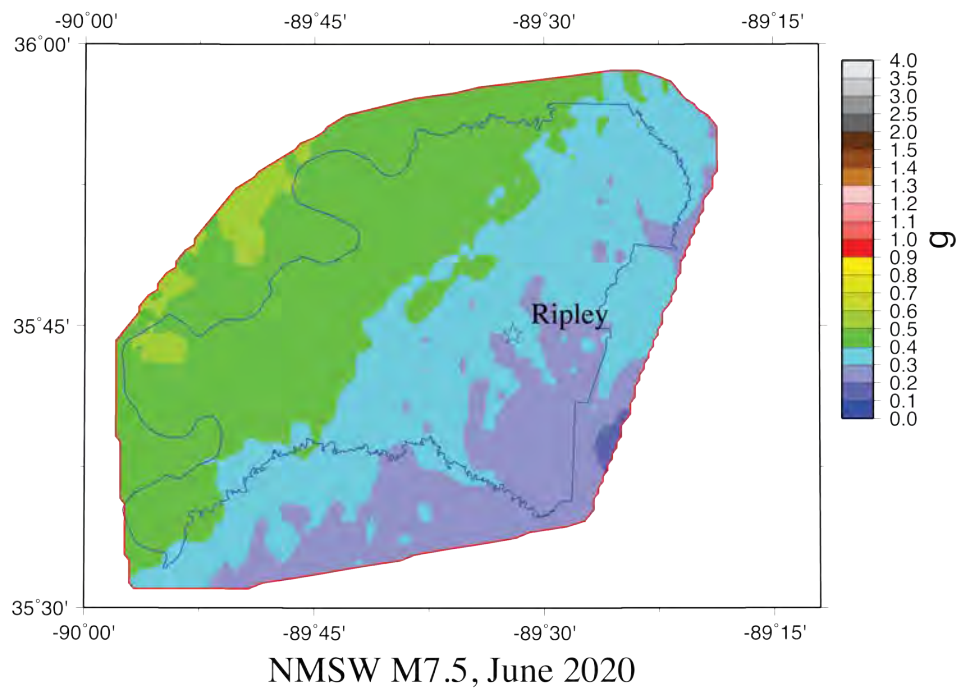
Lauderdale Co 0.2s Hazard



NMSW M7.5, June 2020

Figure 48B: Scenario 0.2 s hazard map for a M7.5 earthquake on the Cottonwood Grove Fault (SW segment of NMSZ) for Lauderdale County with the effects of local geology.

Lauderdale Co 1.0s Hazard



NMSW M7.5, June 2020

Figure 48C: Scenario 1.0 s hazard map for a M7.5 earthquake on the Cottonwood Grove Fault (SW segment of NMSZ) for Lauderdale County with the effects of local geology.

Lauderdale Co PGA Hazard

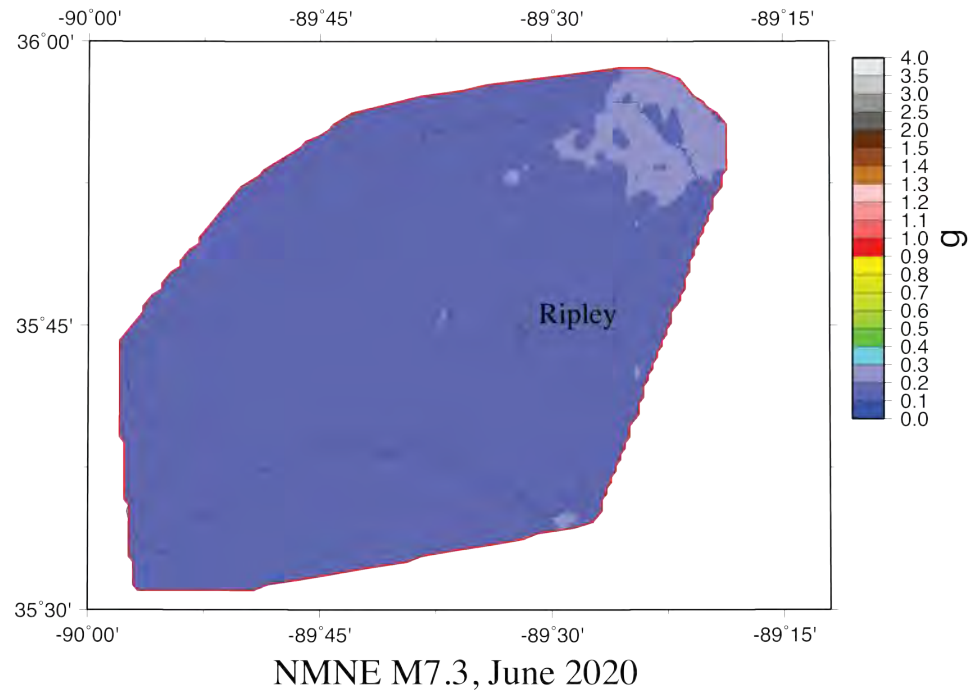


Figure 49A: Scenario PGA hazard map for a M7.3 earthquake on the New Madrid North Fault (NE segment of NMSZ) for Lauderdale County with the effects of local geology.

Lauderdale Co 0.2s Hazard

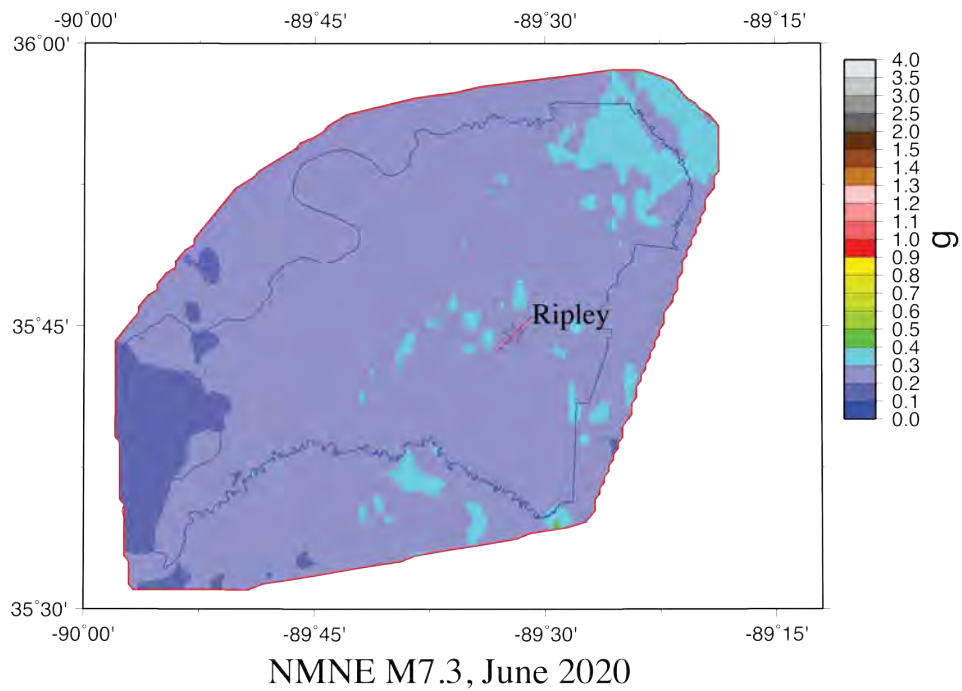


Figure 49B: Scenario 0.2 s hazard map for a M7.3 earthquake on the New Madrid North Fault (NE segment of NMSZ) for Lauderdale County with the effects of local geology.

Lauderdale Co 1.0s Hazard

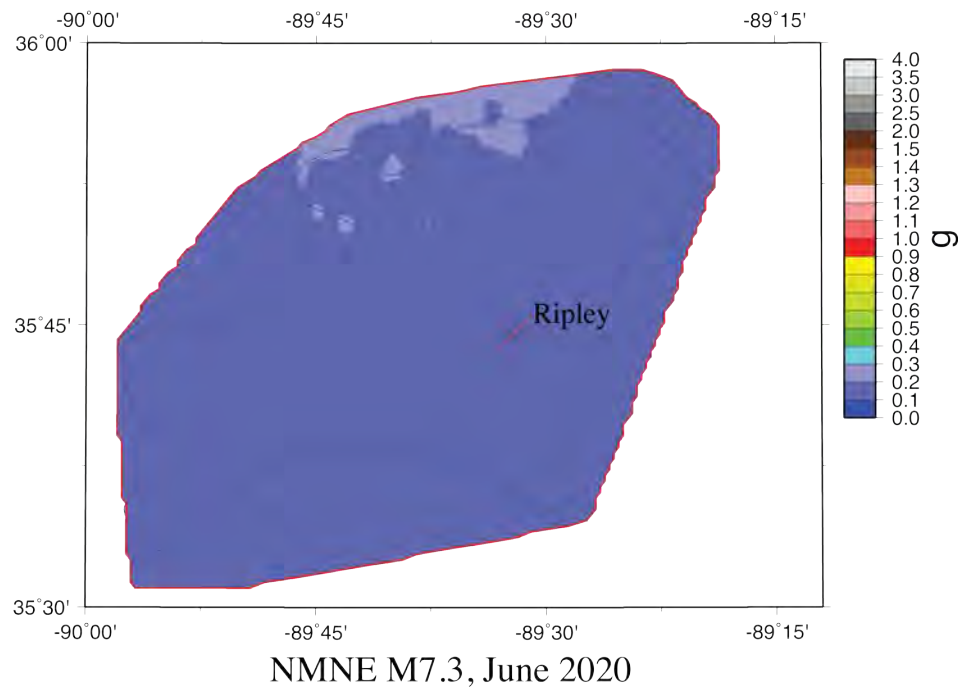


Figure 49C: Scenario 1.0 s hazard map for a M7.3 earthquake on the New Madrid North Fault (NE segment of NMSZ) for Lauderdale County with the effects of local geology.

Lauderdale Co PGA Hazard

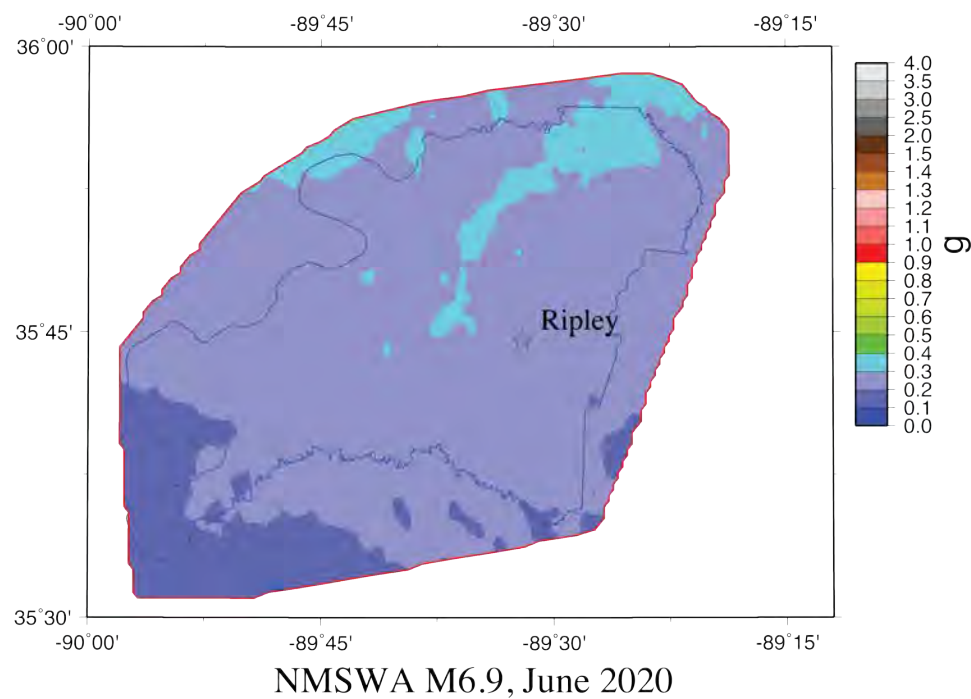


Figure 50A: Scenario PGA hazard map for a M6.9 “Dawn” aftershock (alt. 1) on the Cottonwood Grove Fault (SW segment of NMSZ) for Lauderdale County with the effects of local geology.

Lauderdale Co 0.2s Hazard

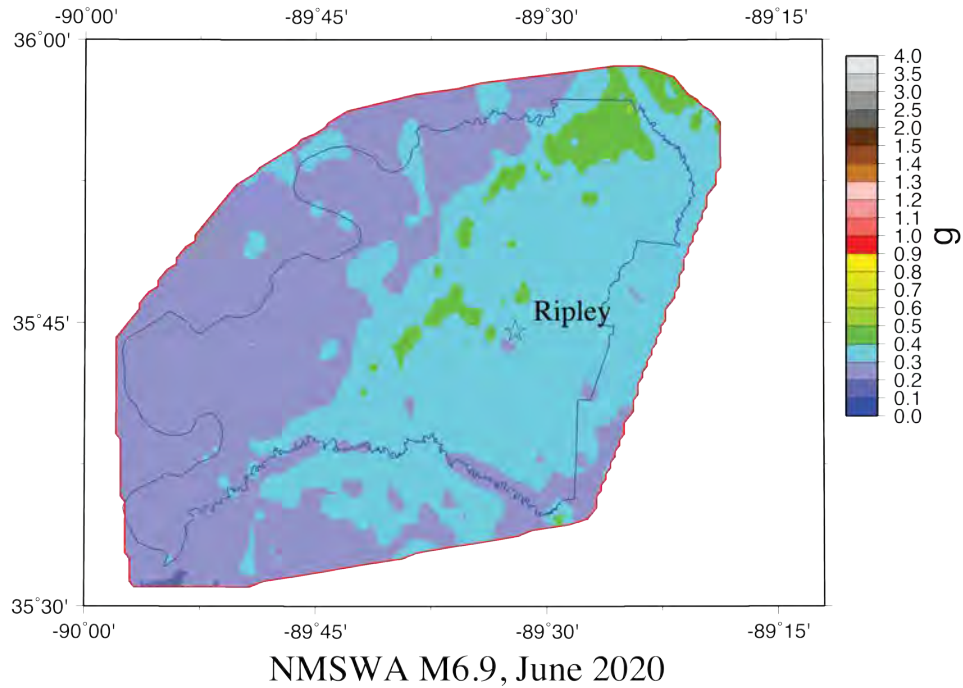


Figure 50B: Scenario 0.2 s hazard map for a M6.9 “Dawn” aftershock (alt. 1) on the Cottonwood Grove Fault (SW segment of NMSZ) for Lauderdale County with the effects of local geology.

Lauderdale Co 1.0s Hazard

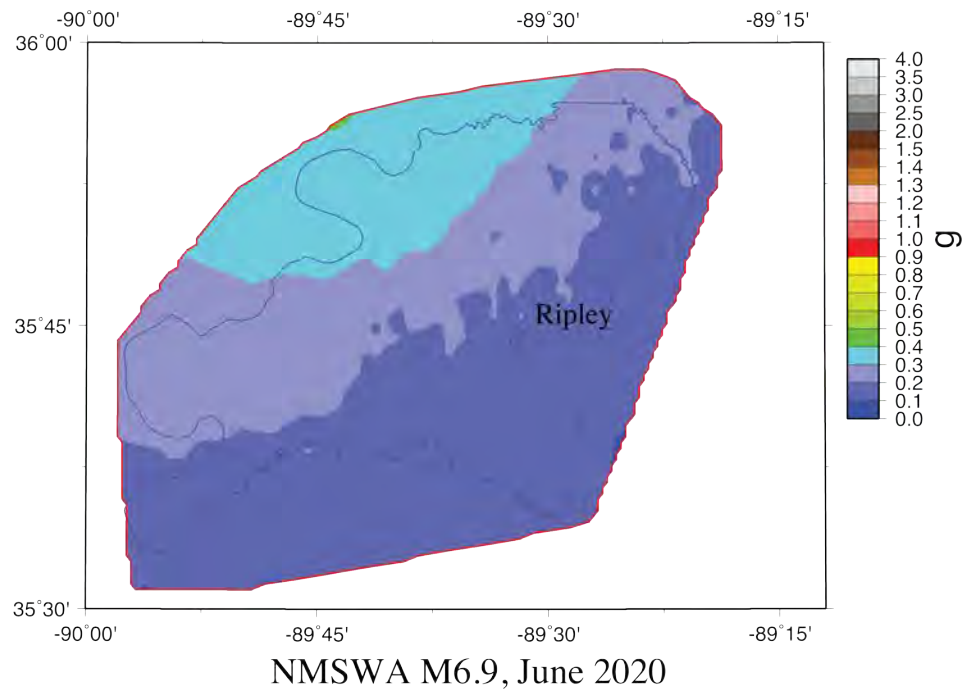
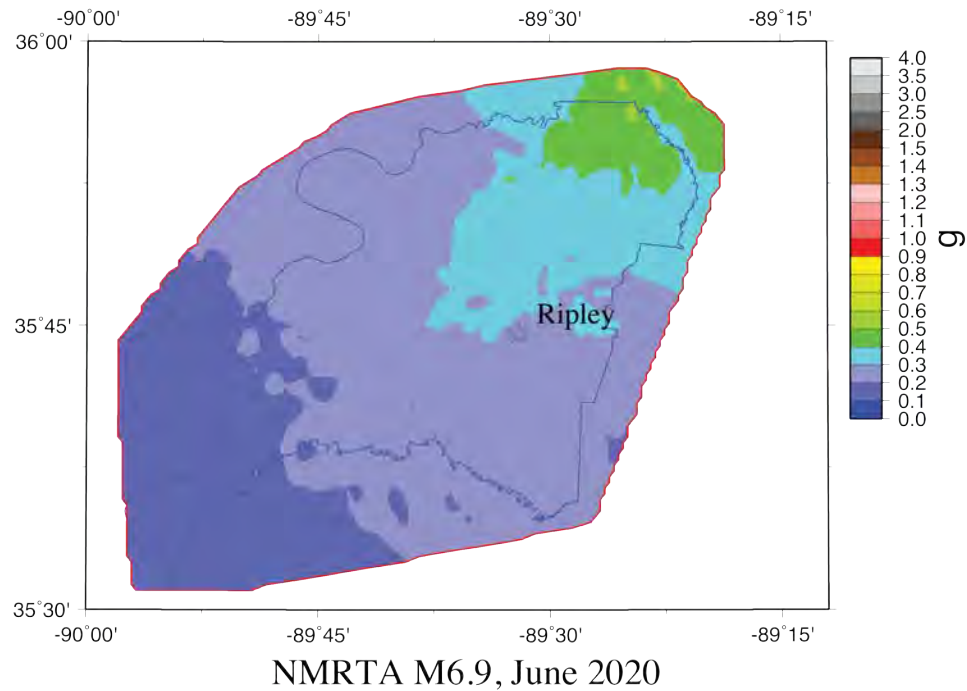


Figure 50C: Scenario 1.0 s hazard map for a M6.9 “Dawn” aftershock (alt. 1) on the Cottonwood Grove Fault (SW segment of NMSZ) for Lauderdale County with the effects of local geology.

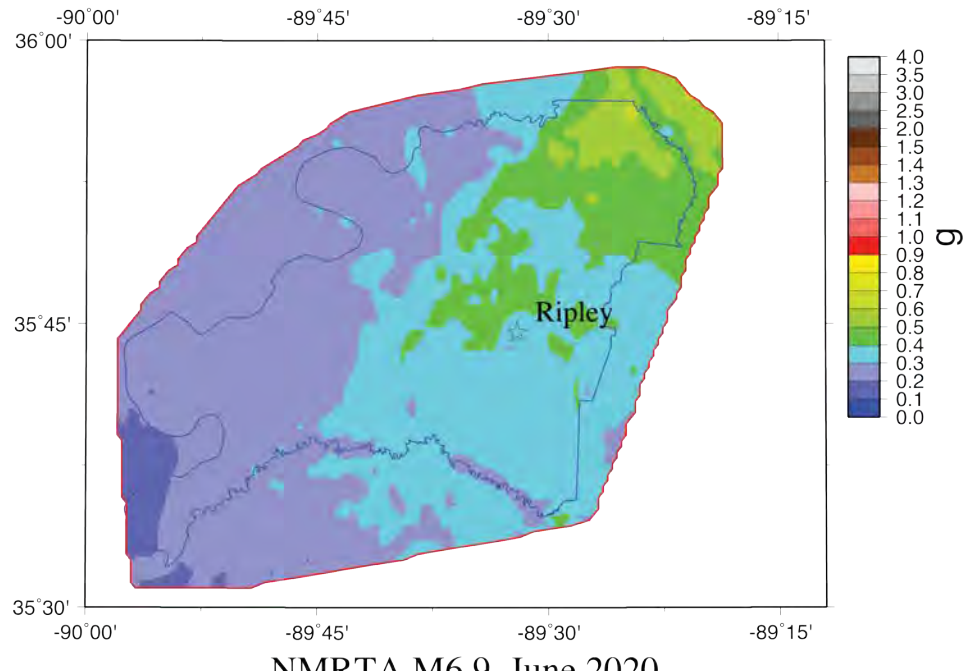
Lauderdale Co PGA Hazard



NMRTA M6.9, June 2020

Figure 51A: Scenario PGA hazard map for a M6.9 "Dawn" aftershock (alt. 2) on the Reelfoot Thrust (central segment of NMSZ) for Lauderdale County with the effects of local geology.

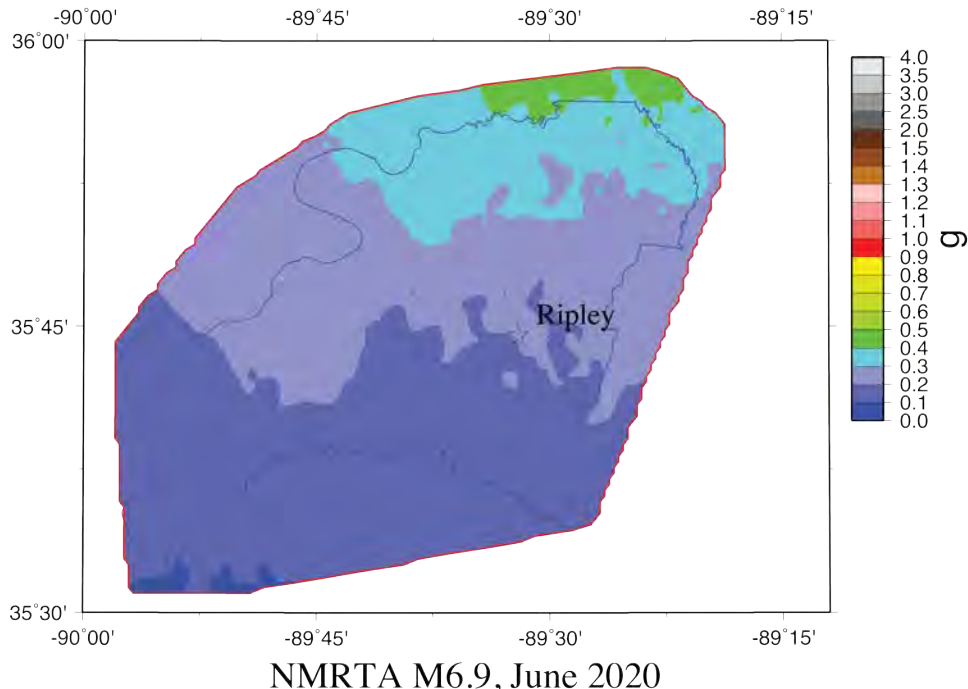
Lauderdale Co 0.2s Hazard



NMRTA M6.9, June 2020

Figure 51B: Scenario 0.2 s hazard map for a M6.9 "Dawn" aftershock (alt. 2) on the Reelfoot Thrust (central segment of NMSZ) for Lauderdale County with the effects of local geology.

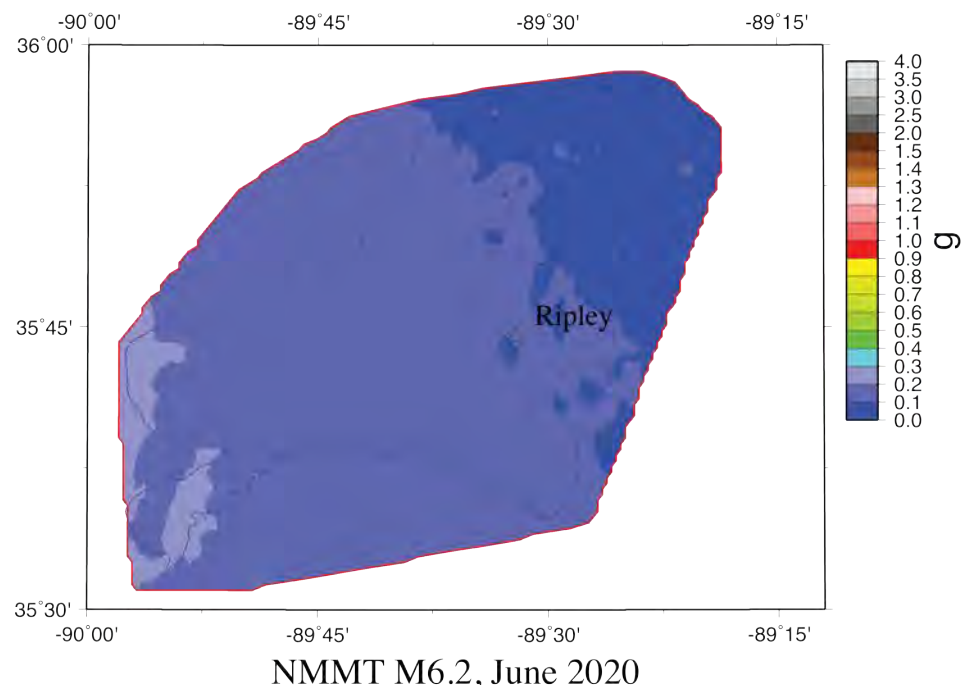
Lauderdale Co 1.0s Hazard



NMRTA M6.9, June 2020

Figure 51C: Scenario 1.0 s hazard map for a M6.9 “Dawn” aftershock (alt. 2) on the Reelfoot Thrust (central segment of NMSZ) for Lauderdale County with the effects of local geology.

Lauderdale Co PGA Hazard



NMMT M6.2, June 2020

Figure 52A: Scenario PGA hazard map for a M6.2 on the Cottonwood Grove Fault (1843 Marked Tree – SW segment of NMSZ) for Lauderdale County with the effects of local geology.

Lauderdale Co 0.2s Hazard

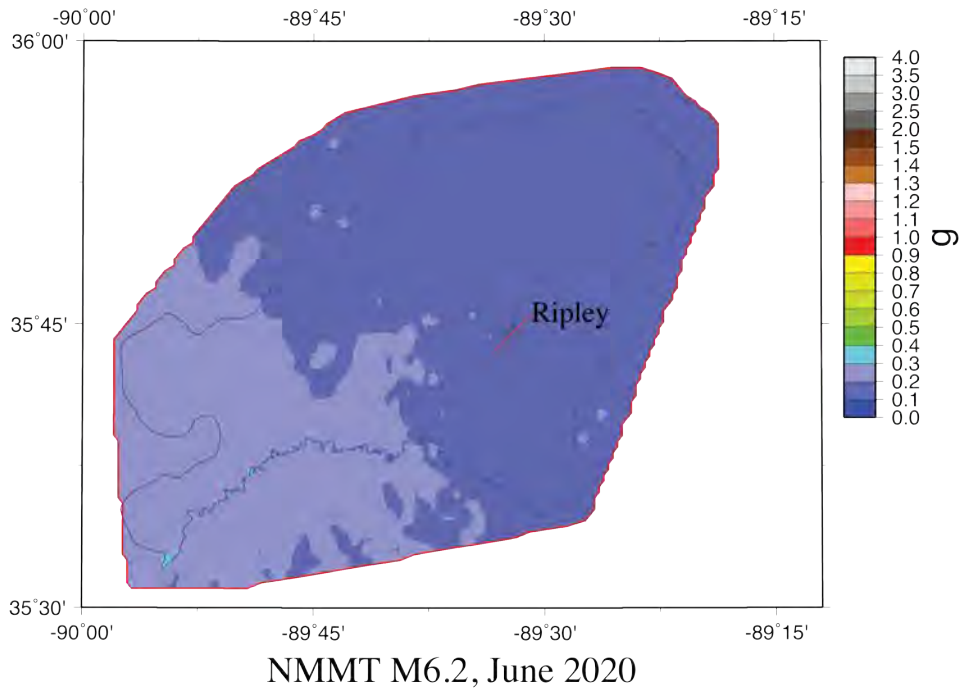


Figure 52B: Scenario 0.2 s hazard map for a M6.2 on the Cottonwood Grove Fault (1843 Marked Tree – SW segment of NMSZ) for Lauderdale County with the effects of local geology.

Lauderdale Co 1.0s Hazard

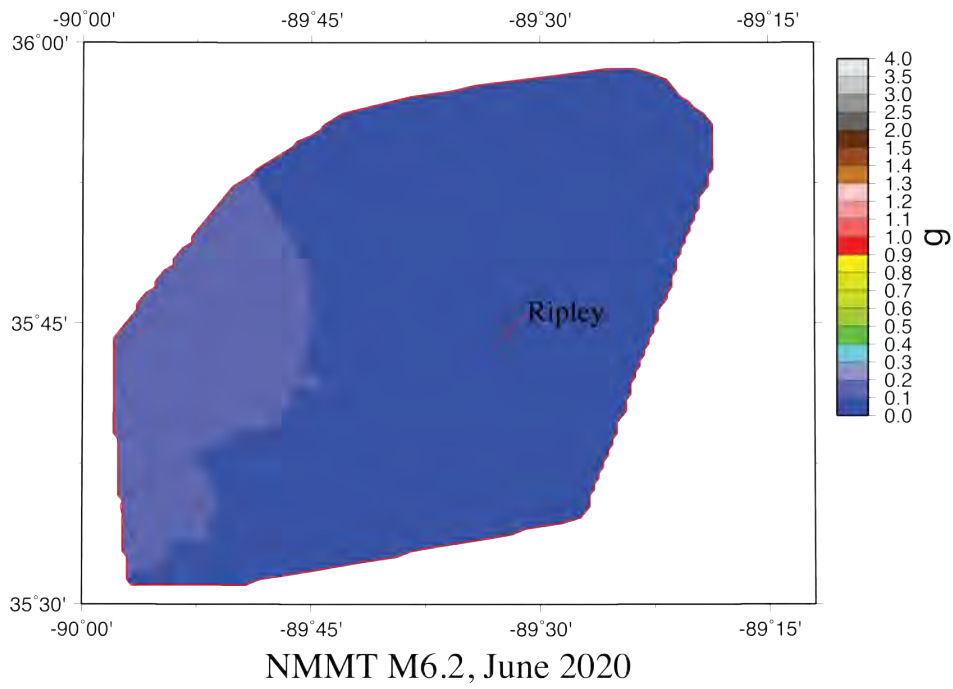


Figure 52C: Scenario 1.0 s hazard map for a M6.2 on the Cottonwood Grove Fault (1843 Marked Tree – SW segment of NMSZ) for Lauderdale County with the effects of local geology.

Lauderdale Co PGA Hazard

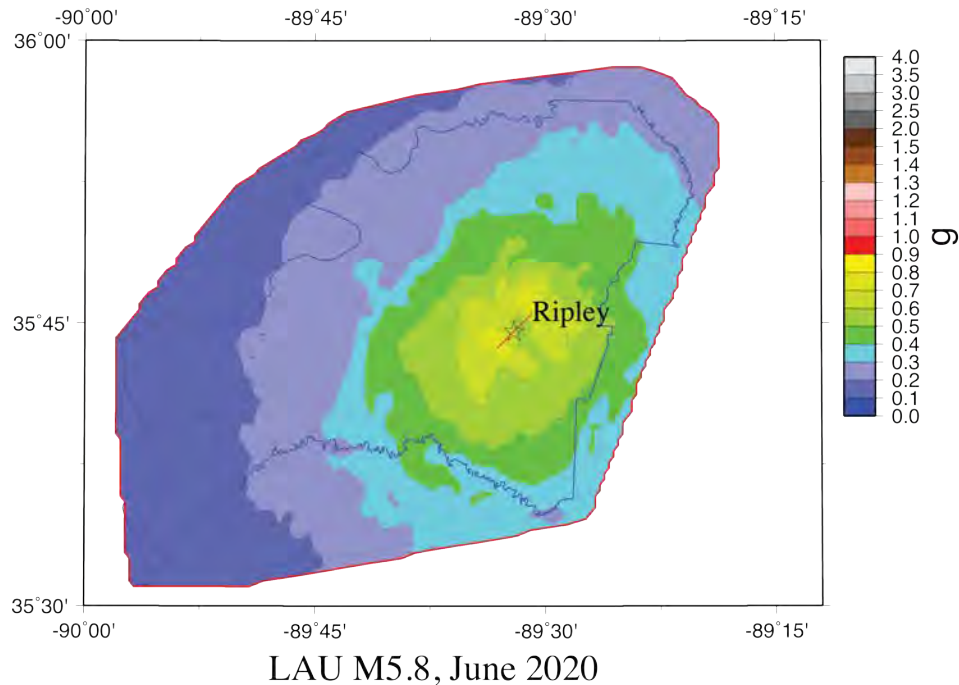


Figure 53A: Scenario PGA hazard map for a M5.8 hypothetical earthquake for Lauderdale County with the effects of local geology. Red line indicates location of source fault.

Lauderdale Co 0.2s Hazard

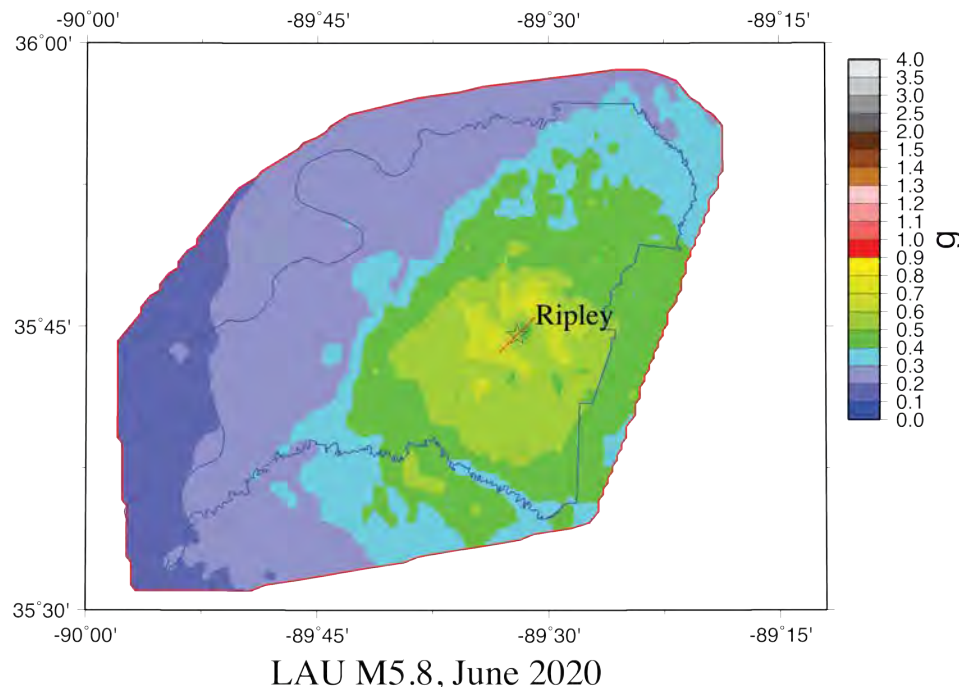
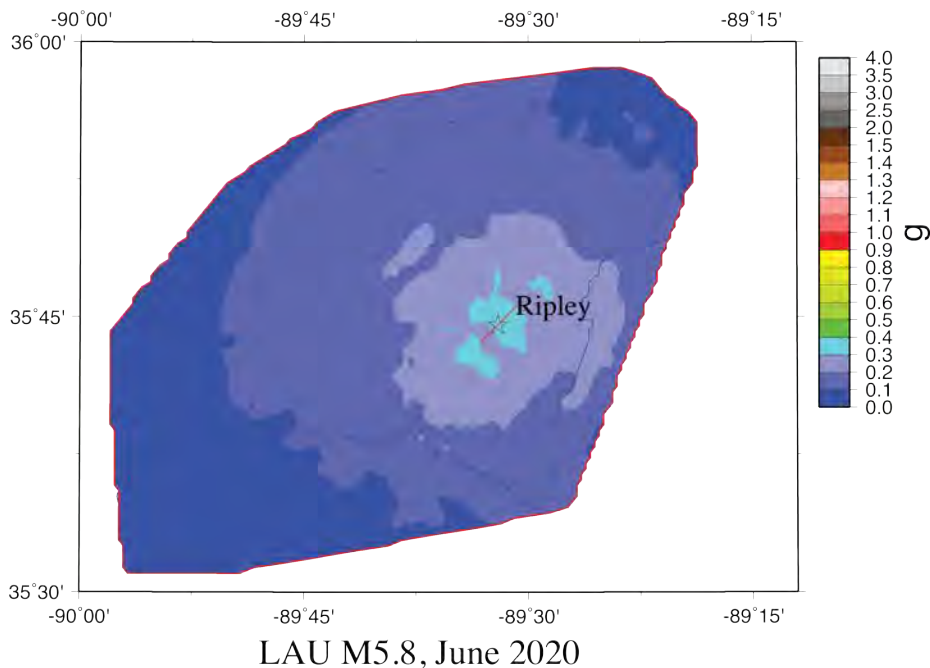


Figure 53B: Scenario 0.2 s hazard map for a M5.8 hypothetical earthquake for Lauderdale County with the effects of local geology. Red line indicates location of source fault.

Lauderdale Co 1.0s Hazard



LAU M5.8, June 2020

Figure 53C: Scenario 1.0 s hazard map for a M5.8 hypothetical earthquake for Lauderdale County with the effects of local geology. Red line indicates location of source fault.

Liquefaction Hazard Maps

To generate the liquefaction hazard maps for Lauderdale County, we used the SPT-based liquefaction probability curves (LPCs) recommended above in Figures 18 and 21 for lowlands and non-lowlands, respectively. The LPCs are for Liquefaction Probability Index (LPI) exceeding 5, which is for the manifestation of liquefaction at the surface (moderate to severe liquefaction). These LPCs were used to maintain compatibility with the liquefaction maps we generated for Lake County (Cramer et al., 2019). Thus, our liquefaction hazard maps are for the probability of moderate to severe liquefaction. If the LPI is for moderate to severe liquefaction LPCs for the effects of non-liquefiable crust of Figures 22 and 23 are used, the liquefaction hazard would be reduced.

Figures 54 - 61 show the two probabilistic and six scenario liquefaction hazard maps derived from the equivalent PGA seismic hazard maps shown above. The probabilistic liquefaction hazard maps show 70 – 80% probability of liquefaction in the lowlands and about 20 – 30% in the non-lowlands for 5%-in-50-years, and about 90% in the lowlands and about 40% in the non-lowlands for 2%-in-50-years probability of liquefaction in Lauderdale County. The M7.7 scenario on the Reelfoot Thrust liquefaction hazard map shows 40 – 80% probability of liquefaction in the lowlands and 10 – 30% in the non-lowlands. For the M7.5 scenario on the SW arm, the liquefaction hazard map shows 50 – 80% in the lowlands and about 10 – 20% in the non-lowlands. The M7.3 scenario on the NE arm shows about 30 – 40% probability of

liquefaction in the lowlands and less than 10% probability of liquefaction in the non-lowlands. The largest aftershock alternatives show 20 – 70% probability of liquefaction in the lowlands and <10 – 20% in the non-lowlands. And the M5.8 hypothetical Lauderdale County earthquake shows 20 – 50% probability of liquefaction in the lowlands and 0 – 20% probability in the non-lowlands. The 1843 and 1895 M6.2 scenarios do not produce any significant liquefaction hazard and are not shown. The liquefaction hazard is high in the lowlands for the near M7 and greater earthquake scenarios.

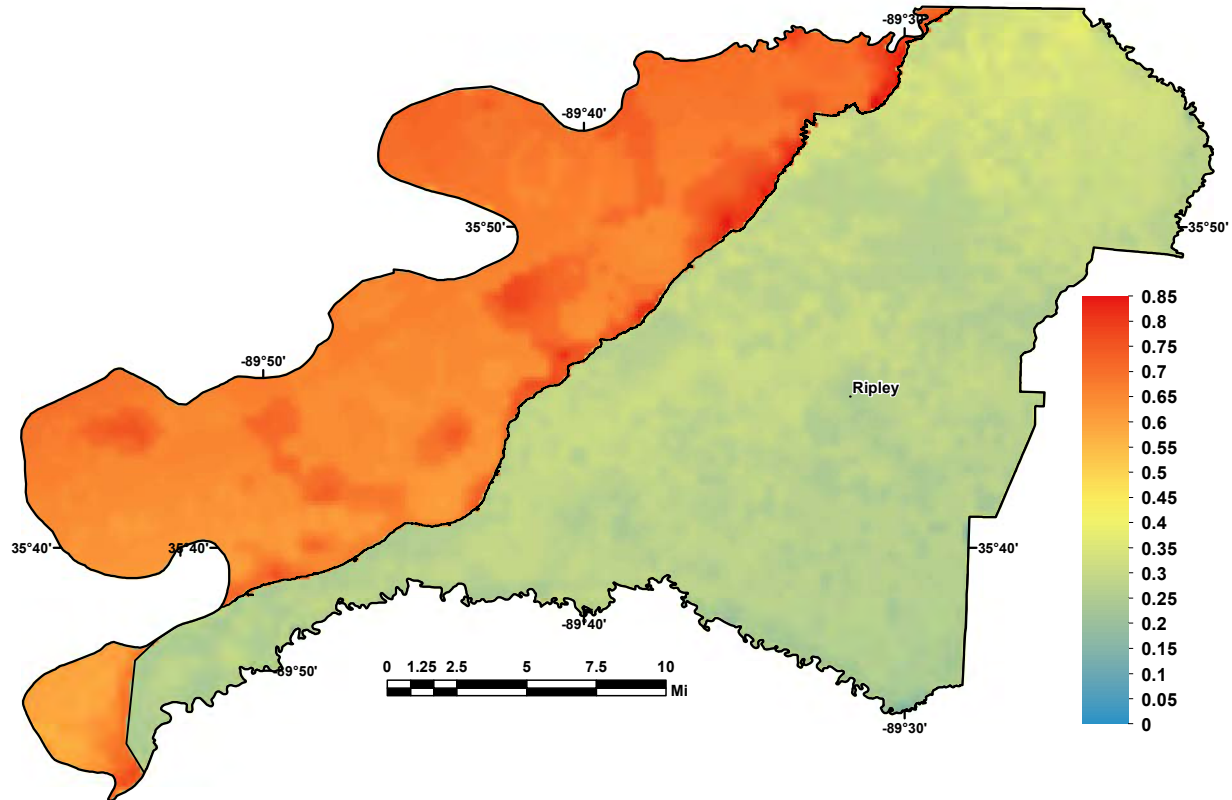


Figure 54: 5%-in-50-year liquefaction hazard map for moderate to severe liquefaction at the surface ($LPI > 5$) for Lauderdale County including the effects of local geology.

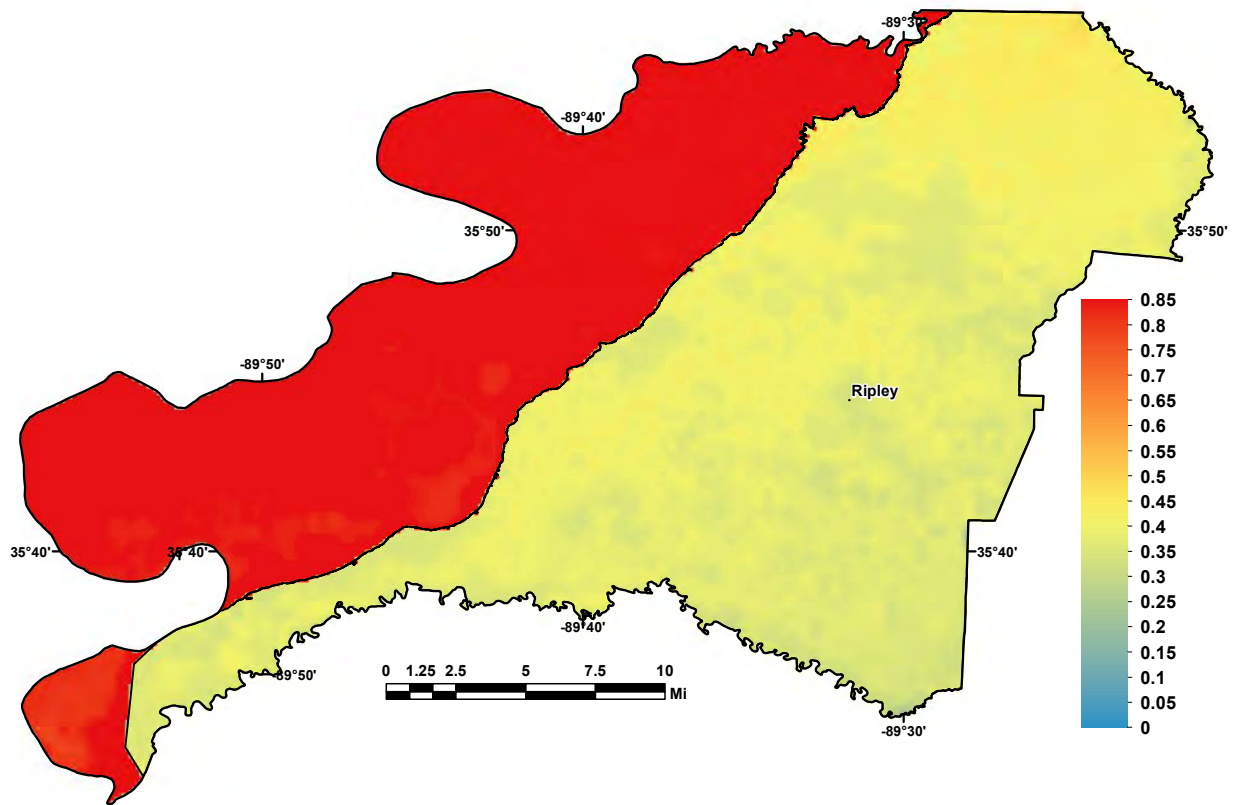


Figure 55: 2%-in-50-year liquefaction hazard map for moderate to severe liquefaction at the surface ($LPI > 5$) for Lauderdale County including the effects of local geology.

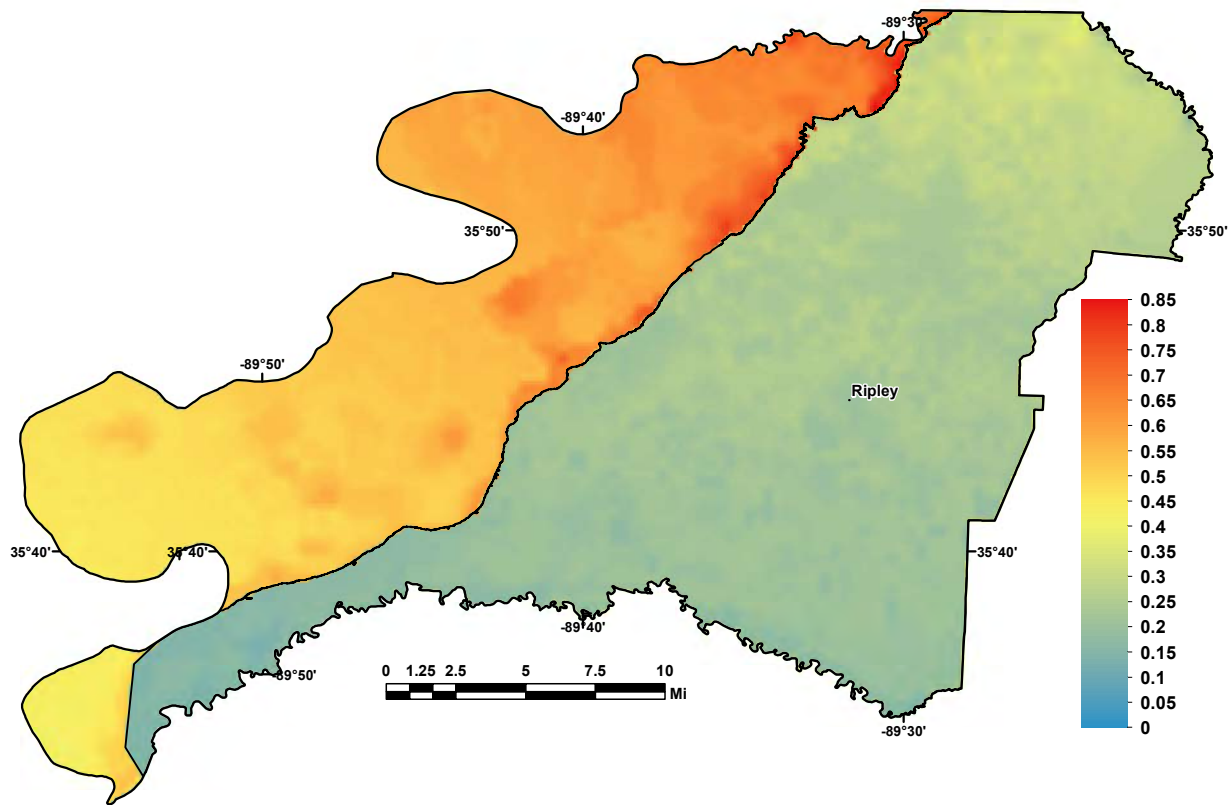


Figure 56: Scenario liquefaction hazard map for moderate to severe liquefaction at the surface (LPI > 5) for a M7.7 earthquake on the Reelfoot Thrust (central segment of NMSZ).

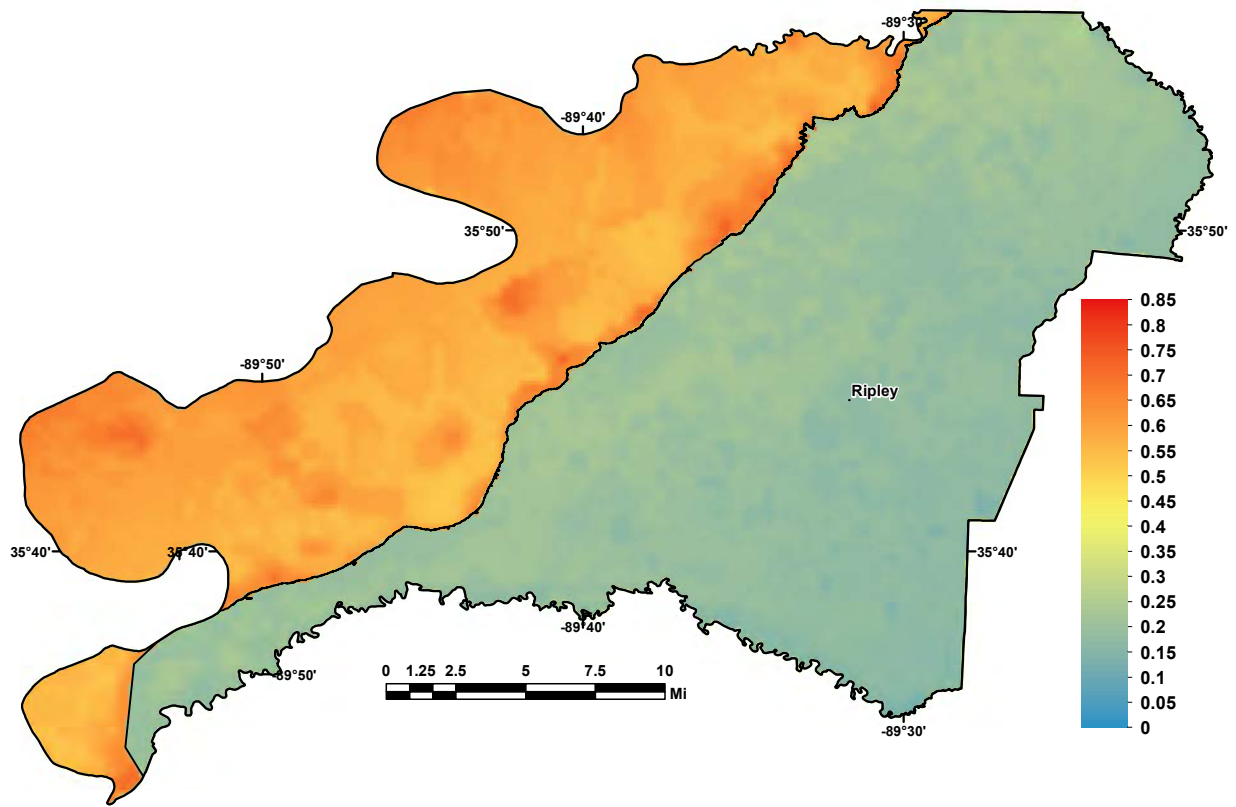


Figure 57: Scenario liquefaction hazard map for moderate to severe liquefaction at the surface (LPI > 5) for a M7.5 earthquake on the Cottonwood Grove Fault (SW segment of NMSZ).

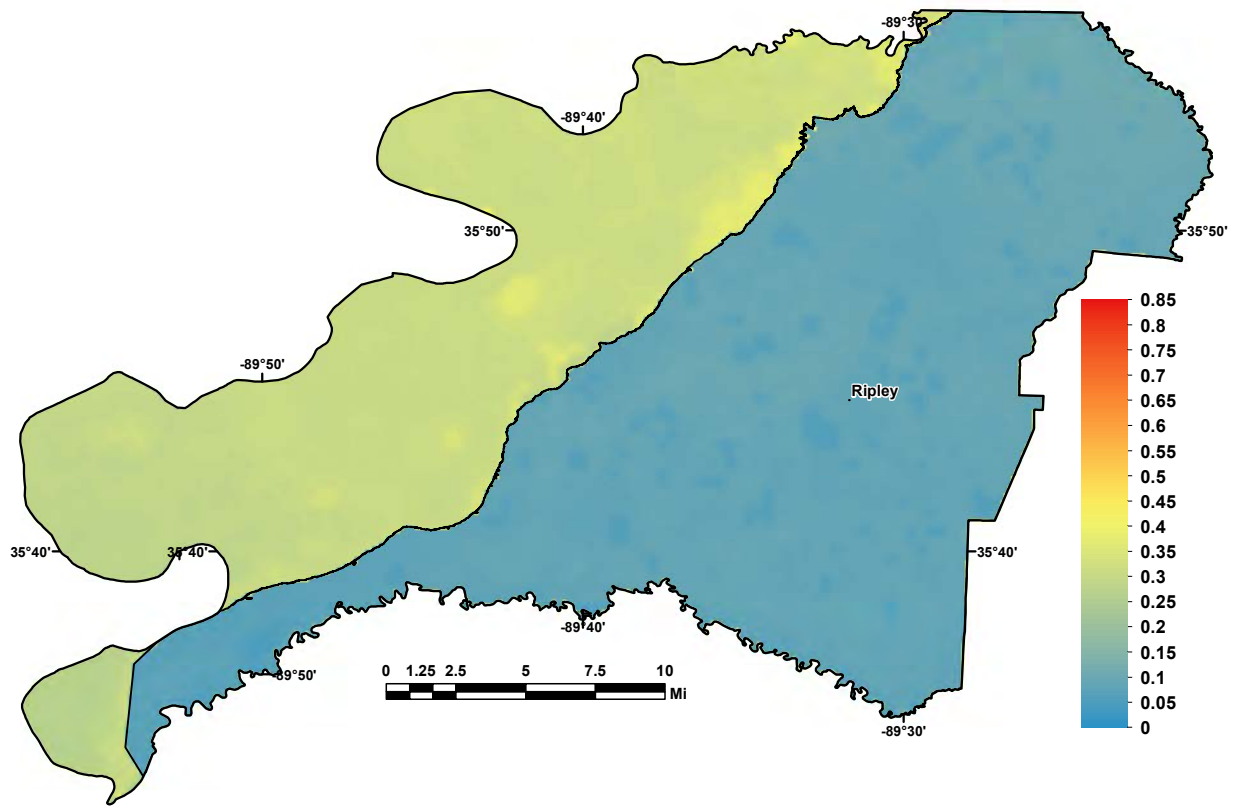


Figure 58: Scenario liquefaction hazard map for moderate to severe liquefaction at the surface (LPI > 5) for a M7.3 earthquake on the New Madrid North Fault (NE segment of NMSZ).

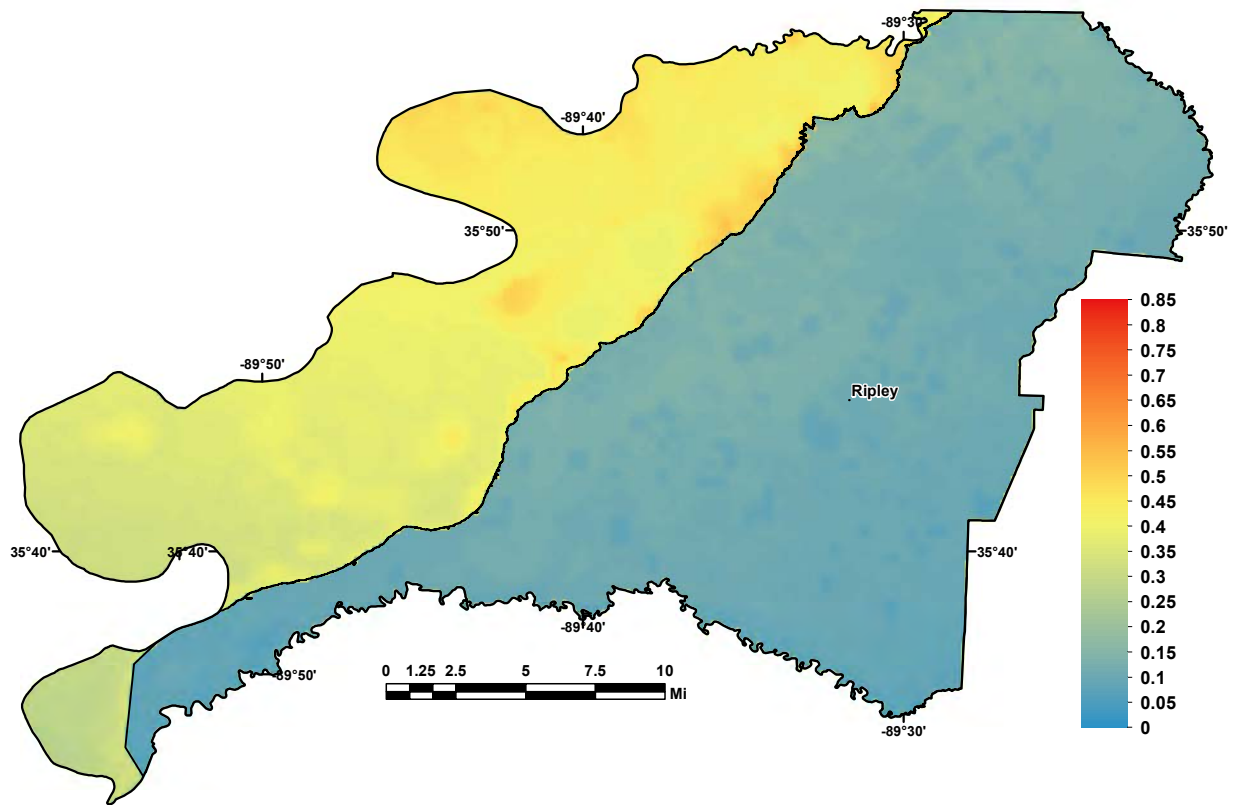


Figure 59: Scenario liquefaction hazard map for moderate to severe liquefaction ($LPI > 5$) for a M6.9 "Dawn" aftershock (alt. 1) on the Cottonwood Grove Fault (SW segment of NMSZ).

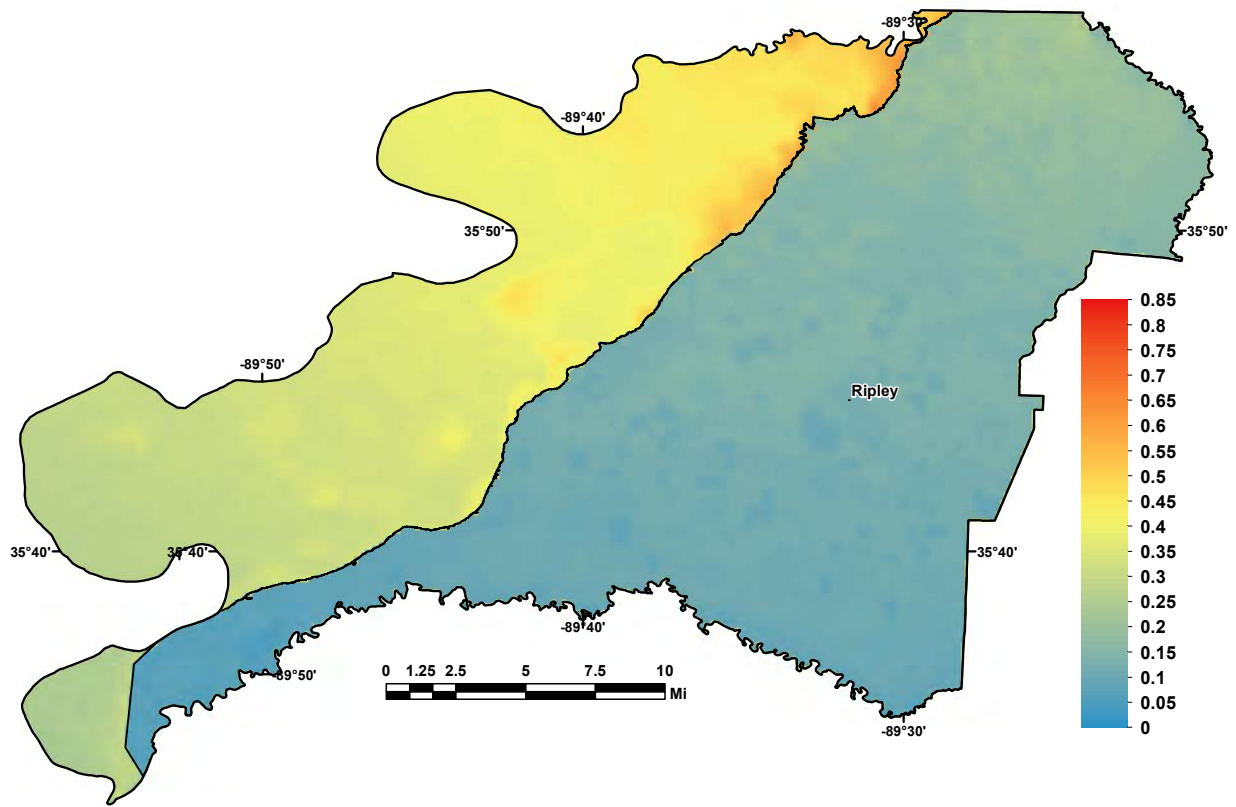


Figure 60: Scenario liquefaction hazard map for moderate to severe liquefaction (LPI > 5) for a M6.9 "Dawn" aftershock (alt. 2) on the Reelfoot Thrust (central segment of NMSZ).

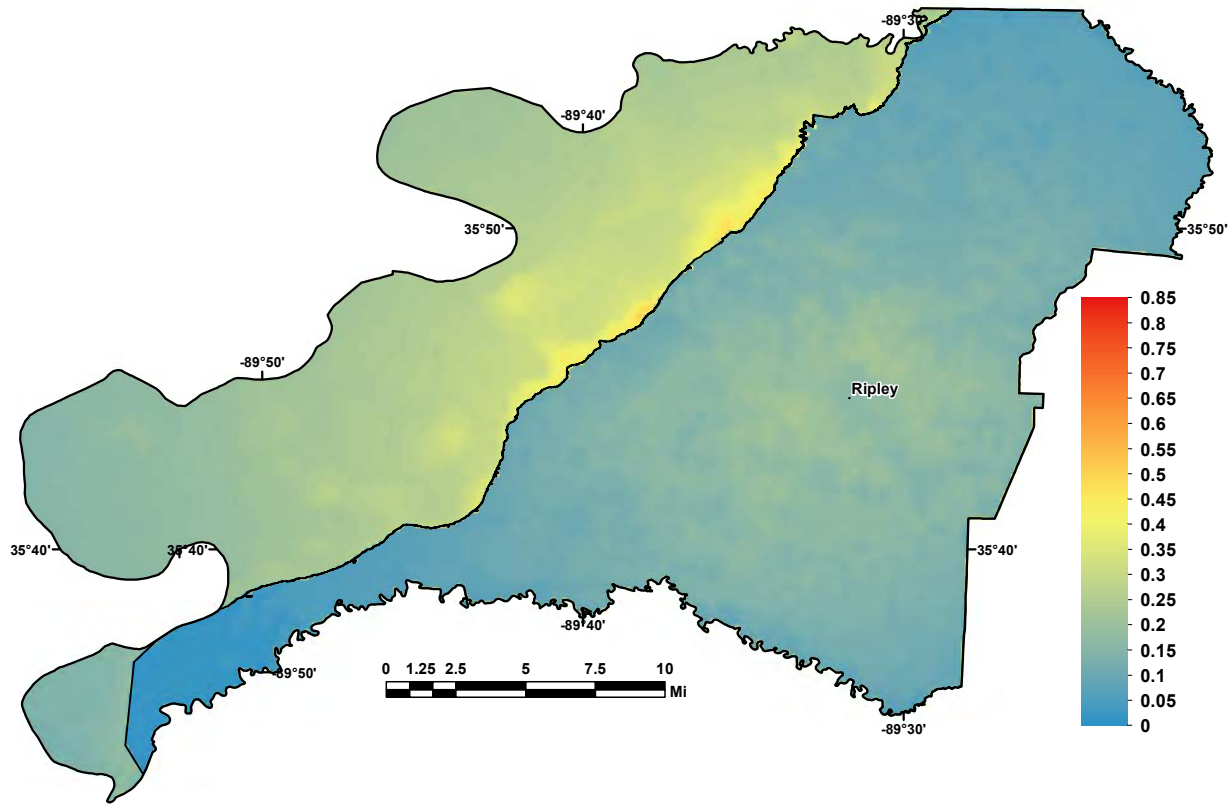


Figure 61: Scenario liquefaction hazard map for moderate to severe liquefaction ($LPI > 5$) for a M5.8 hypothetical Lauderdale County earthquake (near Ripley).

Conclusions

We have produced seismic and liquefaction hazard maps that include the effects of local geology for Lauderdale County. The products from this effort include a 3D geology database and model, a geotechnical database and liquefaction probability curves (LPCs), shear-wave velocity (V_s) measurements and models, and probabilistic and scenario hazard maps for Lauderdale County. The geology model is detailed for the Quaternary sediments down to depths of 200 ft (70 m) and more generalized for the Eocene to Paleozoic formations. Paleozoic limestones form the bedrock of the model. The geotechnical database includes information on water table depths, standard penetration tests (SPT), seismic cone penetration tests (CPT), and shallow V_s information. It was used to generate LPCs based on SPT measurements to add to the published LPCs based on Mississippi embayment CPT measurements. The liquefaction hazard maps for Lauderdale County were based on our developed LPCs for lowlands and non-lowlands. Shallow V_s measurements in 2019 were made at 9 Lauderdale and Dyer County sites. The V_s measurements from Dyer and Lauderdale Counties were used to generate a typical Quaternary V_s profile for non-lowlands areas. Deeper published information from the region

developed for Lake County were used to constrain the Eocene to Paleozoic Vs reference profile used in this study. Seismic and liquefaction hazard maps were generated that include the new geological, geotechnical, and seismological information gathered. The hazard maps are both probabilistic (5% and 2% probability of being exceeded in 50 years) and for seven earthquake scenarios. Seismic hazard maps show a 10-70% decrease in hazard at short periods and a 10-100% increase at long periods compared with USGS NSHMP maps, which are for a uniform standard geology not found in western Tennessee. Liquefaction hazard maps show high hazard in Lauderdale County for four of the five M7 New Madrid scenarios, and low hazard for the M7.3 NE arm and M5.8 hypothetical Lauderdale County earthquakes. The 1843 and 1895 M6.2 scenarios do not produce any significant liquefaction hazard due to more distant epicenters and a shorter duration of strong shaking.

References

- Atkinson, G.M., and I.A. Beresnev, 2002. Ground motions at Memphis and St. Louis from M 7.5–8.0 earthquakes in the New Madrid seismic zone, *Bull. Seism. Soc. Am.* **92**, 1-15-1024.
- Chiu, J. M., Johnston, A. C., and Yang, Y. T., 1992. Imaging the active faults of the central New Madrid seismic zone using PANDA array data. *Seismological Research Letters* **63**, p. 375-93
- Cox, R.T., Van Arsdale, R.B., Harris, J.B., and Larsen, D., 2001, Neotectonics of the southeastern Reelfoot Rift zone margin, central United States, and implications for regional strain accommodation. *Geology* **29**, p. 419-422.
- Cox, R.T., J. Cherryhomes, J. B. Harris, D. Larsen, R. B. Van Arsdale, S. L. Forman, 2006. Paleoseismology of the southeastern Reelfoot rift in western Tennessee and implications for intraplate fault zone evolution. *Tectonics* **25**, p. 1-17.
- Cox, R.T., Lumsden, D.N., and Van Arsdale, R.B., 2014. Possible relict meanders of the Pliocene Mississippi River and their implications. *Journal of Geology* **122**, p. 609-622.
- Cramer, C.H., J.S. Gomberg, E.S. Schweig, B.A. Waldron, and K. Tucker, 2006. First USGS urban seismic hazard maps predict the effects of soils, *Seism. Res. Lett.* **77**, 23-29.
- Cramer, C.H., 2006. Quantifying the uncertainty in site amplification modeling and its effects on site-specific seismic-hazard estimation in the Mississippi embayment and adjacent areas, *Bull. Seism. Soc. Am.* **96**, 2008-2020.
- Cramer, C.H., G. Rix, and K. Tucker, 2008. Probabilistic liquefaction hazard maps for Memphis, Tennessee, *Seis. Res. Lett.* **79**, 416-423.
- Cramer, C.H., and O.S. Boyd, 2014, Why the New Madrid earthquakes are M7–8 and the Charleston earthquake is ~M7, *Bull. Seism. Soc. Am.* **104**, 2884-2903.
- Cramer, C.H., R.B. Van Arsdale, M.S. Dhar, D. Pryne, and J. Paul, 2014. Updating of urban seismic-hazard maps for Memphis and Shelby County, Tennessee: geology and Vs observations, *Seis. Res. Lett.* **85**, 986-996.
- Cramer, C.H., G. Patterson, and David Arellano, 2015. Final Technical Report, Updating Liquefaction Probability Curves, Seismic Hazard Model, and Urban Seismic Hazard Maps with Public Outreach for Memphis and Shelby County, Tennessee, USGS grant G14AP00099, October 30, 2015, 42 pp (available at <http://earthquake.usgs.gov/research/external/reports/G14AP00099.pdf>).

Cramer, C.H., R.A. Bauer, J. Chung, J.D. Rogers, L. Pierce, V. Voigt, B. Michell, D. Gaunt, R.A. Williams, D. Hoffman, G.L. Hempen, P.J. Steckel, O.S. Boyd, C.M. Watkins, K. Tucker, and N. McCallister, 2017. St. Louis area earthquake hazards mapping projects: seismic and liquefaction hazard maps, *Seis. Res. Lett.* **88**, 206-223.

Cramer, C.H., M.S. Dhar, and D. Arellano, 2018a. Update of the urban seismic and liquefaction hazard maps for Memphis and Shelby County, Tennessee: liquefaction probability curves and 2015 hazard maps, *Seis. Res. Lett.* **89**, 688-701.

Cramer, C., R. Van Arsdale, D. Arellano, S. Pezeshk, S. Horton, T. Weathers, N. Nazemi, J.A. Jimenez, H. Tohidi, and L.P. Ogweno, 2018b, Seismic and liquefaction hazard maps for Lake County, northwestern Tennessee, (2018 SE-GSA abstract). Geological Society of America Abstracts with Programs 50. 10.1130/abs/2018SE-312570.

Cramer, C., R.B. Van Arsdale, V. Harrison, D. Arellano, S. Pezeshk, S.P. Horton, T. Weathers, N. Nazemi, J. Jimenez, H. Tohidi, and L.P. Ogweno, 2019. Lake County seismic and liquefaction hazard maps, CERI Report, 129 pp.

Cramer, C., R.B. Van Arsdale, R. Reichenbacher, D. Arellano, H. Tahidi, S. Pezeshk, S.P. Horton, R. Bhattacharai, N. Nazemi, and A. Farhadi, 2020. Dyer County seismic and liquefaction hazard maps, CERI Report, 90pp.

Csontos, R., and Van Arsdale, R., 2008. New Madrid seismic zone fault geometry. *Geosphere* **4**, p. 802-813.

Csontos, R., Van Arsdale, R., Cox, R., and Waldron, B., 2008. The Reelfoot Rift and its impact on Quaternary deformation in the central Mississippi River Valley. *Geosphere* **4**, n. 1, p. 145-158, doi: 10.1130/GES00107.1.

Cupples, W., and Van Arsdale, R., 2014. The Preglacial “Pliocene” Mississippi River. *Journal of Geology* **122**, p. 1-15.

Dhar, M.S., and C.H. Cramer, 2018. Probabilistic seismic and liquefaction hazard analysis of the Mississippi embayment incorporating nonlinear effects, *Seis. Res. Lett.* **89**, 253-267, published online 13 December 2017.

Hardeman, W.D., 1966, Geologic Map of Tennessee: West Sheet. Scale 1:250,000.

Ishihara, K., 1985. Stability of natural deposits during earthquakes. In: Proceedings of the 11th International Conference on Soil Mechanics and Foundation Engineering. San Francisco, CA, USA, 1, pp.321–376.

Iwasaki, T., Tatsuoka, F., Tokida, K. and Yasuda, S., 1978. A practical method for assessing soil liquefaction potential based on case studies at various sites in Japan, Second International Conference on Microzonation for Safer Construction Research and Application 1978.

Iwasaki, T., Tokida, K., Tatsuoka, F., Watanabe, S., Yasuda, S., and Sato, H., 1982. Microzonation for soil liquefaction potential using simplified methods. Proceedings 3rd International Conference on Microzonation, Seattle, USA. 1319-1330.

Louie, J.N., 2001. Faster, Better: Shear-Wave Velocity to 100 Meters Depth from Refraction Microtremor Arrays. *Bulletin of the Seismological Society of America* **91**, 347–364.

Lumsden, D.N., Cox, R.T., Van Arsdale, R.B., and Cupples, W.B., 2016, Petrology of Pliocene Mississippi River alluvium: provenance implications. *The Journal of Geology* **124**, 501-517.

Markewich, H. H., Wysocki, D. A., Pavich, M. J., Rutledge, E. M., Millard, H. T., Rich, F. J., et al. (1998). Paleopedology plus TL, ^{10}Be , and ^{14}C dating as tools in stratigraphic and paleoclimatic investigations, Mississippi River valley, U.S.A. *Quaternary International* **51**, 143–167. doi: 10.1016/s1040-6182(97)00041-4.

Martin, R.V., and Van Arsdale R.B., 2017, Stratigraphy and structure of the Eocene Memphis Sand above the eastern margin of the Reelfoot rift in Tennessee, Mississippi, and Arkansas, USA. *Geological Society of America Bulletin* **129**, 970-996.

Maurer, B. W., Green, R. A., and Taylor, O.-D. S., 2015. Moving towards an improved index for assessing liquefaction hazard: Lessons from historical data, *Soils and Foundations* **55**, 778–787.

Odum, W., Hofmann, F., Van Arsdale, R., and Granger, D., New $^{26}\text{Al}/^{10}\text{Be}$ and (U-Th)/He constraints on the age of the Upland Complex, central Mississippi River Valley. In press with *Geomorphology*.

Parrish, S., and Van Arsdale, R., 2004, Faulting along the southeastern margin of the Reelfoot rift in northwestern Tennessee revealed in deep seismic reflection profiles. *Seismological Research Letters*, v. 75, p. 782-791.

Petersen, M. D., M. Moschetti, P. Powers, C. Mueller, K. Haller, A. Frankel, Y. Zeng, S. Rezaeian, S. Harmsen, O. Boyed, N. Field, R. Chen, K. Rukstales, N. Luco, R. Wheeler, R. Williams, and A. Olsen, 2014, *The 2014 update of the United States national seismic hazard models*, U.S. Geological Survey, OFR 2014-X1091, 255 p.

Rittenour, T.M., Blum, M.D., Goble, R.J., 2007, Fluvial evolution of the lower Mississippi River valley during the last 100 k.y. glacial cycle: response to glaciation and sea-level change. *Geological Society of America Bulletin* **119**, 586-608.

Rodbell, D. T., 1996, Subdivision, subsurface stratigraphy, and estimated age of fluvial-terrace deposits in northwestern Tennessee. U.S. Geologic Survey Bulletin, v. 2128, 24 pp.

Romero, S., and G.J. Rix (2001). Regional variations in near surface shear wave velocity in the Greater Memphis area, *Eng. Geol.* **62**, 137-158.

Saucier, R.T., 1987, Geomorphological interpretations of late Quaternary terraces in western Tennessee and their regional tectonic implication. U.S. Geologic Survey Professional Paper 1336-A, 19 pp.

Saucier, R.T., 1994, Geomorphology and Quaternary Geologic History of the Lower Mississippi Valley: Vicksburg, Mississippi. U.S. Army Engineer Waterways Experiment Station, v. 1, 364 p., and v. 2, map plates.

Schrader, T.P., 2008. Potentiometric surface in the Sparta-Memphis aquifer of the Mississippi embayment, Spring 2007, U.S. Geological Survey Scientific Investigations Map 3014.

Schuler, Juerg, 2008. Joint inversion of surface waves and refracted P and S-wave. Masters Science Thesis, Eidgenossische Technische Hochschule Zurich, Swiss Federal Institute of Technology Zurich.

Seed, H. B., and Idriss, I. M., 1971. "Simplified procedure for evaluating soil liquefaction potential." *J. Geotech. Eng. Div., ASCE*, 97(9), 1249–1273.

Stokoe II, K.H., and J.C. Santamarina, 2000. Seismic-wave-based testing in geotechnical engineering, International Conference on Geotechnical and Geological Engineering, GeoEng 2000, 1490–1536.

Toprak, S., and Holzer, T. L., 2003. "Liquefaction potential index: Field assessment." *Journal of Geotechnical and Geoenvironmental Engineering, ASCE*, 129(4), 315-322.

Tuttle, M. P., Schweig, E. S., Sims, J. D., Lafferty, R. H., Wolf, L. W., and Haynes, M. L., 2002. The earthquake potential of the New Madrid seismic zone, *Bulletin Seismological Society of America* **92**, 2080–2089, doi: 10.1785/01200 10227.

Van Arsdale, R.B., Bresnahan, R.P., McCallister, N.S., and Waldron, B., 2007. The Upland Complex of the central Mississippi River Valley: Its origin, denudation, and possible role in reactivation of the New Madrid seismic zone, in Stein, S., and Mazzotti, S., eds., Continental Intraplate Earthquakes: Science, Hazard, and Policy Issues. Geological Society of America Special Paper 425, p. 177-192.

Van Arsdale, R.B., Arellano, D., Stevens, K.C., Hill, A.A., Lester, J.D., Parks, A.G., Csontos, R.M., Rapino, M.A., Deen, T.S., Woolery, E.W., Harris, J.B., 2012. Geology, Geotechnical Engineering,

and Natural Hazards of Memphis, Tennessee, USA. *Environmental & Engineering Geoscience* **18**, 113-158, doi:10.2113/gseegeosci.18.2.113.

Van Arsdale, R.B., Cox, R.T., and Lumsden, D.N., 2019, Quaternary Isostatic Uplift in the Northern Mississippi Embayment, *Journal of Geology* **127**, 1-13.

Weathers, T., and Van Arsdale, R. 2019, Lake County Tennessee: in the Heart of the New Madrid seismic zone. *Frontiers in Earth Science* **7**, 1-20.

Woolery, E.W., Z. Wang, N.S. Carpenter, R. Street, and C. Brengman, 2016. The Central United States Seismic Observatory: site characterization, instrumentation, and recordings, *Seis. Res. Lett.* **87**, 215-228.

Appendix (separate file)